ABSTRACT

SODIUM AND CHROMATE ION MOVEMENT ACROSS ISOLATED FROG AND FISH SKINS WITH THE EFFECT OF MAGNETIC FIELDS UPON SUCH MOVEMENT

by Jack Knoll

The literature is not in agreement as to what, if any, are the biological effects of magnetic fields. Frog skin provided the opportunity to study the action of magnetic fields on an isolated biological system capable of actively transporting sodium ions. Fish skin was used for comparative purposes. Isotopically labeled chromate ions were utilized in the study, and it was assumed they would not be transported actively and would thus represent a diffusable anion. With the exception of three in vivo observations taken for purposes of comparison, all studies were conducted using isolated frog or fish skin mounted in a short-circuit chamber.

Magnetic fields in the range of 3500 gauss were found to exert no repeatable effects on sodium ion transport across frog skin. This was true both in normal skins and in those that had been stimulated with neurohypophyseal extract or epinephrine. The average total sodium ion short-circuit current output of the frog skins studied was 233 ± 97

microampere hours per cm^2 or 0.20 \pm 0.08 milligrams of sodium transported per cm^2 .

The increased potential that was observed following short-circuiting of frog skin was attributed to chloride ion accumulation in the stratum germinativum cells. This increased potential was unaffected by magnetic fields.

Radiochromate ion crossed frog skin in a two-step process: a rapid initial step completed before the first tenminute aliquot was taken and a slow second step that remained linear over a three-hour observation period. When they were determined by using the slopes of the linear regression lines of the slow component, radiochromate flux ratios of Min/Mout compared closely with calculated values. Because of the close agreement of measured and calculated flux ratios, the second component was assumed to represent radiochromate ion movement caused by the electrochemical potential gradient existing across the frog skin. It was proposed that the rapid component was quenched due to radiochromate ion binding in or on membrane pores, thereby either diminishing the pore size or occluding the pore altogether.

Possible effects of a magnetic field on radiochromate ion movement across frog skin were observed. Such effects could be explained by applying the Lorentz equation.

The possibility of a two-component system of radiochromate ion movement across fish skin was noted. Since the potential difference across isolated fish skin was zero, flux ratios of $M_{\rm in}/M_{\rm out}$ should equal unity. Although variable, the measured flux ratios ranged both above and below one, thus presenting no evidence to doubt that true flux ratios of $M_{\rm in}/M_{\rm out}$ were equal to one.

Isolated fish skin took up radiochromate ion in amounts ten times greater than that present in the Ringer's bathing solutions. Because skin taken from fish living in water containing radiochromate ion showed little activity, it was concluded that radiochromate ion probably does not cross the skin of living rainbow trout to any great extent.

SODIUM AND CHROMATE ION MOVEMENT ACROSS ISOLATED FROG AND FISH SKINS WITH THE EFFECT OF MAGNETIC FIELDS UPON SUCH MOVEMENT

bу

Jack Knoll

A THESIS

Submitted to
Michigan State University
in partial fulfillment of the requirements
for the degree of

DOCTOR OF PHILOSOPHY

Department of Physiology and Pharmacology

1962

ACKNOWLEDGMENT

4 3 3

The author wishes to express gratitude to Dr. P. O.

Fromm for his counsel and interest. Appreciation is expressed to Dr. D. J. Montgomery and A. Smith for their advice and their aid in the preparation of Appendix B.

Both Dr. L. F. Wolterink and Dr. W. L. Frantz provided helpful suggestions. Thanks are also extended to Mr. K.

Irish, both for his help in constructing the short-circuit chambers and for his interest in the project. In addition, the writer is indebted to the Public Health Service,

National Institute of Health, for funds in support of this work.

Whatever contribution this dissertation will make to man's knowledge is dedicated to my wife and son. Their willingness to cheerfully endure five years of disrupted living has made this task a much easier one.

TABLE OF CONTENTS

	Page
INTRODUCTION	1
LITERATURE REVIEW	3
Anatomy of Frog Skin	3
Early Frog Skin Investigations	3
Ussing's Short-Circuit Technique	6
Chloride Ion Movement across Frog Skin	11
Electrical Potential Gradients across Frog Skin	12
Metabolism and Active Transport	16
Water Movement across Frog Skin	19
Other Frog Skin Experiments	28
Magnetic Effects in Biology	29
Magnetic Field Effects upon Animal Orientation	30
Physiological Changes Induced by Magnetic Fields	31
MATERIALS AND METHODS	37
Frog Procurement and Holding Facilities	37
Rationale of the Short-Circuit Technique	38
The Short-Circuit Apparatus	39
Source of the Magnetic Field	45
Positioning of the Magnet	46
Isotopic Techniques	49
Short-Term Biomagnetic Studies	50
Ten-Hour Biomagnetic Studies	50
The Effects of Higher Magnetic Fields	51

	Page
The Effects of Magnetic Fields on Neurohypo- physeally Stimulated Frog Skin	52
The Effects of Magnetic Fields on Epinephrine Stimulated Frog Skin	52
The Effects of Magnetic Fields on the Increased Potential Observed after Short-Circuiting Frog Skin	53
The Movement of Radiochromate Ion across Frog Skin	53
The Movement of Radiochromate Ion across Fish Skin	55
Expression of Data	55
RESULTS	57
Short-Term Biomagnetic Studies	57
Ten-Hour Biomagnetic Studies	58
The Effects of Higher Magnetic Fields	59
The Effects of Magnetic Fields on Neurohypo-physeally Stimulated Frog Skin	61
The Effects of Magnetic Fields on Epinephrine Stimulated Frog Skin	61
The Effects of Magnetic Fields on the Increased Potential Observed after Short-Circuiting Frog Skin	65
The Movement of Radiochromate Ion across Frog Skin	72
The Movement of Radiochromate Ion across Fish Skin	80
DISCUSSION	85
Effects of Magnetic Fields on Sodium Ion Transport across Normal Frog Skin	85

Effects of Magnetic Fields on Sodium Ion	Page
Transport across Frog Skin Stimulated with Neurohypophyseal Extract or Epinephrine	86
Increased Potential Following Short-Circuiting of Frog Skin	87
Radiochromate Ion Movement across Frog Skin .	88
Radiochromate Ion Movement across Fish Skin .	92
SUMMARY AND CONCLUSIONS	96
LITERATURE CITED	99
APPENDICES	
A. SUBSTANCES AFFECTING SODIUM TRANSPORT ACROSS FROG SKIN	106
B. PHYSICAL PROPERTIES OF MAGNETISM	110
The Development of a Magnetic Field	111
Monopoles	113
Dipoles	113
Diamagnetism	114
_	116
Paramagnetism	
Other Types of Magnetism	117
C. SHORT-TERM BIOMAGNETIC STUDIES	118
D. TEN-HOUR BIOMAGNETIC STUDIES	123
E. MOVEMENT OF RADIOCHROMATE ION ACROSS FROG SKIN	132
F. MOVEMENT OF RADIOCHROMATE ION ACROSS	140

LIST OF TABLES

Table		Page
1.	The effect of neurohypophyseal extract on short-circuit current of frog skin	64
2.	The effects of epinephrine on short-circuit current of frog skin	64
3.	Effects of short-circuiting duration on potential	70
4.	The effects of a magnetic field on potential	70
5.	Calculated line equations and flux ratios for radiochromate ion movement across frog skin	75
6.	Activity remaining in the frog skins after rinsing in 50 ml. of Ringer's solution	75
7.	Per cent of activity crossing frog skin in 1, 2 and 3 hours based on corrected activities	78
8.	Calculated regression equations and flux ratios for radiochromate ion movement across frog skin in the presence of a magnetic field	78
9.	Summary of ion exchange studies of Cr^{51} after it had passed through frog skin	79
10.	Summary of pertinent data regarding radio- chromate ion movement across fish skin	84
11.	Uptake of radiochromate ions by isolated fish skin	84
12.	Flux ratios determined using different criteria	90
	APPENDIX A	
A-1.	Agents stimulating active sodium transport in amphibian skin	107
A-2.	Agents inhibiting sodium transport in amphibian skin	108

Table		Page			
A-3.	Effect of various metabolites on 02-consumption of epithelial homogenate	109			
	APPENDIX D				
D-1.	Total short-circuit current (microampere hours) produced by frog skins	124			
	APPENDIX E				
E-1.	Movement of radiochromate ion across frog skin	133			
E-2.	Movement of radiochromate ion across frog skin	134			
E-3.	Movement of radiochromate ion across frog skin	135			
E-4.	Movement of radiochromate ion across frog skin	136			
E-5.	Movement of radiochromate ion across frog skin in the presence of a magnetic field	137			
E-6.	Movement of radiochromate ion across frog skin in the presence of a magnetic field	138			
E-7.	Movement of radiochromate ion across frog skin in the presence of a magnetic field	139			
APPENDIX F					
F-1.	Movement of radiochromate ion across fish skin	141			
F-2.	Movement of radiochromate ion across fish skin	142			
F-3.	Movement of radiochromate ion across fish skin	143			
F-4.	Movement of radiochromate ion across fish skin in the presence of a magnetic field	144			

LIST OF FIGURES

Figure		Page
1.	A schematic drawing of a section through frog skin	4
2.	Equivalent circuit representing the short-circuited frog skin	10
3.	Proposed model of Na ⁺ ion transport across frog skin stratum germinativum layer	14
4.	Equivalent circuit of frog skin under short-circuit conditions	40
5.	Two batteries connected in series and then short-circuited	40
6.	Schematic diagram of the short-circuit apparatus	42
7.	Pictorial views of the short-circuit apparatus	43
8.	A homogeneous field with the magnet placed at a right angle to the frog skin	47
9.	An inhomogeneous field with the magnet placed at an oblique angle to the frog skin	47
10.	The effects of high magnetic fields on Na ⁺ ion transport	60
11.	The effects of high magnetic fields on Na ⁺ ion transport	60
12.	Effects of magnetic fields applied subsequent to neurohypophyseal stimulation of frog skin	62
13.	Effects of magnetic fields applied subsequent to neurohypophyseal stimulation of frog skin	62
14.	Effects of magnetic fields applied prior to neurohypophyseal stimulation of frog skin .	63
15.	Effects of magnetic fields applied following epinephrine stimulation of frog skin	66

Figure		Page
16.	Effects of magnetic fields applied following epinephrine stimulation of frog skin	66
17.	Effects of magnetic fields applied prior to epinephrine stimulation of frog skin	67
18.	Effects of magnetic fields applied prior to epinephrine stimulation of frog skin	67
19.	The effects of short-circuiting duration on voltage	68
20.	The effects of short-circuiting duration on voltage increase	71
21.	The effects of magnetic fields on voltage .	71
22.	Radiochromate ion movement across frog skin	73
23.	Radiochromate ion movement across frog skin	73
24.	Radiochromate ion movement across frog skin	74
25.	Radiochromate ion movement across frog skin	74
26.	Effects of magnetic fields on radiochromate ion movement across frog skin	76
27.	Effects of magnetic fields on radiochromate ion movement across frog skin	76
28.	Effects of magnetic fields on radiochromate ion movement across frog skin	77
29.	Radiochromate ion movement across fish skin	82
30.	Radiochromate ion movement across fish skin	82
31.	Radiochromate ion movement across fish skin	82
32.	Effects of magnetic fields on radiochromate ion movement across fish skin	83
	APPENDIX B	
B-1.	The magnetic field surrounding a closed loop as viewed from a great distance	115

Figure							Page
			APPENI	DIX C			
C-1.	Frog	skin	short-circuit	current	versus	time	119
C-2.	Frog	skin	short-circuit	current	versus	time	119
C-3.	Frog	skin	short-circuit	current	versus	time	120
C-4.	Frog	skin	short-circuit	current	versus	time	121
C-5.	Frog	skin	short-circuit	current	versus	time	121
C-6.	Frog	skin	short-circuit	current	versus	time	122
C-7.	Frog	skin	short-circuit	current	versus	time	122
APPENDIX D							
D-1.	Frog	skin	short-circuit	current	versus	time	125
D-2.	Frog	skin	short-circuit	current	versus	time	126
D-3.	Frog	skin	short-circuit	current	versus	time	127
D-4.	Frog	skin	short-circuit	current	versus	time	128
D-5.	Frog	skin	short-circuit	current	versus	time	129
D-6.	Frog	skin	short-circuit	current	versus	time	130
D-7.	Frog	skin	short-circuit	current	versus	time	131

INTRODUCTION

Biological effects of magnetic fields should be studied in view of the possibility that living systems could easily encounter strong magnetic fields in space travel, that physicists and accelerator operators in the atomic-energy industry are exposed to magnetic fields of varying intensities in the course of operation and maintenance of ion accelerators and finally, as pointed out by Montgomery and Smith (1959), that the literature is not in agreement as to just what, if any, are the biological effects of magnetic fields.

Frog skin was employed in this study because it provided the opportunity to study an isolated biological system that is capable of actively transporting sodium ions and also chloride ions under conditions of epinephrine stimulation. The fact that frog skin is a well-studied system is an exceptionally desirable attribute in an endeavor of this kind. The ability to utilize frog skin in an isolated system, coupled with the ease of obtaining frogs at any time, presents additional reasons for choosing such an experimental system. Another advantage in the use of frog skin is that it, together with the associated apparatus, can be easily placed in magnetic fields, since the entire apparatus is relatively small and can be moved to some extent, and possesses no iron parts that would be affected by strong magnetic fields.

The purpose of this study was to investigate the effects

of a magnetic field in the 3000 to 4000 gauss range upon different aspects of sodium transport.

The short-circuit apparatus utilized in this experiment provided an excellent opportunity to study the movement of chromate ion, CrO_4^- , across both frog and fish skin. In the case of frog skin studies, the short-circuit current along with the non-short-circuit potential difference existing across the skin could be utilized to evaluate the over-all condition of the skin under test.

The fish skin study represented an attempt to consider chromate ion movement across skins from a comparative standpoint. It also permitted continuation of a previous project in which it was stated that chromium movement across rainbow trout skin was probably of little significance (Knoll, 1959; Knoll and Fromm, 1960).

LITERATURE REVIEW

Anatomy of Frog Skin

Frog skin is smooth, moist, loosely attached to the body, with lymph spaces occurring between the skin and the body wall. Histologically the skin consists of an epidermis and an inner corium or dermis. A schematic drawing of a cross-section of frog skin is depicted in figure 1.

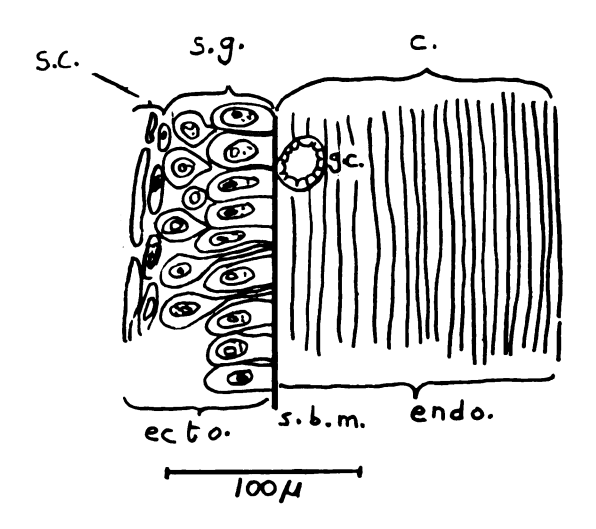
Using an electron microscope, Ottoson et al. (1953) determined that the epidermal cells were delimited by a complete cell membrane and that the frog epidermis did not represent a syncytium. Electron microscopic analysis also revealed that there was a well-defined special basement membrane at the chorio-epidermal junction, 200 to 300 A thick, the dimensions of which were indistinguishable with ordinary light microscopes.

Early Frog Skin Investigations

Although coming long after Galvani discovered the electrical properties of animal tissue in 1791 by conducting experiments on frogs' legs, the measurement of electrical potentials across isolated frog skin ranks among some of the earliest work done in the field of electrophysiology.

As early as 1848, DuBois-Reymond, in addition to studying action potentials and injury potentials in nerves, observed that isolated frog skin maintains an electric potential between the inside and outside. Galeotti, in the

Figure 1. A schematic drawing of a section through frog skin. (Koefoed-Johnsen and Ussing, 1958)



s.c. - stratum cornea

s.g. - stratum germinativum

c. - corium

g.c. - goblet cell

s.b.m. - special basement membrane

ecto. - region of ectodermal origin

endo. - region of endodermal origin

early 1900's, made the important observation that Na⁺ or Li⁺ ions are necessary for the maintenance of this electrical potential. He hypothesized that the skin was more permeable to Na⁺ and Li⁺ ions in a direction from outside to inside than from inside to outside. Galeotti's theory was not well accepted at the time, since it appeared to violate the second law of thermodynamics (Ussing, 1960a).

Francis (1933) demonstrated that a partially short-circuited frog skin was capable of generating electrical energy for several hours. Huf (1935) showed that isolated frog skin was capable of transporting Cl⁻ ions from the outside to inside even when the inside and outside bathing solutions were of the same composition. He considered this phenomenon to represent an active transport of NaCl.

The effects of cyanide on the electrical potential across isolated frog skin were observed by Amberson (1936), who showed that if both the inside and outside bathing solutions were of the same concentration, cyanide caused the P.D. (potential difference) to drop to zero. If the outside solution was more dilute than the inside, cyanide caused a reversal of polarity. He postulated that this was so because the non-metabolically active skin is more permeable to Na⁺ ion than to Cl⁻ ion. Krogh (1937) exposed frogs to repeated changes of distilled water for several days to "wash out" part of the animals' chlorides. He then placed these

"chloride deficient" frogs in dilute NaCl solutions and was able to measure a drop in the NaCl content of the outside medium even though it was far more dilute than the internal medium of the frog. In this manner, Krogh was able to demonstrate an uptake from solutions as dilute as 10⁻⁵ molar. In later experiments (1938), Krogh found that NaCl was taken up by the skin but that CaCl₂ or KCl were not. Katzin (1940), using radioactive sodium, showed that isolated frog skin with Ringer's solution on both sides is capable of transporting Na⁺ ions to the inside. Stapp (1941) and later Lund and Stapp (1947), utilizing lead-lead chloride electrodes to short-circuit the inside and outside bathing solutions, were able to obtain short-circuit currents averaging about sixteen microamperes. They did not relate this current to ionic movement.

Meyer and Bernfeld (1946) discussed a potentiometric method of analyzing ion selectivity, ion dissolving power, and ion mobility. They also analyzed frog skin potentials. Although their conclusion that the P.D. is due to the difference of hydrogen ion concentration on both sides of the skin was erroneous, their technique of analysis could very well have laid the groundwork for Ussing's classical work on frog skin.

Ussing's Short-Circuit Technique

Although much of the groundwork had been laid by his

predecessors, Ussing must be given credit for elucidating the true mechanisms responsible for the frog skin potential. He (Ussing, 1949a) was the first to attempt to quantitate Na⁺ ion movement across frog skin by the use of radioisotopes. He also showed that Na⁺ ion transport inward varied directly with the pH of the inside solution, whereas the pH of the outside solution had little effect on Na⁺ ion transport at values above pH 5. At pH values of the outside solution lower than 5, Na⁺ ion influx dropped to a very low value and Cl⁻ ion influx increased. In this same experimental series, Ussing reported a pronounced parallelism between the P.D. across the skin and the influx of Na⁺ and Cl⁻ ions.

In studies of the movement of iodide ions through frog skin he (Ussing, 1949b) found that for a freely diffusing ion such as this, the ratio between the flux in one direction and the simultaneous flux in the opposite direction was independent of the structure of the membrane. In these experiments it was shown that iodide ions diffused inwards faster than outwards under all conditions studied. No active transport of iodide ions was postulated since the P.D. across the skin was adequate to explain the difference in diffusion rates. Both influx and efflux of iodide ions showed a negative correlation to the P.D.; high P.D. values were found only when the iodide ion permeability was low.

A milestone in the study of active transport of Na+ ions

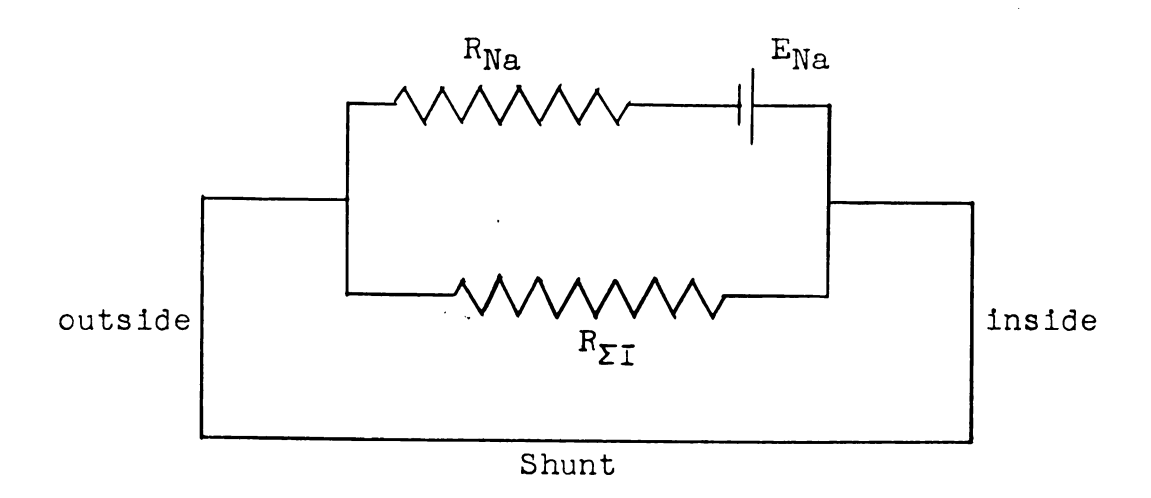
by frog skin occurred with the development of the shortcircuit technique (Ussing and Zerahn, 1951). If a P.D. exists across isolated frog skin where several ions are present in equal amounts on either side. it would be difficult to determine the contributory role of these ions to the P.D. Although radioactive tracers could be used. Ussing and Zerahn solved the problem by reducing the P.D. across the skin to zero by applying a voltage equal to the P.D. produced by the frog skin but opposite in polarity. Since the solutions bathing both sides are identical, net transfer of passive ions would not be expected to take place. ions subject to active transport would continue to move in one direction. The current flowing in the short-circuit loop would be the resultant of all the net active transport processes. Under short-circuit conditions, if the current is greater than the net rate of Na⁺ ion flow inward (both expressed in similar units such as coulombs per hour), other processes in addition to Na ion transport would be contributing to the current and presumably to the voltage. Conversely, if the current is less than or equal to the net Nat ion influx, one could justifiably consider Na+ ion transport as being the main source of current and potential. (The short-circuit technique will be covered in greater detail in the Materials and Methods section.)

By employing the above technique, Ussing and Zerahn (1951)

determined that under normal conditions with Ringer's solution on both sides of the skin, the Na⁺ ion influx is on the average 105 per cent of the current, while the efflux is about 5 per cent of the current. Thus the current was equal to the net active transport of Na⁺ ions. They determined the influence of Cu⁺⁺ ions, epinephrine, neurohypophyseal hormone and CO₂ upon Na⁺ ion flux and total current values obtained on isolated frog skin. The effects of these and other agents are summarized in Appendix A.

In addition to the above, Ussing and Zerahn (1951) used the voltage clamp technique to study the effect of P.D. on Na⁺ ion transport. They maintained the potential across the skin at a series of levels by adjusting the external voltage. The results indicated that with increasing potential, the influx diminished and the outflux increased in magnitude. Although their results showed considerable variability, it appeared that influx and efflux became equal at a potential of about 110 mV (millivolts). These authors suggested that such a P.D., just sufficient to equalize influx and efflux, represented the maximum force that can be exerted by the Na⁺ ion transport mechanism under a given set of conditions. They also proposed an equivalent circuit diagram for the short-circuited frog skin shown in figure 2 and derived the basic formula involved in active Na⁺ ion transport to be:

Figure 2. Equivalent circuit representing the short-circuited frog skin (Ussing and Zerahn, 1951)



 E_{Na} - E.M.F. of sodium transporting mechanism

 ${\tt R}_{\tt Na}$ — resistance to the sodium current

 $R_{\Sigma T}$ - resistance to passive ions

Shunt - net effect of the applied E.M.F.

$$\frac{M_{\text{in}}}{M_{\text{out}}} = e^{-\frac{zF}{RT}} \cdot E_{\text{Na}}$$

$$E_{\text{Na}} = \frac{RT}{zF} \ln \frac{M_{\text{in}}}{M_{\text{out}}}$$

where:

 $M_{in} = Na^{\dagger}$ ion flux inward R = gas constant

 $M_{out} = Na^{+}$ ion flux outward T = absolute temperature

z = ionic charge E_{Na} = P.D. across skin due

F = Faraday constant to Na⁺ ion active transport.

Hodgkin, Huxley and Katz (1952) have presented data pertaining to current-voltage relations in the membrane of the giant axon of Loligo. The similarity of this work to frog skin short-circuit technique was that both experiments utilized the voltage clamp procedure. Hodgkin et al. attributed this procedure to Cole (1949) and Marmont (1949).

Chloride Ion Movement across Frog Skin

Koefoed-Johnsen, Levi and Ussing (1952) showed that the movement of Cl⁻ ions across isolated frog skin could be explained on the basis of the electrochemical potential gradient. The flux ratio for Cl⁻ ions as determined by tracers turned out to be of the same magnitude as that calculated for a passively diffusing monovalent negatively charged ion.

Koefoed-Johnsen, Ussing and Zerahn (1952) demonstrated that epinephrine stimulation of frog skin aroused an extra source of electric current, which amounted to approximately ninety per cent of the Na⁺ ion current. The determination of influx and efflux of Cl⁻ ions utilizing Cl³⁶ and Cl³⁸ indicated that the non-sodium current evoked by epinephrine stimulation of the skin was due to active transport of Cl⁻ ions in an outward direction. It was concluded that this active outward Cl⁻ ion transport during epinephrine stimulation was performed by the mucous glands of the skin.

Electrical Potential Gradients across Frog Skin

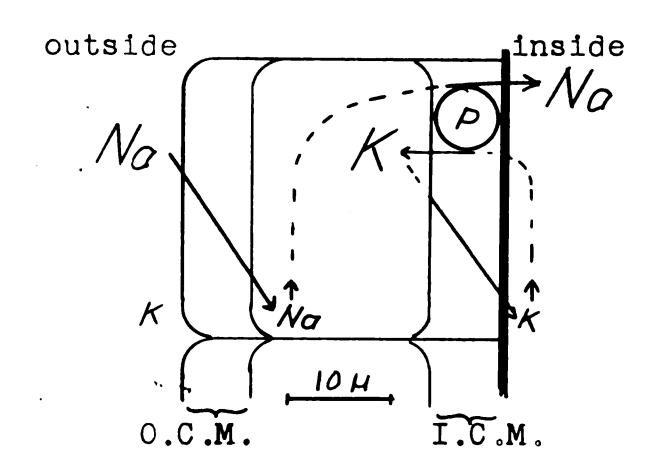
Ottoson et al. (1953) determined that the removal of the corium layer had little effect on the resting potential of the skin. However, even slight damage in the dermoepidermal junction region caused a marked decrease of the potential. This group concluded that the main part of the skin resting potential is located across the submicroscopic membrane which demarcates the epithelium from the connective tissue of the corium. Linderholm (1954) also assumed a single membrane to be the major diffusion barrier in frog skin. Hoshiko and Engbaek (1956) and Engbaek and Hoshiko (1957) reported that in most instances, the total skin potential (73 to 145 mV) was reached in two, rarely three, distinct potential jumps. Comparison with measurements of the frog skin thickness indicated that the site of the first

jump is in the epidermis whereas the second potential jump corresponded to the junction between the epidermis and the corium. The electrical potential profile of the isolated toad bladder was also reported as being a two-step profile (Frazier, 1962).

Koefoed-Johnsen and Ussing (1956; 1958) reported that the outward facing side of the skin behaved like an almost ideal sodium electrode over a wide range of sodium concentrations (1-120 mM), whereas the inward facing side of the skin behaves like a potassium electrode. Under these conditions, the skin potential thus seems to be the sum of a sodium diffusion potential and potassium diffusion potential. They proposed the model presented in figure 3.

Hoshiko and Ussing (1960) tested this model further. They reasoned that if Na²⁴ were suddenly added to the solution bathing one side of the skin, the isotopic flux or the rate of appearance of radioactivity in the opposite bathing solution would increase exponentially with time to a final steady state value. In twenty-three out of twenty-four experiments, the data could be fit by a single exponential curve plotted against time. The average half time of 3.9 minutes for flux build-up was similar for frog skin, toad skin and toad bladder. These observations correlated with the skin model of Koefoed-Johnsen and Ussing (1958) who visualized a large number of identical compartments (stratum

Figure 3. Proposed model of Na⁺ ion transport across frog skin stratum germinativum layer (Koefoed-Johnsen and Ussing, 1958).



- O.C.M. outer cell membrane passively permeable to Na⁺ ions
 I.C.M. inner cell membrane passively permeable to K⁺ ions
 P pump
- 1. The transporting epithelial cells have a high concentration of K^+ ions and a low concentration of Na^+ ions.
- 2. The outward-facing membrane of the cells is impermeable to all cations except Na⁺ ions and Li⁺ ions.
- 3. The inward-facing membrane of the cells is permeable to K⁺ ions, while the permeability to free Na⁺ ions (as distinguished from Na⁺ ions passing through the "sodium pump") is extremely low.
- 4. The active sodium transport mechanism is located at the inner border, and should possibly be considered a forced exchange of Na⁺ ions from the cells against K⁺ ions from the inner solution. (H⁺ ions might to some extent substitute for K⁺ ions.)

germinativum cells) in parallel that contained a single pool. They felt such a single sodium pool concept was in agreement with the finding that a single exponential curve suffices to describe the time course of Na²⁴ flux across either skin or bladder. They reasoned that such a time course would not be expected if diffusion through the interspace between cells were the limiting step. Their minimal estimate of the sodium pool size was 6.07 µeq/cm², an amount much too large to be located in the 250 A thick basement membrane, the site proposed by Linderholm (1954). They then concluded that the actively transported sodium passes through and not between cells.

Hoshiko (1960) reported that almost all skin resistance was located across the outer potential barrier of the stratum germinativum cells, indicating that the presumed Na^+ ion permeability of the outer border is much lower than the K^+ ion permeability of the inner border of the skin epithelial cell.

Gatzy and Clarkson (1962) stated that the serosal surface of toad bladder is permeable to K^{+} ions, while the mucosal surface is predominantly permeable to Na^{+} ions.

Scheer (1962) applied the methods of irreversible thermodynamics to the problem of steady state linear diffusion and concluded that the flux across any system of parallel membranes or phase boundaries can be expressed as a linear function of the differences of electrochemical potential

across the system.

To date, no explanation of sodium transport based on the endoplasmic reticulum (Brachet, 1961; Robertson, 1962), the extensive cavities, sinuses and canals that run throughout the typical cell, has been proposed. In addition, no information has been found relating possible correlation between pinocytic microvesicles (Holter, 1960) and movement through cells.

Metabolism and Active Transport

The active transport of Na ions across frog skin requires metabolic energy derived from oxidative metabolism.

Zerahn (1956), in correlating O_2 consumption with Na⁺ ion transport, measured O_2 consumption when non-sodium ions were substituted in the outside bathing solution and subtracted this value from that obtained when the skin was transporting Na⁺ ions. The consumption of O_2 observed when the skin was transporting Na⁺ ions increased at a rate that was proportional to the active transport rate of Na⁺ ions. His data showed a transport of approximately 18 Na⁺ ions per molecule of O_2 utilized. This ratio held rather constantly over varying rates of Na⁺ ion transport.

In the absence of O₂, active Na⁺ ion transport drops off rapidly but generally never reaches zero. Leaf and Renshaw (1957) noted an increase in lactic acid production under conditions of anoxia and hypothesized that glycolysis

could provide energy under such conditions.

Leaf et al. (1957) reported that the mean net Na⁺ ion flux across the bladder wall measured with radioactive isotopes, Na²⁴ and Na²², just equalled the simultaneous short-circuit current. Under anerobic conditions the mean net Na⁺ ion flux was found to be slightly less than the short-circuit current.

Huf et al. (1957), in their study of the effects of O_2 consumption and metabolic inhibitors and drugs on Na^+ ion transport across isolated frog skin, reported that the inhibition of net NaCl transport was found to be accompanied by decrease, increase, and unaltered O_2 consumption and, as a result, they did not calculate sodium to oxygen ratios. Their technique of inhibiting Na^+ ion transport with metabolic inhibitors such as fluoroacetate may have contributed to the variability of the data.

Hokin and Hokin (1960) presented data supporting the hypothesis that phosphatidic acid participates in a cyclic carrier mechanism for the transport of Na⁺ ions across the apical membranes of the avian salt gland.

Kirschner (1953) reported that inhibitors of cholinesterase inhibit active Na⁺ ion transport in frog skin. These inhibitors were more effective when applied to the "inside" of the frog skin. It was later shown (Kirschner, 1955) that atropine, tubocurarin, histamine and pilocarpine were powerful stimulants of active transport when they were added to the "outside" of the skin, but showed little stimulatory effect when added to the inside.

Koblick (1958) estimated that more than ninety per cent of the skin cholinesterase was located in the tela subcutanea, a cellular layer that constitutes the internal surface of the dermis. Later, he (1961) isolated materials that exhibited acetylcholine activity from frog skin.

Skjelkvale et al. (1960) described a simple method for complete separation of the epithelial layer from the corium in frog skin. Their metabolic studies on this isolated epithelium and its homogenate pointed to the operation of the Krebs cycle. Citrate, α -ketoglutarate, succinate, and fumarate, which led to stimulation of 0_2 consumption of the epithelial homogenate, could indicate that through the operation of the Krebs cycle, malate and oxaloacetate were formed for pyruvate consumption via the citric acid cycle. When the only substrate present was pyruvate, the 0_2 consumption was not stimulated greatly.

In the toad urinary bladder, the decline in Na⁺ ion transport was prevented or sharply reversed by glucose, pyruvate and lactate (Maffly and Edelman, 1961). In the same study, iodoacetate inhibited Na⁺ ion transport, but lactate delayed its onset and reduced the degree of this inhibition.

Huf et al. (1962) stated that electron transport, oxidative phosphorylation and active ion transport in frog skin are intimately related processes.

Spectrofluorometric studies have enabled identification of RPN (reduced pyridine nucleotide) in the intact toad bladder. The same experiment showed that measurements of short-circuit current with pyruvate or succinate as a substrate indicated the initiation of a rapid drop in sodium transport at the point of ADP addition. The changes occurred pari passu with RPN oxidation and the acceleration of oxygen consumption. Vasopressin increased the reduction of pyridine nucleotide after the acceleration of Na⁺ ion transport. This indicated that sodium could be acting as a metabolic pacemaker (Canessa et al., 1962).

In summary, it appears that energy for the active transport of Na⁺ ions across frog skin can be derived from the aerobic citric acid cycle or to a lesser extent from the anerobic Embden-Meyerhof pathway.

Water Movement across Frog Skin

One would assume that if water penetrates a membrane passively, the fluxes of water from side I to side II of the membrane and from side II to side I would be proportional to the water activities in the solutions bathing sides I and II respectively. However, Hevesy, Hofer and Krogh (1935), measured frog skin permeability by both osmosis and the

diffusion rate of D₂O (heavy water) and found that the net uptake of tap water measured directly by volume change was three to five times higher than the values calculated from either the heavy water flux or the difference in the osmotic pressure across the skin. They theorized that water transfer across frog skin was due to the osmotic pressure difference because frogs placed in isotonic glucose did not take up water while those sitting in tap water did. In opposition to this theory Huf (1937) demonstrated the presence of a net water transport through frog skin with Ringer's solution on both sides.

Ussing (1952) proposed a hypothetical explanation of the above findings: "If water penetrates a membrane through pores an osmotic or hydrostatic pressure difference across the membrane will cause a bulk flow of water through the pores. If so, molecules going in the direction of flow will be speeded up, whereas molecules moving in the opposite direction will be slowed down, thus making the ratio between influx and outflux different from the ratio of outside and inside activity of water." The actual transport of sodium ions through the skin could provide an additional force bringing about water transfer, which would be created by the flow of sodium and chloride ions through narrow pores. Ussing termed this a simple "drag effect."

In a later paper (Koefoed-Johnsen and Ussing, 1953),

the pore theory was further developed. In this experiment. a 0.1 Ringer's solution was placed on the outside of the skin and normal Ringer's on the inside. Neurohypophyseal extracts increased the net transfer of water by 100 to 200 per cent and also increased the net Na⁺ ion transport across the skin. However, the inward flux of water as measured by the amount of DoO passing through was little affected by the hormone. They hypothesized that neurohypophyseal hormones act by increasing the pore size in some layer of the skin without increasing the total area available to diffusion. "In other words if the total area remained constant the diffusion of water - as opposed to the net flow measured osmotically - would be unaffected, whereas the flow - to which Poiseuille's law of flow might be applicable - would be favored by the increase in diameter of the pores." (Davson, 1959). Koefoed-Johnsen and Ussing (1953) hypothesized that small pores possibly were able to fuse together, creating a larger pore, but with no change in the actual pore area available for diffusion. The validity of this explanation depends on whether an osmotic pressure can really be considered in the same light as hydrostatic pressure (Davson, 1959).

The calculation of permeability coefficients from the inward movement of D_2O has produced values that were significantly lower than those obtained by directly measuring

slight volume changes in many different biological situations. The explanations of these results have not always agreed with those of Ussing's.

Capraro and Bernini (1952) discussed this same phenomenon prior to the time Ussing's group reported it, but concluded that neurohypophyseal hormone produced an active transport of water possibly coupled with a decreased permeability to water diffusion in the opposite direction.

Prescott and Zeuthen (1953) used both D_20 and direct volume change measurements to determine permeability constants of numerous amoebae, fish eggs and amphibian eggs. In all cases the permeability constant was greater when determined by volume changes. Kitching and Padfield (1960) reported that D_20 penetrates ciliates less rapidly than does H_20 .

Hodgkin and Keynes (1955) studied the movement of K⁴² across DNP poisoned giant nerve axons. Using a voltage clamp technique to vary the potential, they compared flux ratios across the axon with those predicted by the equation derived by Ussing (1949b) for independent passive transport of ions such as potassium. When the nerve was at equilibrium, that is, when not clamped, the fluxes measured conformed to those predicted by Ussing's equation. It was found, however, that under voltage clamp conditions there were wide ranges of deviation from the predicted values. The isotopic technique

showed flux ratios varying as much as 100 times from the predicted values. Hodgkin and Keynes explained these variations, which were quite analogous to those obtained by Ussing, as being the result of molecular interaction. Their model considers that ions moving through a small pore of molecular dimensions would be forced to do so in single file. An isotopic ion striking the pore would dislodge one at the other end of the pore. If an ion struck the pore from the opposite direction, the radioactive ion would be dislodged. After the isotope first entered the pore, it would have to be followed by another molecule going in the same direction to be able to remain in the pore. Hodgkin's and Keynes' explanation of why flux ratios were as predicted under non-clamp conditions was simply that both fluxes were much lower than the actual K' ion exchange taking place, but the per cents of flux in both directions were equal.

This group modified Ussing's formula to include the number of molecules in the pore:

$$\frac{\text{Influx}}{\text{Efflux}} = e^{-\frac{n'F}{RT}} (E - E_K)$$

where:

n' = number of molecular sites in pore

E = P.D. across the membrane

 $E_{K} \ = \ \mbox{equilibrium potential for potassium}$ Their data gave a value of n' equal to 2.5, although they

cautioned against placing great reliance upon this numerical figure in view of the considerable scatter of results.

Anderson and Ussing (1957) measured relative fluxes of S^{35} and C^{14} labeled thiourea and acetamide across frog skin in the presence of a continuous osmotic flow. They demonstrated that the drag force exerted by water is proportional to the osmotically induced rate of net water transfer across toad skin and that the ratio between the drag effects on the two substances is equal to the inverse ratio between their respective free diffusion coefficients. They used these observations to support their hypothesis that toad skin contains a porous layer and that neurohypophyseal hormone increases the permeability to both solutes and water by increasing the pore size in this porous layer.

Lindley and Hoshiko (1962) determined the effects of a 100 per cent solution of D_2 0-sulfate Ringer's solution on frog skin potential. They reported a 70 per cent decrease in potential when the D_2 0-sulfate Ringer's solution was on the outside, a 27 per cent decrease when it was placed in the inside, and a 47 per cent decrease when it was used for both bathing solutions. This change of potential was reversible even after one hour of exposure to the D_2 0. They reported that there was a net water flow from the water-Ringer's into the D_2 0-Ringer's solution that took place across frog skin as well as across Visking membranes. They

concluded that D_20 was osmotically active and that the depression of skin potential following exposure of the outside surface to D_20 was in large part due to a solvent drag effect.

One should not consider heavy water (D₂O) as being the same as ordinary water (H₂O) since its physical properties differ greatly. Deuterium has twice the mass of ordinary hydrogen; heavy water has a 10 per cent higher density, and a 25 per cent greater viscosity than does water. Its freezing point (4 O) and boiling point (1 O) are both distinctly higher. Many salts and some gases, including carbon dioxide and oxygen, are less soluble in heavy water, and acid solutions of D₂O are distinctly more acid than corresponding solutions of H₂O (Katz, 1960).

Because a universally accepted model of water transport has not been resolved, considerable interest is still present in the study of water movement. Leaf (1960), studying the actions of neurohypophyseal hormones on toad bladder, reported that the action of the hormone in enhancing the movement of water and urea through the membrane is a passive phenomenon, and could be attributed to a simple dilatation of aqueous channels.

Sidel and Hoffman (1961), using two aqueous phases (0.1 molal and 5.0 molal NaCl), separated by a liquid non-aqueous mesityl oxide membrane, produced greater net water movement

than predicted by the Ussing flux ratio. These investigators hypothesized that the deviation was due to a difference in water content at the two interfaces.

Ussing (1960b) measured volume changes in frog skin epithelium to show that the outward facing boundary of the epithelium was much less permeable to water than the inside. He also determined that antidiuretic hormone or oxytocic hormone when added to the inside bathing solution increased the water permeability of the outward facing boundary of the epithelium.

Clarkson (1962) concluded that NaCl and water share a common pathway of absorption which allows strong frictional interaction between the flows of salt and water across the isolated rat ileum.

Other investigators (Peterson and Edelman, 1962) produced experimental results that indicated water and urea migrate through the same passages, but raised the possibility that ADH stimulates Na⁺ ion transport directly rather than by altering Na⁺ ion permeability of the cell surface. They also raised the possibility that calcium inhibition of ADH may be due to competition for binding sites on the membrane. Contrary to this, Curran et al. (1962) and Curran and Gill (1962) obtained experimental data that suggested that the Na⁺ ion permeability of the outer membrane may control the rate of Na⁺ ion transport across the skin. They reported that

calcium caused a decrease in permeability, pool size, and net Na^+ ion transport.

There is still some controversy regarding water movement across permeable membranes. The rate of water movement, or flux, when determined by actual volume changes, was greater than when it was calculated by D₂O dilution techniques or based on osmotic pressure differences. Two explanations have been presented to account for this. Ussing's group has introduced the concept of solvent drag whereby ions moving through a pore will enhance water movement through the pore in the same direction as ion movement. In frog skin, both Na⁺ ions and Cl⁻ ions are moving into the skin and thus presumably drag water in with them. Although such an explanation is entirely plausible, it doesn't explain why D₂O calculated values are lower than those obtained by direct volume change measurements.

Hodgkin and Keynes provide a good explanation of why D_2O or isotopically calculated water flux values are less than those obtained by direct measurement of volume changes. In their model, ions must move single file through membrane pores that are only slightly larger than the ion itself. A labeled molecule entering one end would be displaced by a collision on the opposite end. In order to remain in the pore, a labeled ion must be struck by an ion also traveling in the same direction. If the opposite end of the pore were

struck, the labeled ion would be displaced.

Probably both of the above models could be present in biological membranes.

Other Frog Skin Experiments

Numerous other experiments have been conducted using frog skin. The effects of temperature have been investigated. Huf and Doss (1959) showed NaCl transport to be maximal at 20° C. and 02 consumption to be decreased when the temperature was lowered from 28° C. to 10° C. Karger (1962) and Karger and Krause (1962) reported that raising the temperature from 14° C. to 20° C. produced a large rise in the P.D. that was of a transitory nature, lasting approximately one hour. A similar rise but of shorter duration was observed at higher temperatures. Lowering the temperature from 20° C. to 14° C. produced a temporary drop in potential of nearly one hour's duration.

Brown (1962) compared <u>in vivo</u> short-circuit Na⁺ ion transport techniques with <u>in vitro</u> measurements of Na⁺ ion transport made on the same skin. He reported that the average short-circuit current as determined by <u>in vitro</u> measurements was 63 per cent of that determined by <u>in vivo</u> methods and that the average <u>in vitro</u> potential measurement was 73 per cent of that obtained by the <u>in vivo</u> technique.

Hoshiko and Seldin (1962) developed a technique to observe the secretion of frog skin glands with the aid of

a microscope. They reported that the presence of SO4⁼, I⁻, Li⁺, or Mg⁺⁺ ions in the internal bathing solution greatly reduced secretion by the skin glands.

Huber and Phillips (1962) reported that there was a response elicited in the short-circuit current of frog skin by products of <u>V</u>. cholera. They identified at least two components of the active melange, one enhancing frog skin potential and short-circuit current, the other inhibiting these properties.

Hoshiko (1961) in comparing the properties of frog skin with those of the nerve, concluded that Na⁺ ion selectivity of the outside surface of frog skin appears somewhat different from the selectivity of active nerve or muscle membrane.

Magnetic Effects in Biology

Constant or slowly varying magnetic fields are not detected directly by any of the human senses. As such, magnetic fields are different from other physical agents, many of which act as external stimuli. Light, sound, heat, pressure, acceleration, gravitational forces, electric potentials and chemicals - all may be perceived directly by at least one of the human sensory organs. There is no theoretical reason for this insensitivity to magnetic fields (Ackerman, 1962).

Magnetic Field Effects upon Animal Orientation

Brown and his group of investigators (Brown, Brett and Webb, 1959; Brown, Bennett and Brett, 1959; Brown, Webb, Bennett and Barnwell, 1959; Brown, Brett, Bennett and Barnwell, 1960) have intensively studied the effects of magnetic fields on snail orientation. These studies represent continuing investigations to support Brown's concept (1959) that during the timing of cycle lengths of the rhythms in animals and plants in so-called "constant conditions," the organisms are still continuously receiving information from the external environment about the natural geophysical cycles.

These workers measured the average amount of clockwise or counterclockwise turning of snails as they traversed a 3-cm. course immediately following their emergence from a straight, narrow corridor into an illuminated, symmetrical, constant field 9 to 10 times stronger than the normal magnetic field. Experimental results indicated that the mean paths of snails were statistically significant to the left of the controls, particularly between the hours of 7 a.m. through 9 p.m. Also, the mean amount of turning, either clockwise or counterclockwise, was increased significantly over that of the controls; this increase also followed a daily rhythm.

This same group (Brown, Webb and Brett, 1960) reported

that the mean amount of turning in snails initially directed southward displayed a lunar-day rhythm, with minimum turning about the time of moonrise and maximum turning at lunar nadir. This group concluded that the specific character of the lunar-day rhythm of the response to the experimental magnetic fields gave further support for the view that magnetic fields are normally involved in snail orientation.

Brown, Bennett and Webb (1961) stated that snails were able to differentiate between directions of weak magnetic fields. The relative influence of the experimental N-S and E-W magnetic fields displayed both solar-daily, lunar-daily, and semi-monthly rhythms. They concluded that the solar and lunar clock-regulated discriminatory responses for magnetic fields indicate the snail to be significantly oriented as if by internal magnetic compass needles, which in turn are hands of horizontal solar and lunar day "clocks."

Physiological Changes Induced by Magnetic Fields

Among the most spectacular of all results claimed in the field of biomagnetism are those described by the Barnothys' (Barnothy, Barnothy and Boszormenyi-Nagy, 1956; Barnothy and Barnothy, 1958; M. F. Barnothy, 1959; J. M. Barnothy, 1959), all of which have been incorporated into a single review article (Barnothy, 1960).

Mice were confined in a plastic cage, 3.5" by 1.4" in dimension, and placed in a magnetic field with the following

results:

(1) Development:

A pregnant female mouse exposed to a 2500 gauss field gave birth to healthy young, but they remained 20 per cent smaller than normal throughout life. When pregnant females were exposed to 3100 gauss, the newborn lived for only a few days, and when the dose was raised to 4200 gauss, the embryos were reabsorbed into the uterus.

(2) Mortality:

Mice placed in the field before puberty were capable of adaptation to the field and were capable of withstanding even the strongest homogeneous or inhomogeneous fields.

Male mice who had passed puberty died when placed in high field strengths while female mice were unaffected.

(3) Body temperature:

Rectal temperatures dropped $0.8\pm0.1^{\circ}$ C. during magnetic exposure and remained at that level for approximately one month following exposure.

(4) Activity:

In mice between the ages of six weeks and one year, a 50 per cent increase in activity was reported.

(5) Food consumption:

After exposure to 4200 gauss, mice ate 14 per cent less than the controls during the remainder of their life spans, but during exposure, their food intake was slightly greater

	:
	;
	:
	ŧ
	;
	•
	•
	:
	Ş
	â
	:
	<i>†</i>
	£.

than that of the controls.

(6) Appearance:

C₃H strain mice did not age as rapidly as the control mice. After 400 days of age the fur of the experimental animals presented a smooth, youthful appearance. The difference in appearance and behavior was so striking that "persons unfamiliar with mice could pick out the experimental subjects from the controls." These mice had been exposed to 4200 gauss for 4 weeks. The final examination was conducted one year after the exposure was completed.

(7) Fertility:

The estrus cycle disappeared when mice were exposed to magnetic fields exceeding 3000 gauss, but it reappeared immediately after removal from the field. Female mice who were kept in a 5500 gauss field for 4 weeks became pregnant immediately after they were removed from the field. A homogeneous field of 4200 gauss reduced the fertility of C57BL/G strain mice. An inhomogeneous field of 3000 gauss prevented fertility between exposed females and exposed males, but either were capable of producing offspring when mated with unexposed animals.

(8) Hematologic changes:

The erythrocyte count of mice exposed to 4200 gauss for 3 to 6 weeks was unaffected. The segmented leucocyte

count, however, was reduced 30 to 40 per cent during the first ten days and remained so during the time of exposure. After removal from the field this count rose to as much as 100 per cent of the pre-exposure level, but returned to the original within three weeks time.

(9) Radiation syndrome:

Since X-ray irradiation decreases, while magnetic irradiation increases the leucocyte count, the effect of magnetism on the radiation syndrome was tested. At an X-irradiation dose causing death to 30 per cent of the controls, none of those died that were exposed to magnetic fields of the same magnitude and duration as for the hematologic studies. However, when the X-irradiation dose was increased to cause an 80 per cent mortality of the controls, the magnetically exposed mice suffered only slightly less mortality.

(10) Pathological changes:

The liver weight of male mice that died as a result of exposure to 4000 gauss was only 50 per cent of that of the controls. Also neoblasts were found in the spleen of 8 out of 9 animals examined.

(11) Tumors:

J. M. Barnothy (1959) reported that white mice of the same litter, inoculated with T2146 adenocarcinoma, showed complete recovery in 80 per cent of the cases if kept in a field of several thousand gauss strength; against 100 per

cent mortality of the controls. Also the C₃H strain, which has a 98 per cent expectancy of spontaneous mammary tumors, showed a considerable delay in the occurrence of the mammary tumor and a parallel increase in their average life span, when treated for several weeks in magnetic fields at an early age. In his 1960 review article, the same author stated that pathologic examinations showed magnetic fields prevent metastasis even in cases when it could not prevent the growth of the primary tumor.

Eiselein et al. (1961) were unable to repeat the Barnothys' results. This group used a large air core electromagnet with a core large enough to accept a stainless steel container capable of containing up to 80 mice. The field strength along the long axes of the magnet core varied from 8800 to 14400 gauss. Movements of the animals were not restricted. The magnet was operated continuously twenty-four hours per day during the experimental periods. The results of the Eiselein group follow:

(1) Ascites tumor growth:

One-hundred-forty white Swiss female mice were injected intraperitoneally with 1 x 10^6 ascites tumor cells. Half were exposed to the above described magnetic field intensities. The growth rate of the ascites tumor was not significantly altered by the magnetic field. Also, the mean survival time of the 12 mice living in the magnet until death

was 11.3 \pm 0.8 days, while that of nine control animals left alone until death was 13.1 \pm 1.2 days.

(2) Growth rate:

The mice maintained in the magnet did not show a significant change in growth rate when compared with the growth rate of the animals in the control cage.

(3) Blood counts:

No significant alterations in the white blood count, differential blood count, hematocrit, red blood count, or liver and spleen weights were observed.

In summation, Ackerman (1962) commented that "No changes reported in the past due to magnetic fields have ever been confirmed."

A discussion of some of the physical aspects of magnetism may be found in Appendix B,

MATERIALS AND METHODS

Frog Procurement and Holding Facilities

Leopard frogs, <u>Rana pipiens</u>, obtained from Steinhilber Inc. of Oshkosh, Wisconsin, were used in this study. These frogs were held at 13.5° C., under constant illumination in stainless steel containers, and were continuously exposed to a fine spray of water. This procedure was adopted after trying various other holding techniques. Since these were the same frogs that were used for classroom purposes, it was possible to select those that were most active and showed no indications of disease such as erythemia (Red Leg). Only female frogs were used throughout this series of experiments, and they were equilibrated to room temperature before use.

The frogs were double-pithed, placed in a glass Petri dish containing Ringer's solution and the skin was removed and mounted in the short-circuit chamber all within an elapsed period of 5 minutes. In certain procedures where a control was desirable, one skin was bisected both along the dorsal and along the ventral mid-points and each half was placed in one of the two short-circuit chambers. In cases where a separate control was unnecessary, the abdominal region of the skin was used. These skins were placed in the short-circuit chambers with the "inside" facing to the left of the apparatus as viewed from the front.

Rationale of the Short-Circuit Technique

In correlating a measured potential with ionic movement, the potential should be considered as the resultant of the passive diffusion of all ion species present plus the unique contribution of the active inward transport of the sodium ion (Ussing, 1960a). Evidence of active transport can be shown by placing similar bathing solutions such as Ringer's on both sides of an isolated frog skin membrane. If a P.D. (potential difference) were detected in such a situation, active ionic transport would be indicated. But even using radioactive ions to quantitate the amount of transport, it would be difficult to show the true relationship between active Na[†] ion transport and the output of electric energy by the frog skin when using a mixed ionic solution such as Ringer's, which is preferable for the inside bathing solution.

An obvious method for eliminating the effects of passive diffusion would be to short-circuit the two sides of the bathing solutions so that no passive diffusion of ions caused by the P.D. would take place. As discussed elsewhere, this had been tried prior to Ussing's approach by using a conductor to make the electrical contacts between the inside and outside solutions. All such systems tried still left a rather high external resistance which made it impossible to eliminate the P.D. across the skin. Ussing's (1949a) approach was to place an opposite but equal external potential across

the skin. The current flowing in the external circuit is equal to the "current" flowing across the membrane when the potential difference equals zero.

In figure 4, when the external battery voltage, EMF_{ext}, is adjusted so that voltmeter E reads zero volts, both "batteries" must be of the same potential but opposite in polarity. This circuit is analogous to connecting two identical batteries in series and then shorting them.

In the circuit of figure 5, the ammeter A_1 will have an identical reading to ammeter A_2 . Thus an ammeter in the external short-circuiting circuit will accurately indicate the net amount of active ion transport.

The Short-Circuit Apparatus

The actual equipment used is depicted schematically in figure 6 and pictorially in figure 7. Mr. Keith Irish constructed the short-circuit chamber from 1 inch and 1/2 inch lucite rods. The remaining material was fabricated by the author.

Each half of the short-circuit chamber had a volume of 25 ml., 9 ml. of which was in the reservoir (res.) and could be pipetted out at will for analysis without interfering with the experiment. Small air bubbles entering at the base of the hollow rod connecting the reservoir to the chamber proper aerated the bathing solution and also served to circulate the fluid in each half of the short-circuit chamber. Aerated.

Figure 4. Equivalent circuit of frog skin under short-circuit conditions.

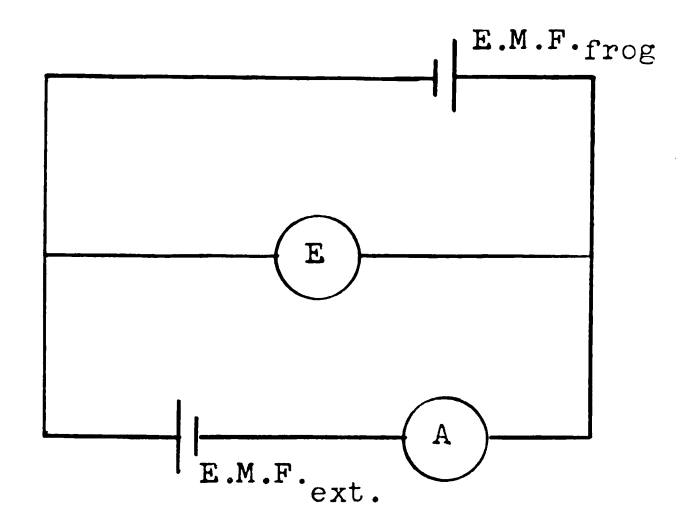


Figure 5. Two batteries connected in series and then short-circuited.

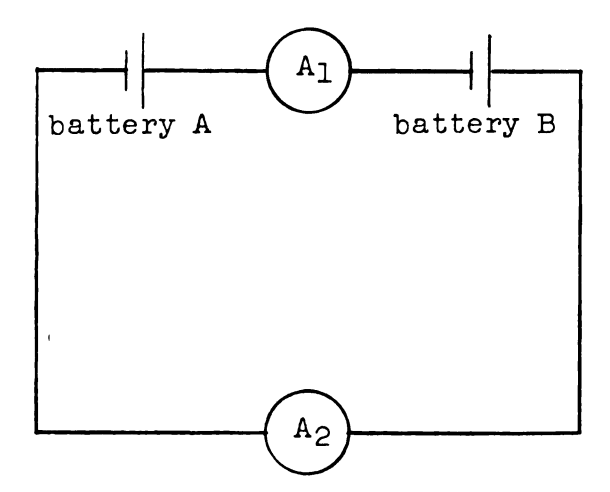


Figure 6.

AgCl - silver-silver chloride electrode

c.c. - calomel cell

c.p. - anti-splash cover

c.t. - circulation tube

 $\mathbf{E}_{\texttt{ext}}$ - external battery source

f.s. - frog skin

KCl - potassium chloride, saturated solution

μA - microammeter

mV - millivoltmeter

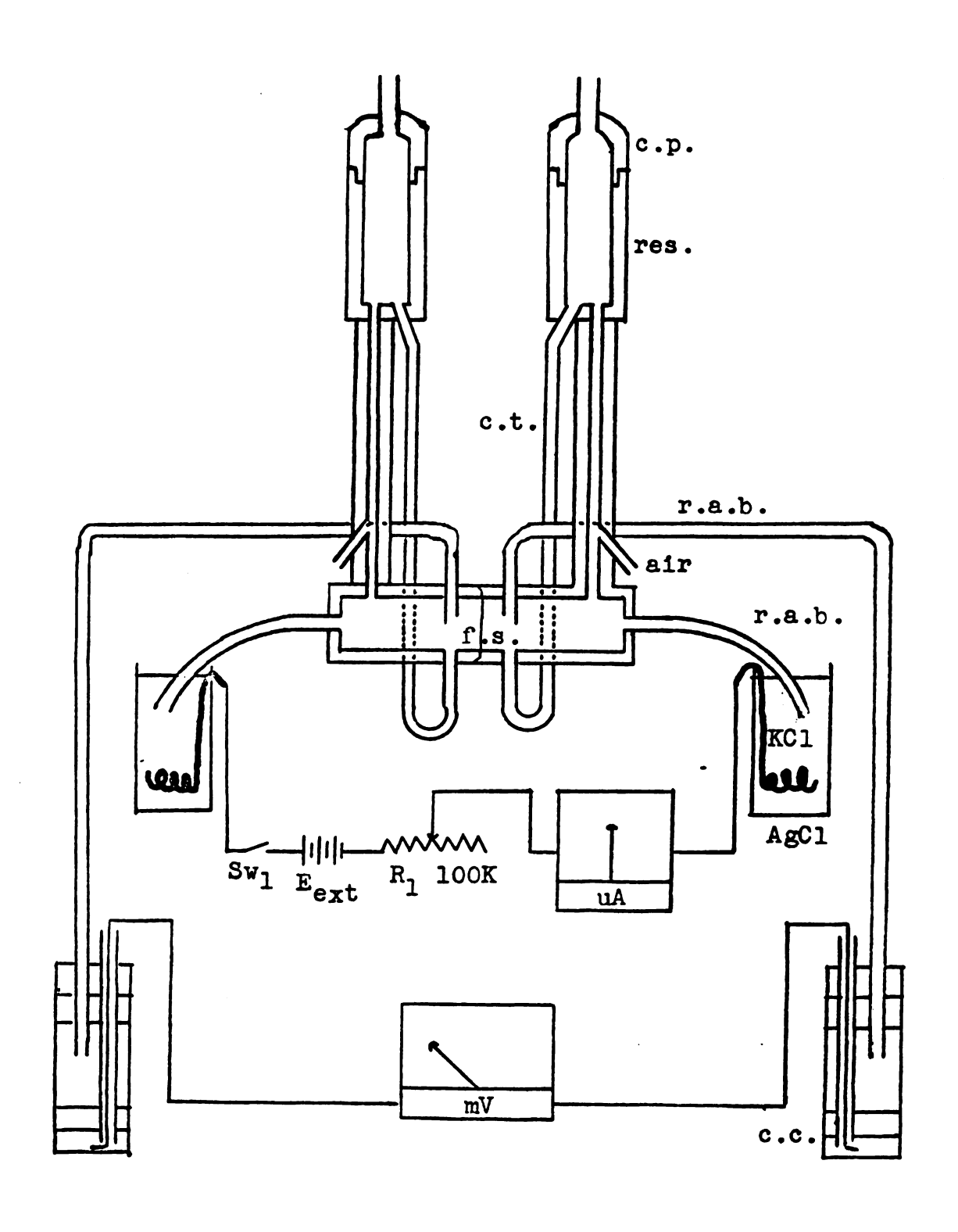
 R_1 - variable resistor, 100 kilohm

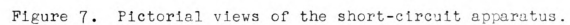
r.a.b. - Ringer-agar bridge

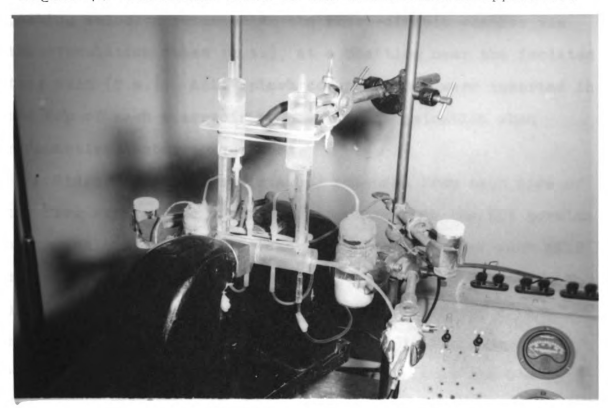
res. - reservoir

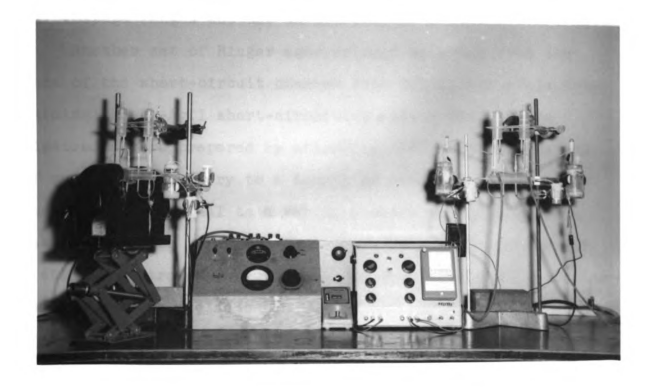
Sw₁ - short-circuiting switch

Figure 6. Schematic diagram of the short-circuit apparatus.









bathing solution returned to the short-circuit chamber via the circulation tubes (c.t.), at a position near the isolated frog skin (f.s.). Anti-splash covers (c.p.) were inserted in the top of each reservoir to prevent contamination when radioactive isotopes were used.

Ringer-agar bridges (r.a.b.) extended from each side of the frog skin in the short-circuit chamber to the KCl portion of the calomel half cells (c.c.). Construction of such half cells is described in most physical chemistry textbooks. The platinum wire in contact with the metallic mercury of the calomel cell was attached to a YSI Model 81 dual channel recorder (Yellow Springs Instrument Co.) set on the 0 - 100 mV scale. This recorder has a 1 megohm input resistance on all voltage ranges and has an accuracy of $\pm 2\%$.

Another set of Ringer-agar bridges extended from the ends of the short-circuit chamber into KCl filled vials containing the Ag-AgCl short-circuiting electrodes. These electrodes were prepared by attaching the positive terminal of an external battery to a length of clean silver wire and the negative terminal to a variable resistor which in turn was connected to a length of platinum wire. The silver and platinum electrodes were then placed in a dilute HCl solution and the current was adjusted to produce a slow rate of electrolysis. The short-circuit apparatus itself was used in this case with the current adjusted to one milliampere. In

the process of short-circuiting under actual experimental conditions, AgCl is deposited on the outside electrode while it is depleted from the inside one. To compensate for this, the electrodes were reversed each day. The remainder of the short-circuit section consisted of a switch (Sw_1) , external battery $(E_{\rm ext})$, a 100,000 ohm variable resistor (R_1) to control current flow, and a 0 - 150 microampere meter to measure the current flow. Although not shown on the schematic diagram, an additional resistance circuit was constructed so that it could be switched in series with the variable resistor. This circuit made it possible to insert any resistance from 0 to 7 megohms in series with the battery.

In actual operation, the voltage was recorded automatically by the YSI recorder. To short-circuit the frog skin, Sw_1 was closed and R_1 was varied until the voltage read zero. At this point, the microammeter reading was recorded. Calomel cells, while providing one of the most satisfactory non-polarizing electrodes, do exhibit small voltage differences between themselves. To compensate for this, it was necessary to measure the calomel difference before starting an experiment. In short-circuiting frog skin, this difference between cells was taken into account.

Source of the Magnetic Field

A large permanent magnet weighing approximately 18 kilograms was used in most of the experiments. The base of

> 01 01 7e

¥£

8]

3;

171

13

this magnet measured 9.5 cm. by 28 cm. and the maximum distance between poles was 4.5 cm. The magnetic field was measured at 3500 gauss under the homogeneous field conditions used in this experiment. Inhomogeneous fields were produced by placing differently shaped iron pieces on one of the magnetic poles.

Positioning of the Magnet

In early experiments, the magnet was maintained in a fixed position while the entire short-circuit cell assembly was moved into the magnetic field. This technique was altered, after it was observed that jarring the short-circuit cell could produce an artifact that might be errone-ously attributed to magnetic effects. In all the later experiments, the magnet was moved in and out of the experimental area with the aid of a modified automobile scissors jack. In this way the short-circuit cell was undisturbed.

In most of the experiments, the magnetic field was placed at right angles to the short-circuit chamber as illustrated in figure 8. In certain other studies, however, the magnet was placed at an angle depicted in figure 9.

The following pattern of notations was used throughout the study to indicate the particular type of magnetic field involved:

Figure 8. A homogeneous field with the magnet placed at a right angle to the frog skin.

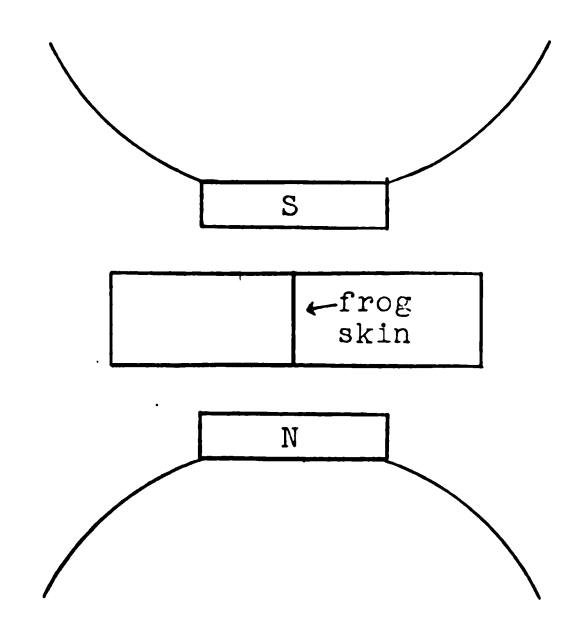
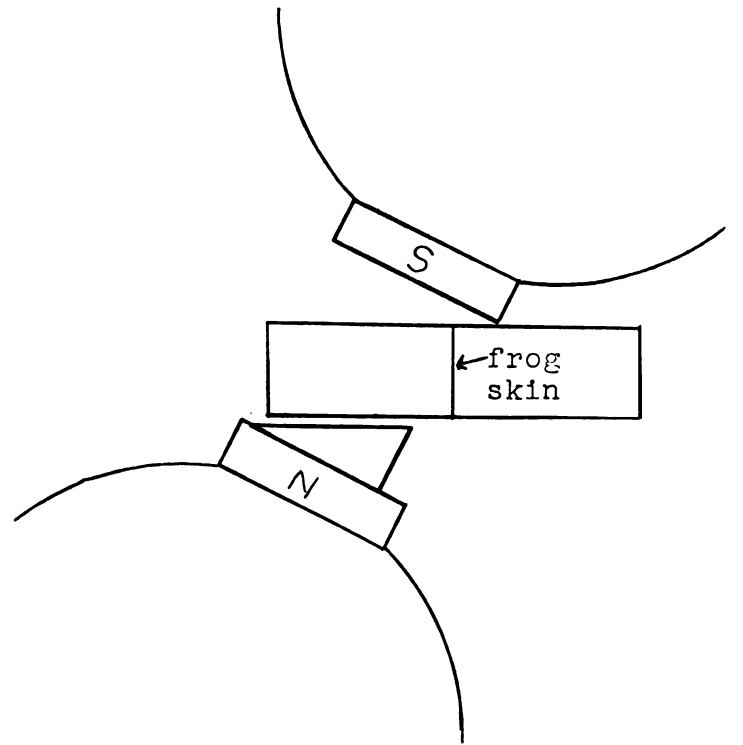


Figure 9. An inhomogeneous field with the magnet placed at an oblique angle to the frog skin.



The type of magnetic field is represented at position (1) by the letters H or U,

where:

H = homogeneous field, or

U = inhomogeneous field

The outward facing pole of the magnet is represented at position (2) by the letters N or S.

where:

N = north pole extends out towards operator, or

S = south pole extends out towards operator

The method of producing an inhomogeneous field is represented at position (3) by the following notations:

C = a solid iron cone placed on one of the magnetic
 poles, or

W = a solid iron blunt wedge placed on one of the magnetic poles, or

T = a solid iron right triangle placed on one of the magnetic poles, or

X = other means used to produce an inhomogeneous field

R + number means the magnet was reversed during the period.

The interval of time in minutes between reversals is indicated by the number. This is also represented at position (3), since the magnet was rotated in homogeneous fields only.

In those cases where the magnet was turned to form an

oblique angle to the short-circuit cell, the direction of the outward facing pole of the magnet is represented at position (4) by the letters L or R:

where:

L = outward pole turned to left, or

R = outward pole turned to right

As an example of the above notation procedure, the setup in figure 8 can be described as HN, while that of figure 9 is $^{\rm UST}_{\rm L}$.

Isotopic Techniques

The counting equipment consisted of the following components: a well-type scintillation detector, model DS 5-5, with suitable shielding, a radiation analyzer, model 1810, and a model 183 scaling unit, all manufactured by the Nuclear Instrument and Chemical Corporation of Chicago, Illinois. Use of the radiation analyzer enabled differentiation against all energy levels except that to which it was set. This instrument, with the window width set at 5 volts, was adjusted to produce a maximum count from a Cr⁵¹ standard. The efficiency of the counting equipment was maintained at a constant level during the total counting period by counting the standard at hourly intervals. If a significant change in standard count occurred, the equipment was readjusted and samples counted during such periods of malfunction were recounted.

Short-Term Biomagnetic Studies

These first studies were conducted to ascertain whether or not magnetic fields exerted any major effect on Na⁺ ion transport. The magnet was inserted for time intervals ranging from 10 to 60 minutes, then removed for a period of time, or the type of magnetic field was changed. Three experiments were conducted utilizing a single cell where the overall current-time curve itself served as the control. Four other experiments utilized an additional short-circuit chamber that facilitated the analysis of any possible magnetic effects. The magnet insertion times and duration were purposely varied in an effort to detect any subtle changes. Both homogeneous and inhomogeneous fields were studied.

Ten-Hour Biomagnetic Studies

These studies were conducted to ascertain whether or not the short-circuit current versus time relationship was affected by magnetic fields over a longer period of time. In the first four experiments, no control was used. The short-circuit current of two frog skins was studied without any magnet present, then two others were observed while continuously exposed to a 3500 gauss magnetic field. In six subsequent experiments, a control was used. Half of the skin of a single frog was placed in either chamber. In all of these experiments, the magnetic field was applied either at the start of the experiment or after approximately 100

minutes, and left there until the termination of the experiment 10 to 12 hours later.

The total short-circuit current, expressed as microampere hours, was calculated for each of the graphs.

These data are also expressed as coulombs (coulombs =
amperes x seconds). The average value of all observations
was expressed as the actual amount of Na ion transported,
calculated by the following equation:

$$W = \frac{Ite}{F}$$

where:

W = number of grams of sodium transported

I = current in amperes

t = time in seconds

e = equivalent weight

F = one faraday= 96,500 coulombs

The Effects of Higher Magnetic Fields

This experiment was conducted in cooperation with Mr. Adolph Smith of the Physics Department. Homogeneous magnetic fields of variable intensity up to 10,000 gauss were applied across the short-circuit chamber. The magnetic source was a 135 kilogram Precision Scientific Co. Model R-3 electromagnet. The spacing between poles approximated 2.2 cm. Current was applied to the electromagnet for approximately 15 seconds at values of 1, 1.5, 2, 2.5, 3, and 3.2 amperes. After the 15

second exposure, the magnet was turned off for approximately 45 seconds before going to the next higher current value. The current value of 3.2 amperes represented the maximum output of the system, approximately 10,000 gauss.

The Effects of Magnetic Fields on Neurohypophyseally Stimulated Frog Skin

Neurohypophyseal extract enhances Na⁺ ion transport presumably by increasing pore size so that Na⁺ ion movement to the active transport site is facilitated. If this movement to the site were passive, then conceivably the presence of magnetic fields could affect it. Two different techniques were utilized in studying the effects of neurohypophyseal extracts. The first consisted of equilibrating the frog skin for 155 minutes, adding 0.1 unit of Pituitrin, observing the effects and then applying the magnetic field. The second technique consisted of equilibrating the skin, applying the magnetic field across the short-circuit chamber and then adding 0.1 unit of Pituitrin to each side of the chamber. An inhomogeneous field was applied in all cases.

The Effects of Magnetic Fields on Epinephrine Stimulated Frog Skin

Since epinephrine is reputed to bring about an active transport of Cl ion in an outward direction, the addition of this hormone would enable one to observe any possible

effects of magnetic fields on active Cl ion transport.

Procedures similar to that used in the neurohypophyseal extract study were followed. In the first procedure the frog skin was equilibrated, 1 cc. of 1:10,000 epinephrine was added to each side of the chamber, the effects observed and then the magnetic field was applied. The second technique consisted of equilibrating the skin, applying the magnetic field and then adding 1 cc. of 1:10,000 epinephrine.

Again an inhomogeneous magnetic field was applied across the chamber.

The Effects of Magnetic Fields on the Increased Potential Observed after Short-Circuiting Frog Skin

A transient rise in voltage was observed following the short-circuiting of frog skin. An Esterline Angus 0 - 1 ma recorder was substituted for the Rustrak 0 - 1 ma recorder built into the YSI model 81 dual channel recorder. This was done so that a more precise record could be obtained of this transient voltage change. Observations of the increased after-potential were made with and without a magnetic field present.

The Movement of Radiochromate Ion across Frog Skin

The movement of a non-actively transported negative ion was observed using radioactive chromate ion $(\mathrm{Cr}^{51}\mathrm{O}_{4}^{=})$. In the first experiment, after suitable equilibration time, 6 µc of radiochromate ion were added to the outside reservoir

and 1 ml. aliquots were removed every 20 minutes. The magnetic field was applied 80 minutes after the radiochromate ion had been added. The second study was similar in all respects except that the radiochromate ion was added to the inside chamber.

Due to the fact that movement of chromate ion across frog skin has not been previously reported, a detailed study without the addition of any external magnetic fields was made. This series of experiments lasted 3 hours after skin equilibration. Radiochromate ion (6 µc) was added to one chamber, short-circuit current was recorded and 2 ml. aliquots were removed and counted from each side after 10, 60, 120 and 180 minutes. After this, each chamber was drained and flushed with Ringer's 5 times over a 1/2 hour period without disturbing the frog skin. Following this flushing, radiochromate ion was added to the side opposite the one in which it was placed for the first part of the experiment, and the entire procedure repeated.

An effort was made to ascertain in what form the Cr^{51} existed after it had crossed the frog skin. At the termination of one experiment in which the $\mathrm{Cr}^{51}\mathrm{O}_{\downarrow}^{=}$ ion had been added to the inside bathing solution, the remaining outside bathing solution, which contained Cr^{51} that had crossed the frog skin, was saved and tested in the following manner. First a 2 ml. portion of this fluid was counted,

while the remainder was run through an anion exchange column (Dowex 1 - X100). A sample of the bathing solution was counted after it had passed through the anion exchange column. The remainder of the solution was then passed through a cation exchange resin (Amberlite IR-120) and a sample of this was counted. Each column was then washed three separate times with 10 ml. of distilled water and 2-ml. samples of each wash were counted.

The Movement of Radiochromate Ion across Fish Skin

Skin from the abdominal region of rainbow trout was placed in the short-circuit chamber. Fish skin is attached to the underlying musculature firmly as opposed to a loose attachment in the case of frog skin. For this reason, it was necessary to place a greater stress on the trout skin when removing it. The experimental procedure was the same used for radiochromate ion diffusion across frog skin.

Expression of Data

Most of the data are presented in a graphic manner, with each experimental datum indicated by a dot. In the non-isotopic studies, results are uniformly expressed as microamperes per cm² of skin versus time in minutes. Although these data could be expressed as conductances or micromoles of Na⁺ ion transported, the actual measurements were in microamperes and were so expressed.

A line connecting the various experimental points on a graph indicates that the magnetic field was being applied. The type of magnetic field is indicated by the scheme described previously.

The data referring to radiochromate ion diffusion have been expressed graphically in the Results section and in tabular form in Appendix E (frog skin) and Appendix F (fish skin).

RESULTS

Short-Term Biomagnetic Studies

To enhance readability, all data pertaining to this section have been placed in Appendix C. Each individual study has been represented graphically as a function of short-circuit current versus time. A line connecting the data is utilized to indicate those times when a magnetic field was present.

In all experiments prior to March 19, 1962, the entire short-circuit chamber was moved into the magnetic field, producing mechanical jarring of the chamber. The spacing between the magnetic poles was just sufficient to accept the short-circuit chamber in the data of figure C-1, causing the chamber to touch one or both of the magnetic poles as it was lowered into place.

A possible increase in variability of the short-circuit current was observed in two instances (figures C-3 and C-4). In both cases, this variability occurred between 100 and 200 minutes time.

Even though opposite halves of the same frog skin were utilized as controls, it was not possible to obtain equal short-circuit current for each of them. Generally speaking, the skin in the right chamber produced lower values than did the one in the left chamber.

Alternating the magnet from one chamber to the other had negligible effect on the general direction of the short-circuit current versus time curve (figures C-5 and C-7). In one experiment (figure C-5), the left chamber was accident-ally jarred when inserting the magnet with a resultant loss of fluid. New fluid was added. The right chamber was then purposely drained and refilled with fresh Ringer's solution. The rise in short-circuit current of the right chamber at 350 minutes time was caused by draining and refilling, and it is probable that the rise in the left chamber current at 325 minutes was due to fluid loss and refilling with fresh Ringer's.

Ten-Hour Biomagnetic Studies

Due to their bulk, these data have been placed in Appendix D. The general information given for the graphs of the previous section is applicable to this study.

The results of all observations that extended over a period of 10 or more hours indicate that no major changes were brought about in short-circuit current versus time correlation by an exposure to 3500 gauss. The observations of 2-9-62 and 2-14-62 in figure D-1 were conducted under a continuous magnetic field. The resulting data were designated differently to aid in differentiating between them.

No magnetic field was present in the observations on 2-12-62 and 2-13-62 of figure D-1.

In the two-chambered experiments, the data were similar if the inherent chamber difference itself was considered.

A possible exception occurred in figure D-3, where considerable irregularity was observed in the short-circuit current of the left chamber when the magnetic field was applied.

The total short-circuit current produced by each frog skin was calculated. These data were placed in table D-1 of Appendix D. The average total short-circuit current was 233 ± 97 microampere hours per cm². This is equivalent to 0.84 ± 0.35 coulombs and can be expressed as 0.20 ± 0.08 mg. of sodium transported per cm² by the average skin.

A generalized short-circuit current versus time curve could be characterized by a negative slope during the first hour, followed by a positive slope during the second and third hours after which time the slope again became negative and continued so until the termination of the experiment.

The Effects of Higher Magnetic Fields

No major changes occurred in short-circuit current, even when magnetic fields up to 10,000 gauss intensity were applied. These results are depicted in figures 10 and 11, where the letter corresponding to each circled experimental datum represents the current in amperes applied to the electromagnet for approximate 15 second intervals. The slight decrease of short-circuit current, in figure 10, when 2 amperes were applied, is no greater than that often seen under normal conditions.

Figure 10. The effects of high magnetic fields on Na⁺ ion transport.

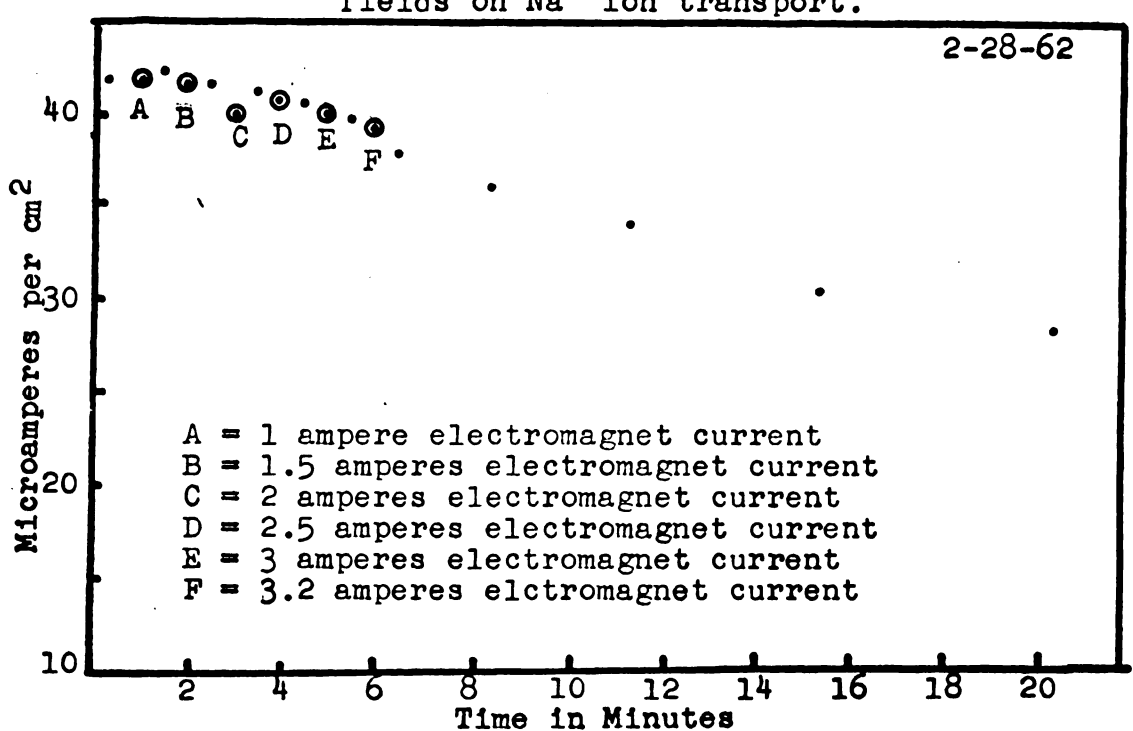
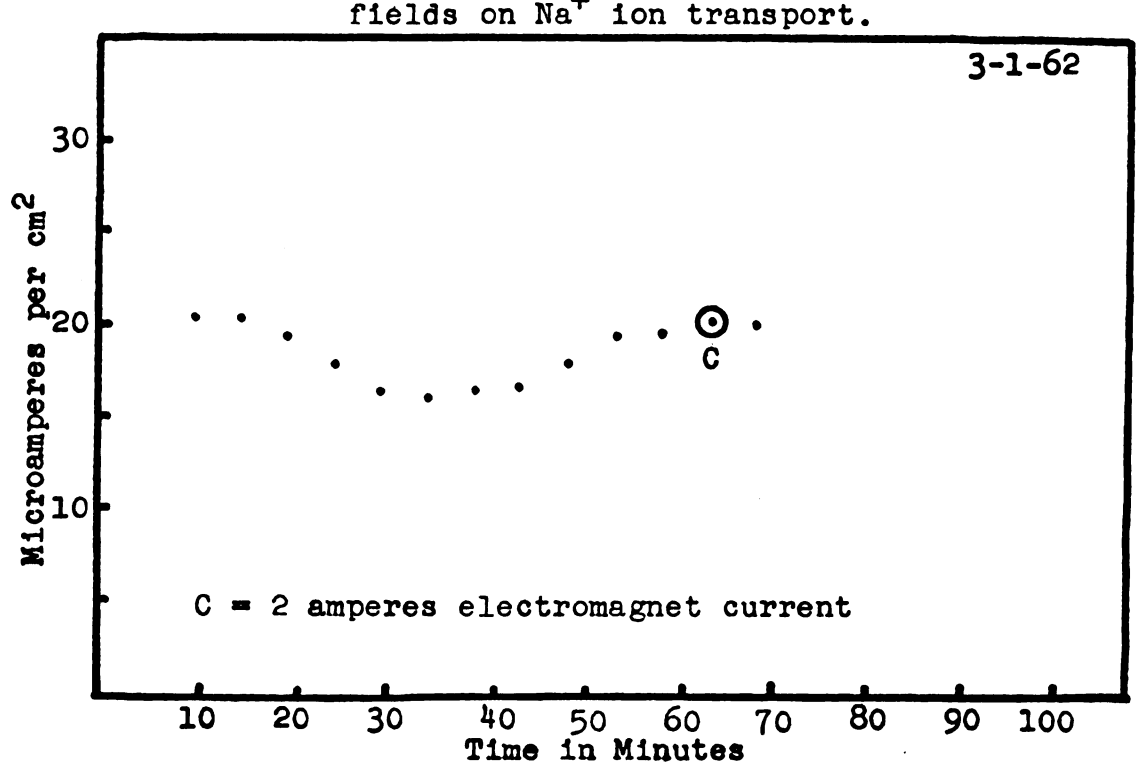


Figure 11. The effects of high magnetic fields on Na⁺ ion transport.



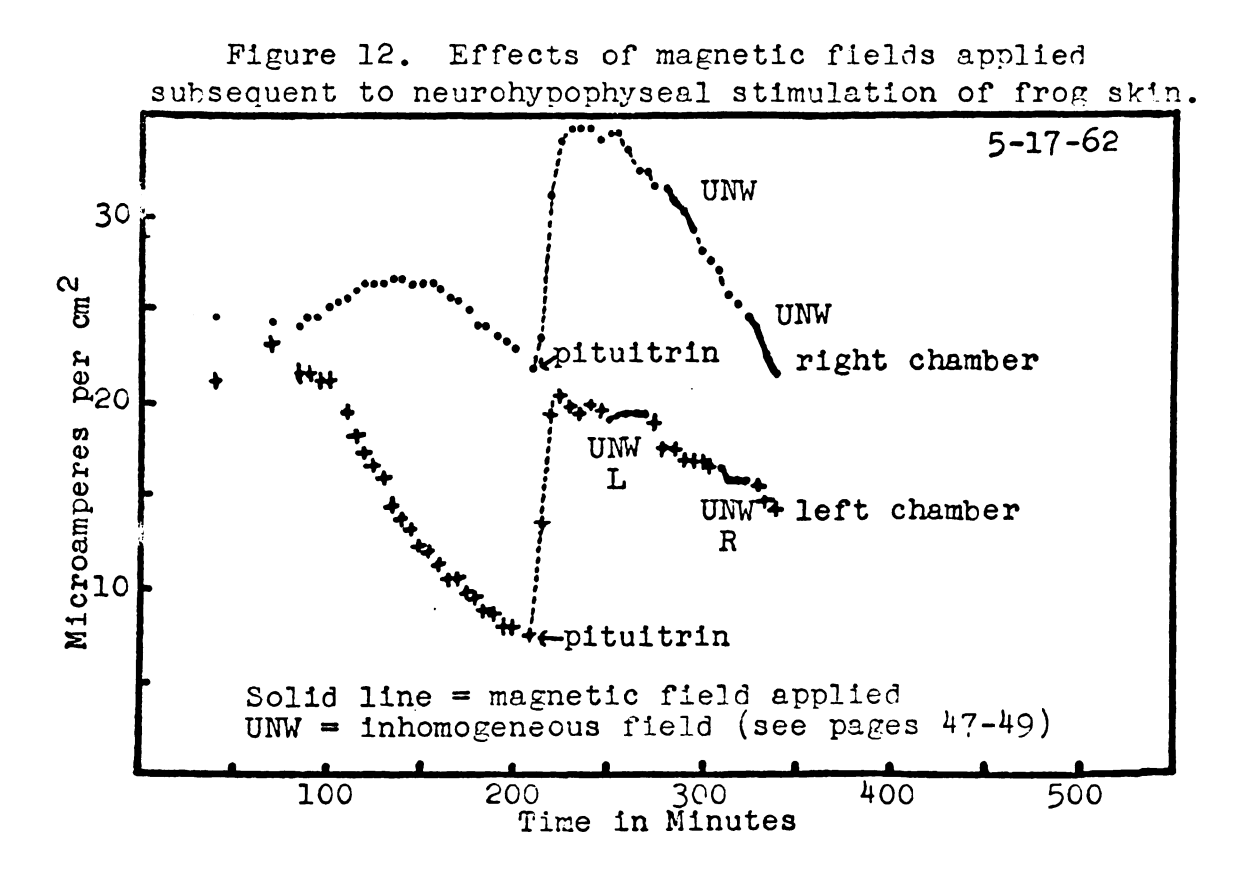
The Effects of Magnetic Fields on Neurohypophyseally Stimulated Frog Skin

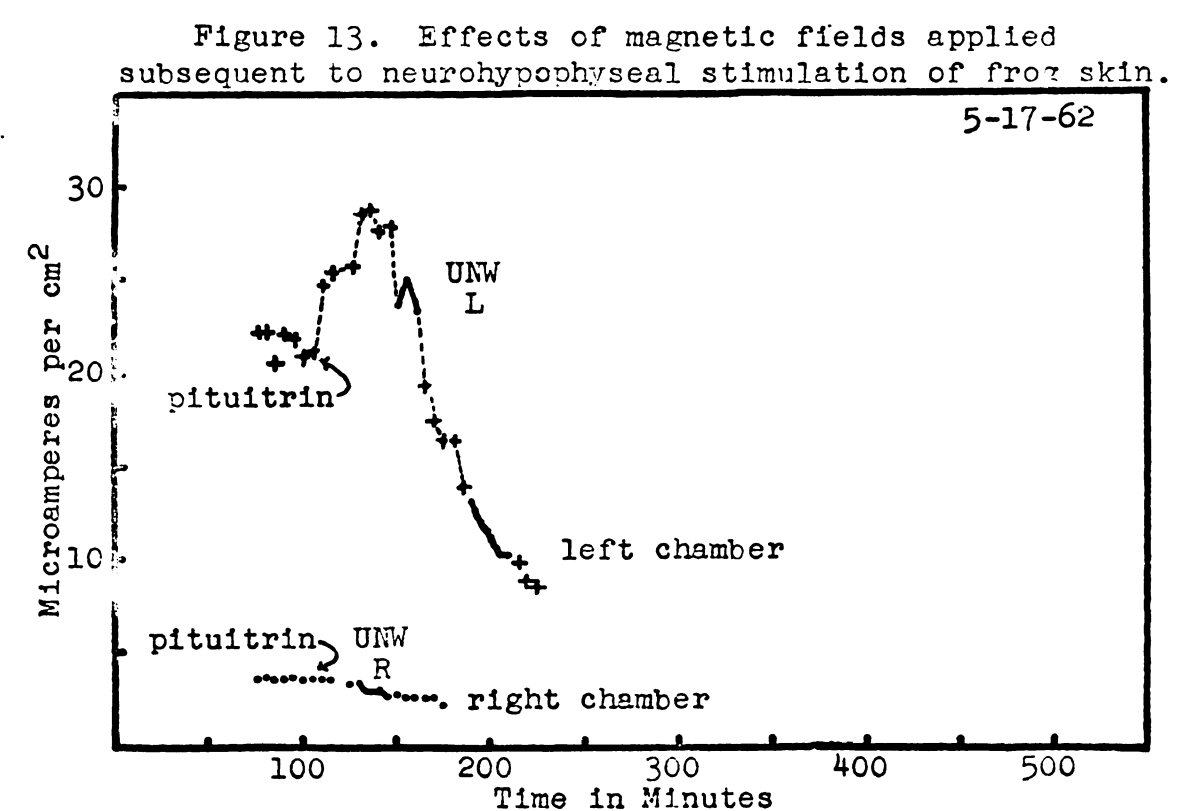
The addition of 0.1 unit Pituitrin to both sides of the short-circuit chamber resulted in an increase in short-circuit current in 5 out of 6 frog skins, as shown in figures 12, 13, and 14, and in table 1. The minimal increase of short-circuit current was 37 per cent, while the maximal increase was 236 per cent greater than the pre-stimulation conditions. The sixth frog skin produced approximately 3.5 microamperes per cm², which diminished to near 2.5 microamperes per cm² after Pituitrin administration. The initial short-circuit current of this frog skin was abnormally low.

In those cases where neurohypophyseal hormone was added prior to the application of a magnetic field, there is little evidence to show any effects by the magnetic field. The effects were more prolonged when the magnetic field was applied prior to neurohypophyseal administration. It was noted, however, that the curve obtained before Pituitrin® administration in this experiment did not diminish as rapidly as similar curves obtained in the other Pituitrin® experiments.

The Effects of Magnetic Fields on Epinephrine Stimulated Frog Skin

Although epinephrine increased the short-circuit current across frog skin, the effects were not as prolonged as those obtained with Pituitrin. The results of adding 1 ml. of a





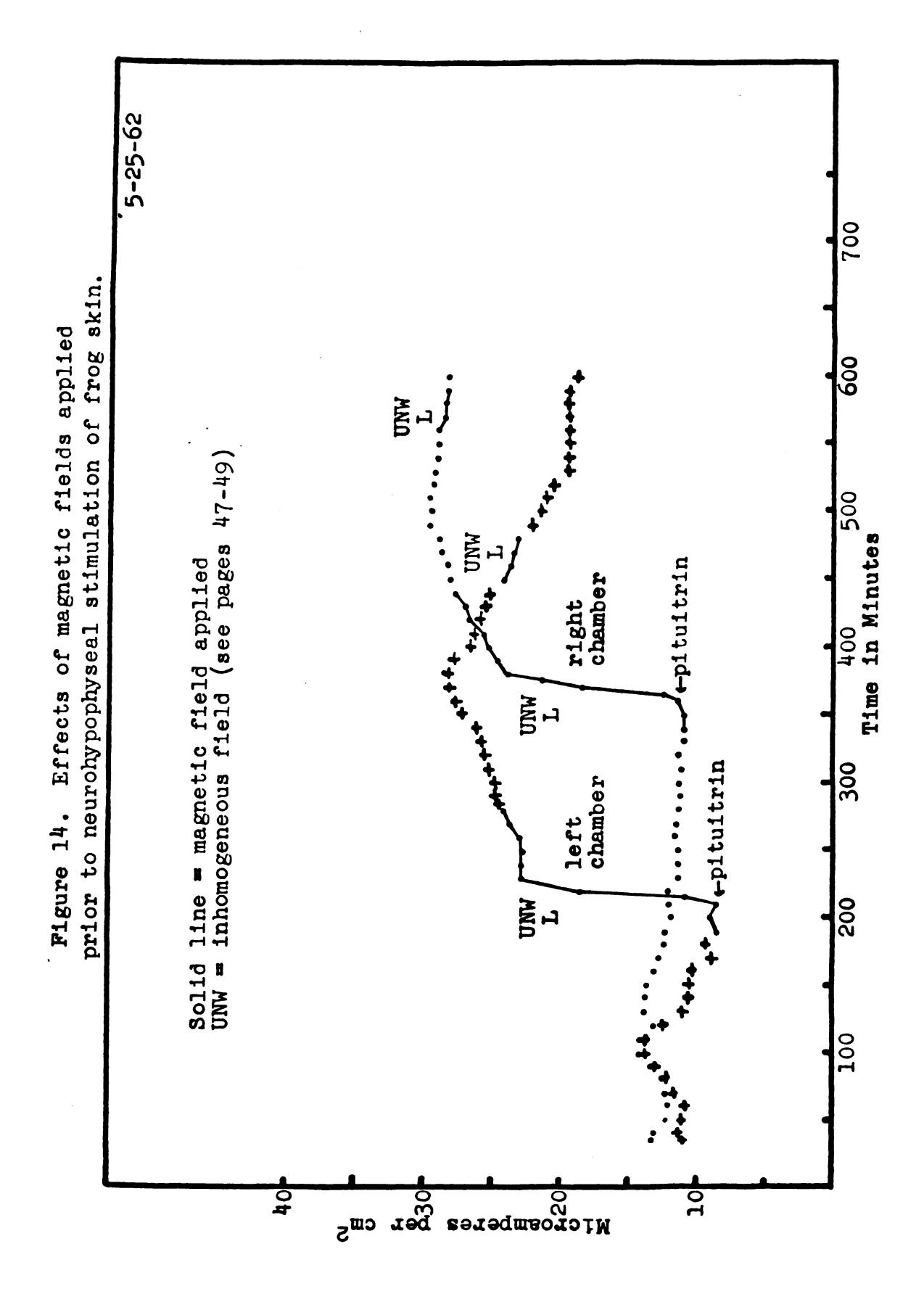


Table 1. The effects of neurohypophyseal extract on short-circuit current of frog skin.

Short-Circu Pre-Pituitrin	uit Current Post-Pituitrin®	Difference	Per Cent Increase
7.4 µA	20.4 µA	13.0 µA	175.7
21.8 µA	Aیر 35.0	13.2 µA	60.6
21.0 µA	28.7 Au	7.7 µA	36.7
8.4 µA	Au, 28.2	Aپر 19.8	235.7
11.8 µA	29.4 µA	17.6 µA	149.2
3.5 µА	Au 2.5	-1.0 µA	-28.6

Table 2. The effects of epinephrine on short-circuit current of frog skin.

Short-Circu Pre-Epinephrine	uit Current Post-Epinephrine	Difference	Per Cent Increase
21.4 µA	32.3 µA	10.9 µA	50.9
31.9 µA	38.2 µA	6.3 µA	19.7
24.0 µA	36.2 µА	12.2 גע	50.8
13.2 μΑ	21.0 µA	7.8 µA	59.1

1:10,000 solution of epinephrine to each side of the short-circuit chamber are depicted in figures 15 through 18, and in table 2. As before, solid lines indicate when the magnetic field was applied.

The Effects of Magnetic Fields on the Increased Potential Observed after Short-Circuiting Frog Skin

This phenomenon has not been previously reported in the literature so it was necessary to obtain normal values which are shown in figure 19. These values were observed on the same frog skin within a 2 hour period of time. The rise in potential following short-circuiting increased over pre-short-circuit voltage in proportion to the duration of short-circuiting. In figure 19, the durations of shortcircuiting time (0.05, 0.1, 0.2, 0.3, 0.4, and 1.0 minutes) are indicated for each curve. The short-circuit current and pre-short-circuit voltage are also listed on the same figure. The curve obtained for 0.1 minutes of shortcircuiting time does not fit in sequence with the other curves. With the exception of this 0.1 minute time, all values were obtained in sequence starting with 0.05 minutes of short-circuit time and progressing to 1 minute. values for 0.1 minute of short-circuit time were obtained subsequent to the other values. The magnitude of the shortcircuit currents, as well as that of the normal frog skin potentials, was increasing during this time. As a result

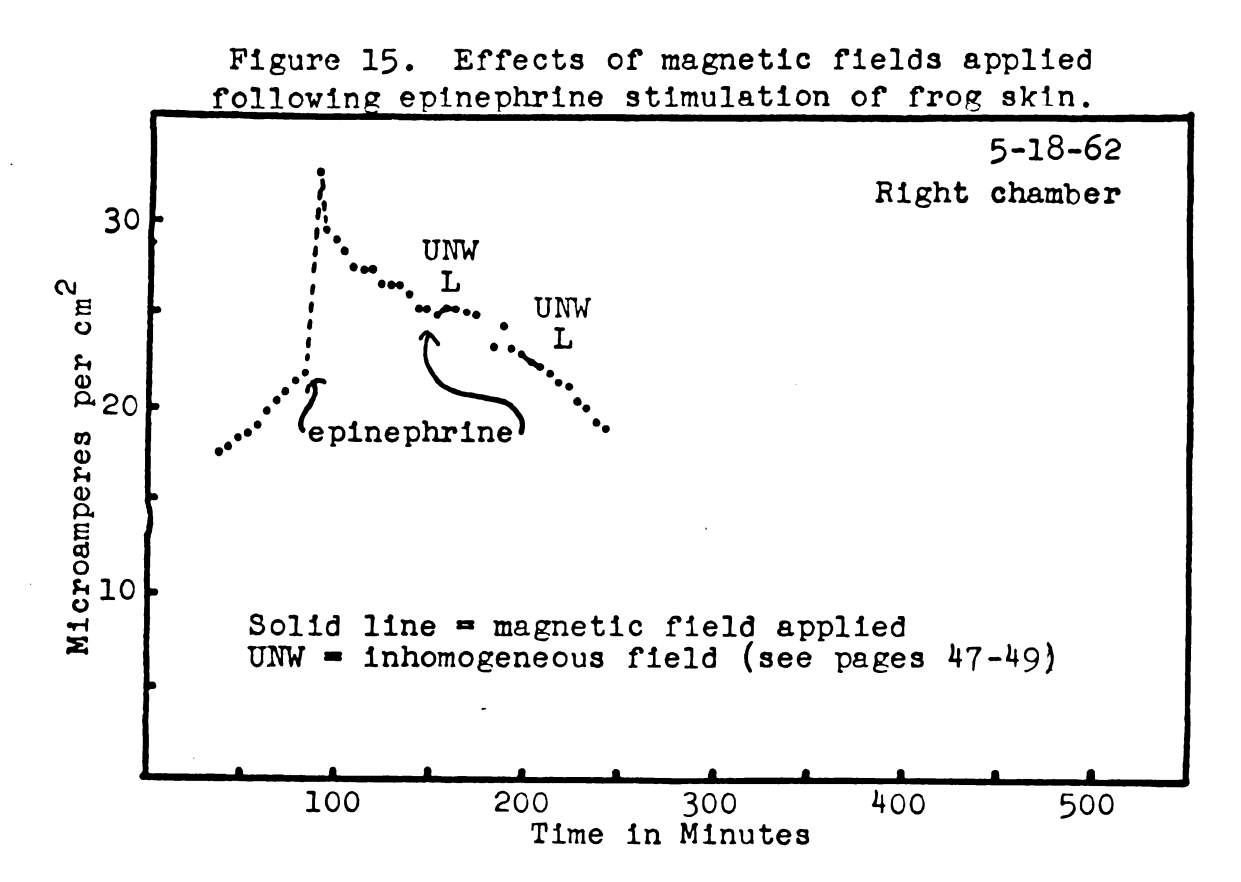
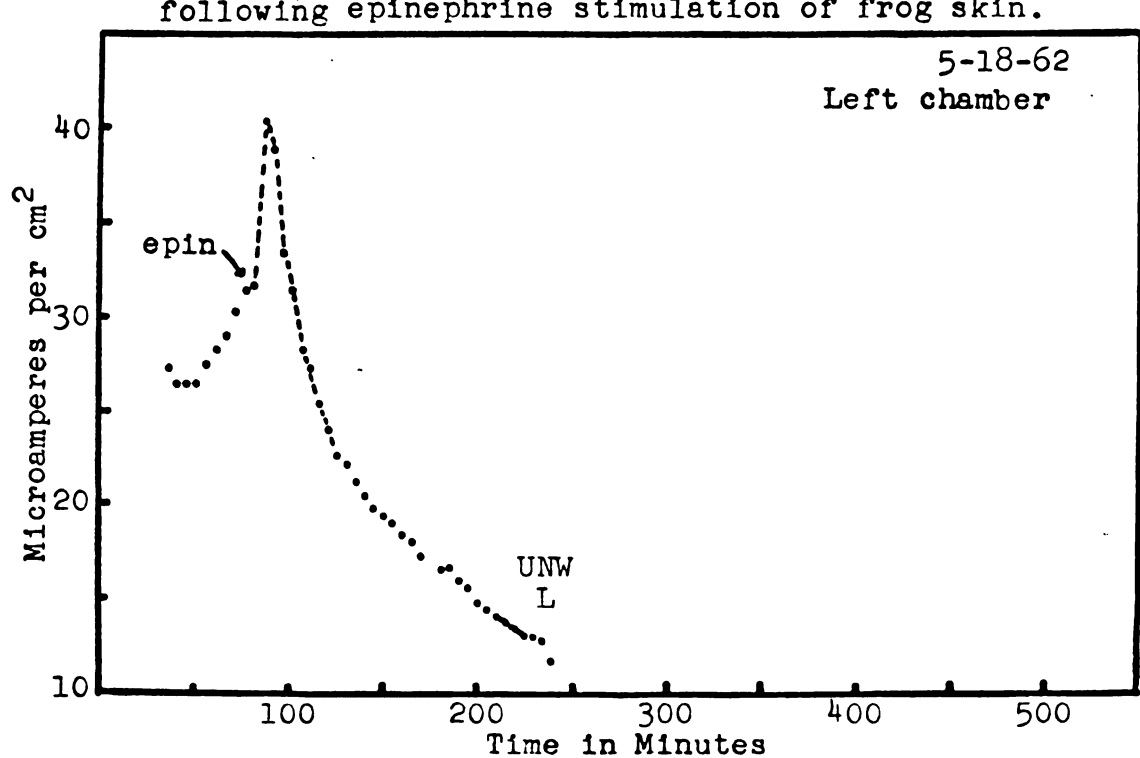
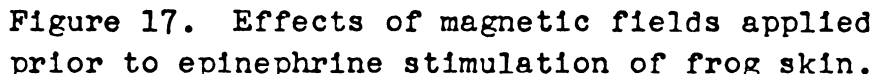


Figure 16. Effects of magnetic fields applied following epinephrine stimulation of frog skin.





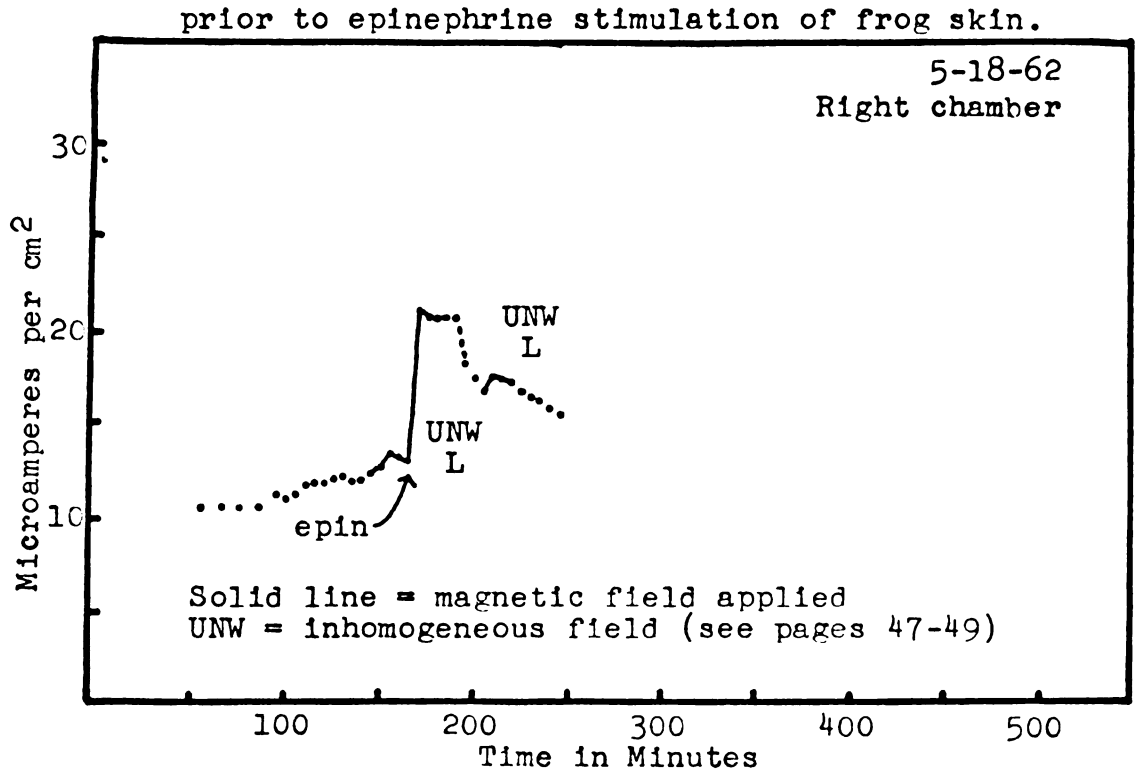
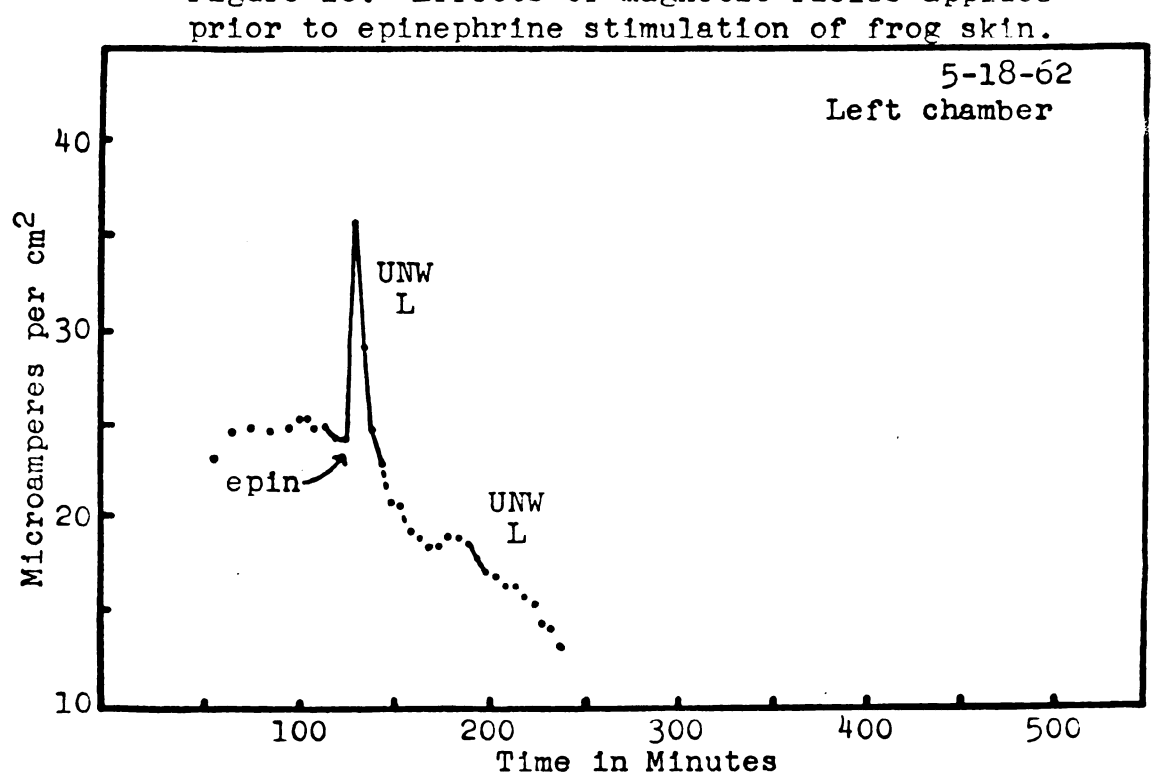
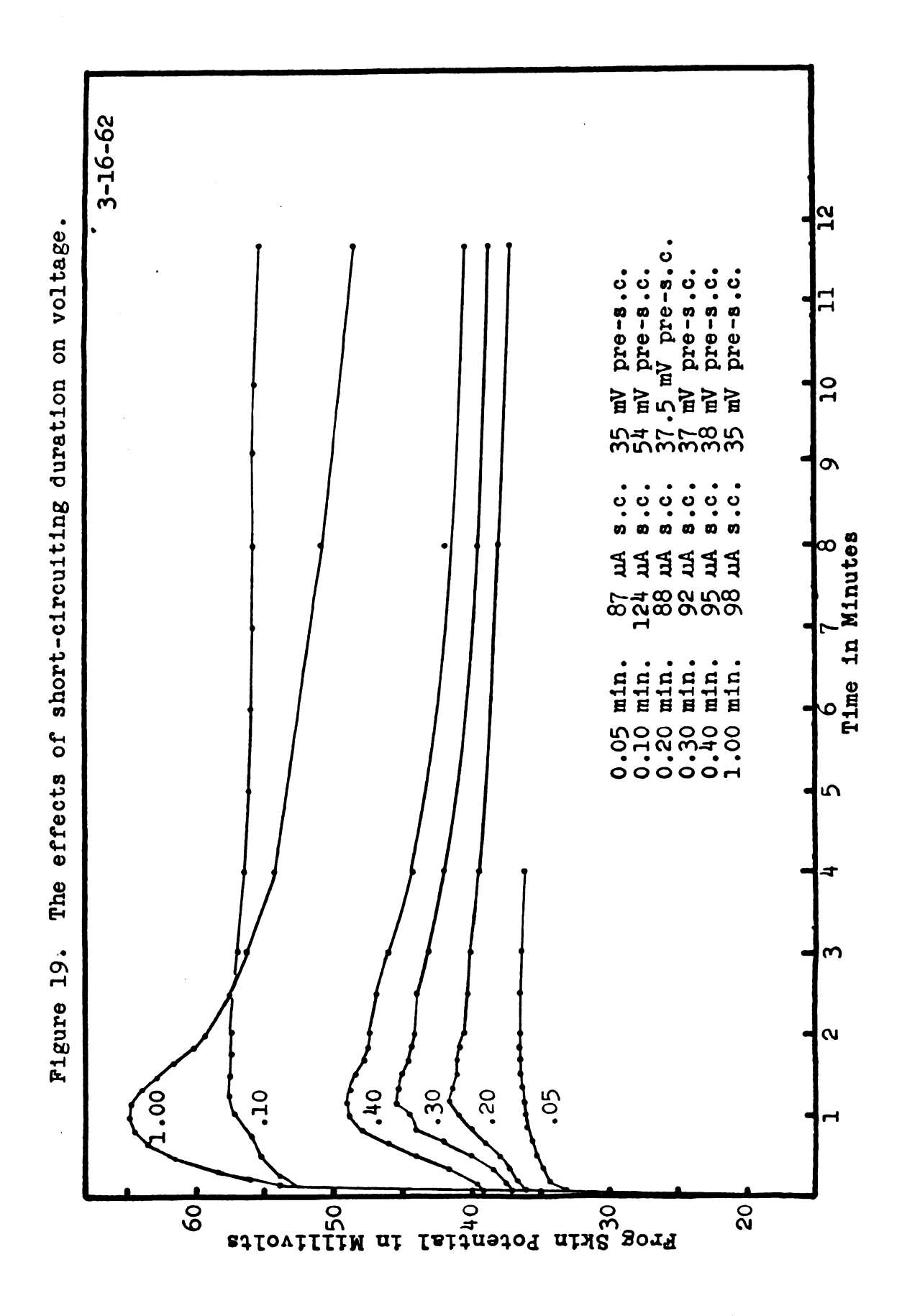


Figure 18. Effects of magnetic fields applied





the curve following the 0.1 minute short-circuiting time would not be expected to fit between 0.05 minutes and 0.2 minutes. However table 3 indicates that the per cent increase in potential is relatively constant for a given period of short-circuit time in the case of this one skin, even though the initial potentials varied.

In determining the per cent increase of the increased after-potential, the voltage was recorded one minute after short-circuiting, and also at the point of maximum voltage (generally occurring at 1.1 minutes). A plot of these per cent increases versus short-circuit time proved to be linear. These data along with a fitted linear regression line are presented in figure 20.

The same frog skin utilized in the above series of normal experiments was used in experiments involving an applied magnetic field. The results are expressed in figure 21. In this experiment, the frog skin was short-circuited 0.1 minutes. Pertinent data referring to this experiment is given in table 4. A homogeneous magnetic field did not produce any noticeable effect on the positive after-potential.

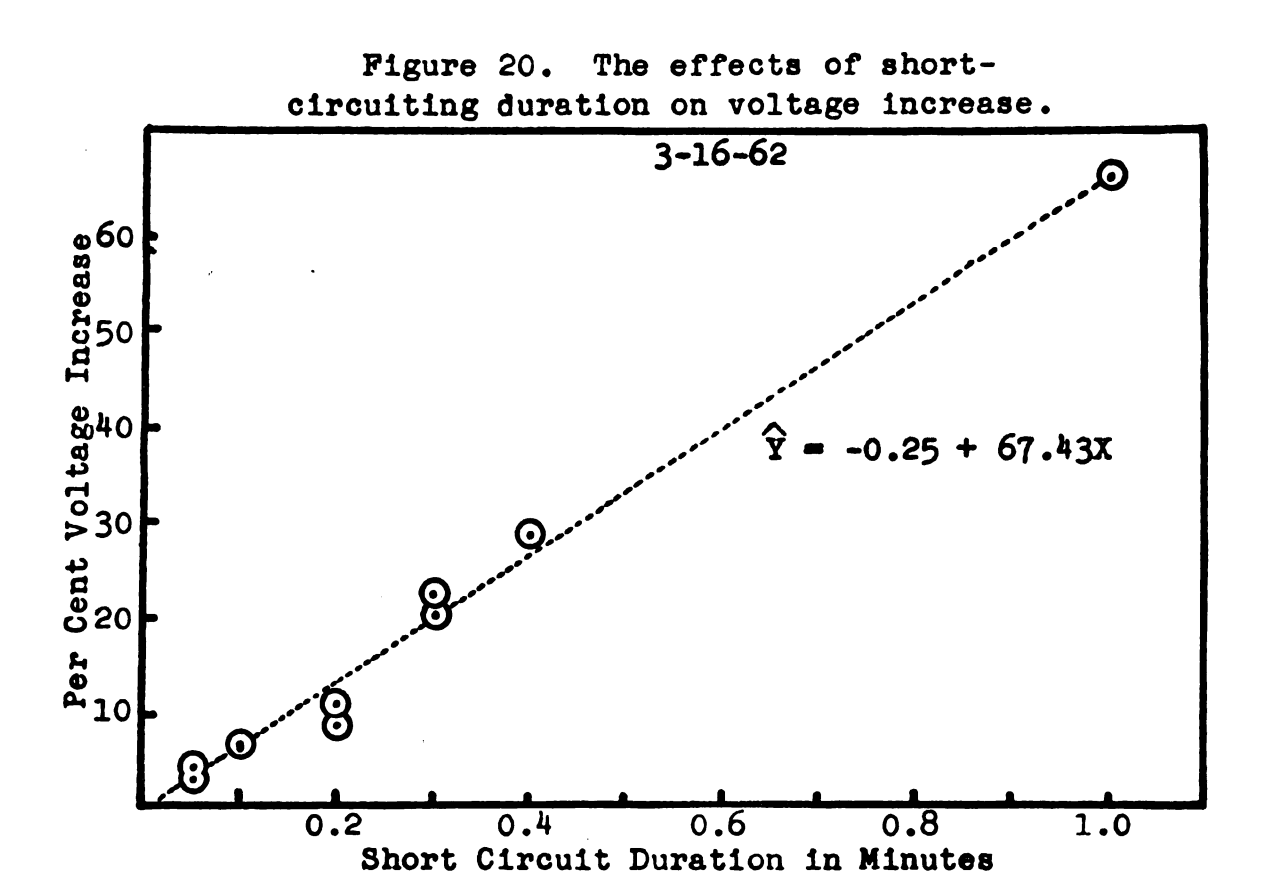
Electrical stimulation was capable of eliminating the short-circuit potential. The return of potential following electrical stimulation was slow, with the potential not returning to its original value during a 30 minute observation period. Excessive electrical stimulation destroyed the potential difference across frog skin.

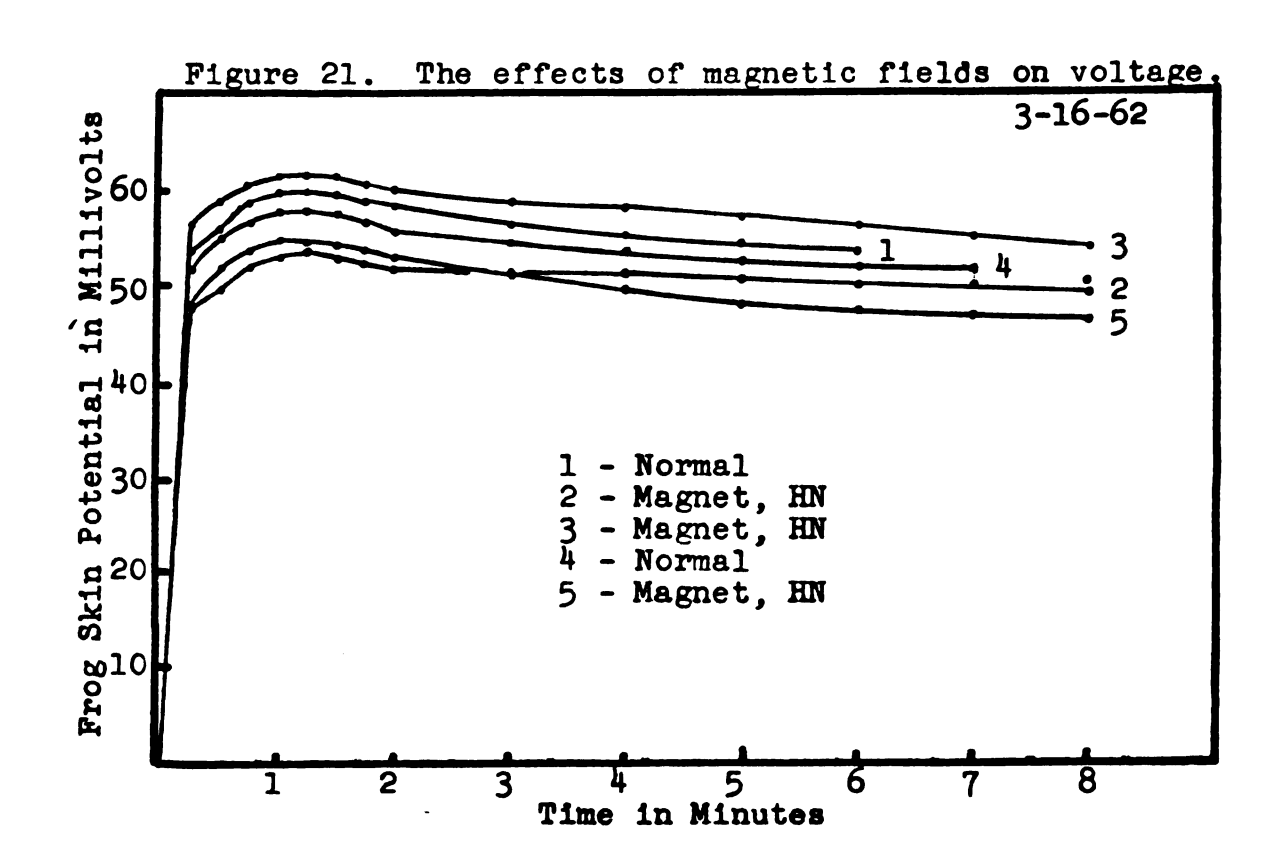
Table 3. Effects of short-circuiting duration on potential.

S.C. Time	S.C.	Pre-S.C. LMF	Post S EMF (。C。 mV)		Per Cent Increase		
(Min.)	Current (µA)	(mV)	l min. Post	Max. Post	l min. Post	Max. Post		
.05	87	35	36	36.3	2.9	4.3		
.10	124	54	57.3	57.7	6.1	6.9		
.20	88	37↓5	40.8	41.5	8.8	10.7		
.30	92	37	44.5	45.3	20.3	22.4		
.40	95.5	38	48.7	49	28.2	28.9		
1.00	98	39	65	65	66.7	66.7		

Table 4. The effects of a magnetic field on potential.

Obser-	S.C.	Pre-S.C. EMF	Post S EMF (1	.C. mV)		Per Cent Increase		
vation Number	Current (µA)	(mV)	l min. Post	Max. Post	l min. Post	Max. Post		
1-normal	150	56.5	60.2	60.2	6.6	6.6		
2-magnet	138	53.5	57.5	57.4	7.5	7.7		
3-magnet	141	58	60.9	61.0	5.0	5.2		
4-normal	143	56.2	59.0	59.2	5.0	5.3		
5-magnet	145	54	56.6	57	4.8	5.5		





The Movement of Radiochromate Ion across Frog Skin

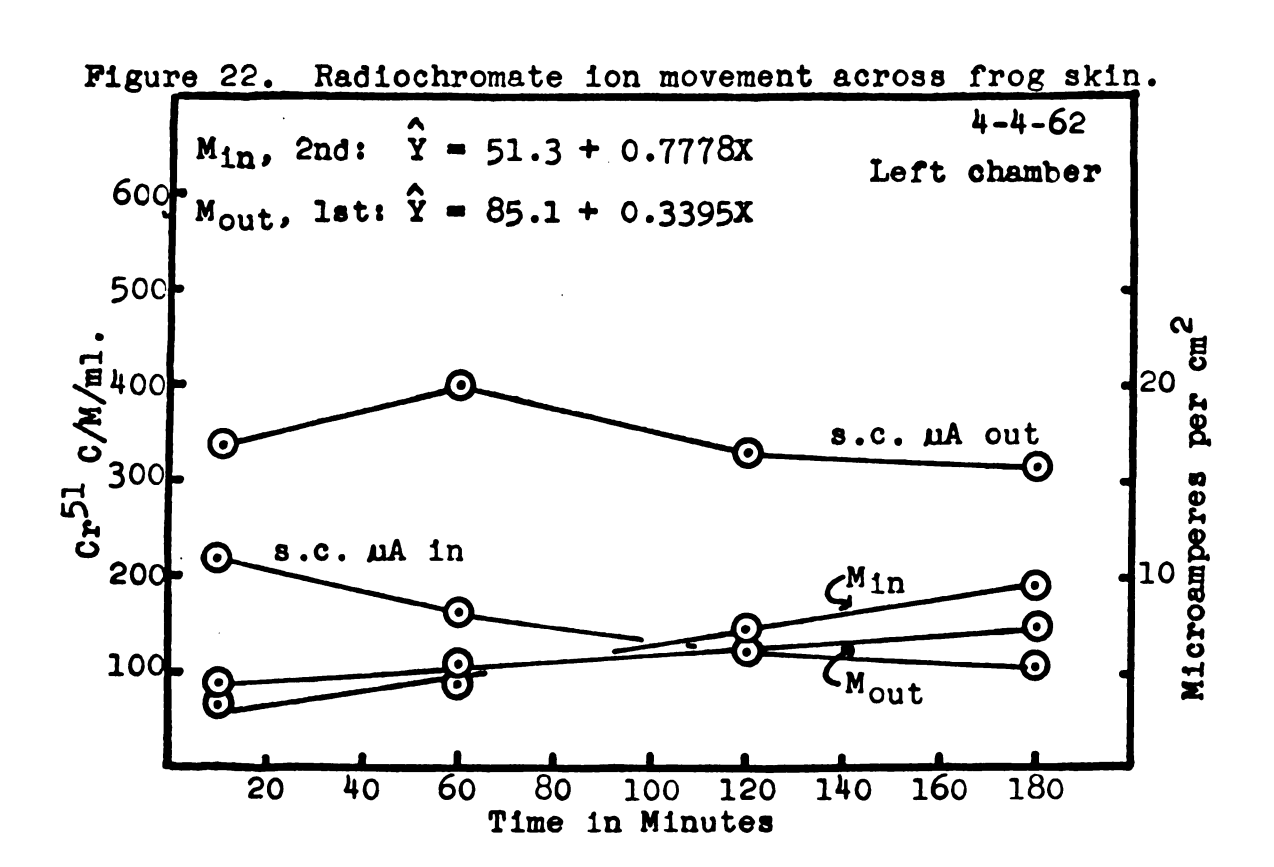
Results of radiochromate ion movement across frog skin under non-short-circuit conditions are shown in figures 22 through 25. These studies were conducted to obtain normal values, since radiochromate ion movement through frog skin has not been previously investigated. In these figures, calculated regression lines of influx (Min) and efflux (Mout) are plotted for the experimental data. Relative Na⁺ ion fluxes are indicated by a plot of short-circuit current versus time.

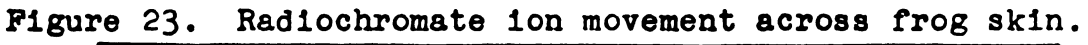
Data were corrected for volume changes occurring due to removal of samples for counting. The graph plots represent these corrected data. The data pertinent to this series are tabulated in Appendix E. Corrected linear regression equations for these lines, along with radiochromate flux ratios, are summarized in table 5. Flux ratios were calculated by Ussing's method (1949b):

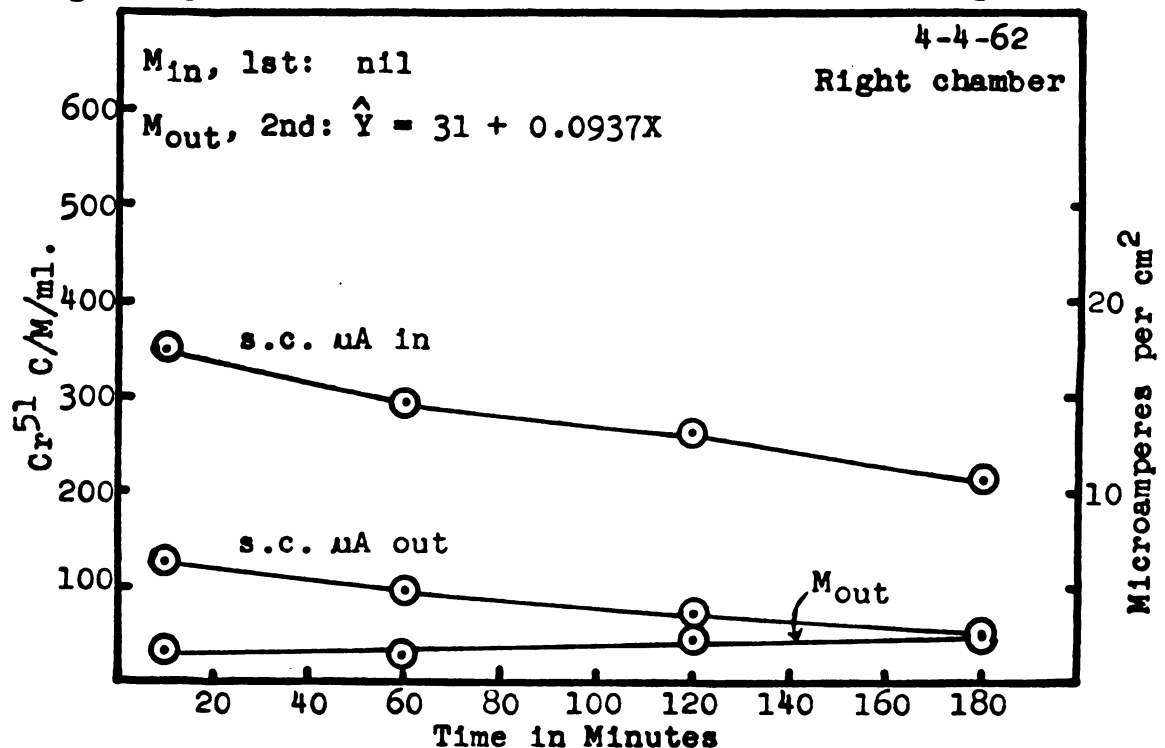
$$\frac{M_{in}}{M_{out}} = e^{-F/RT \cdot (E_1 - E_2)}$$

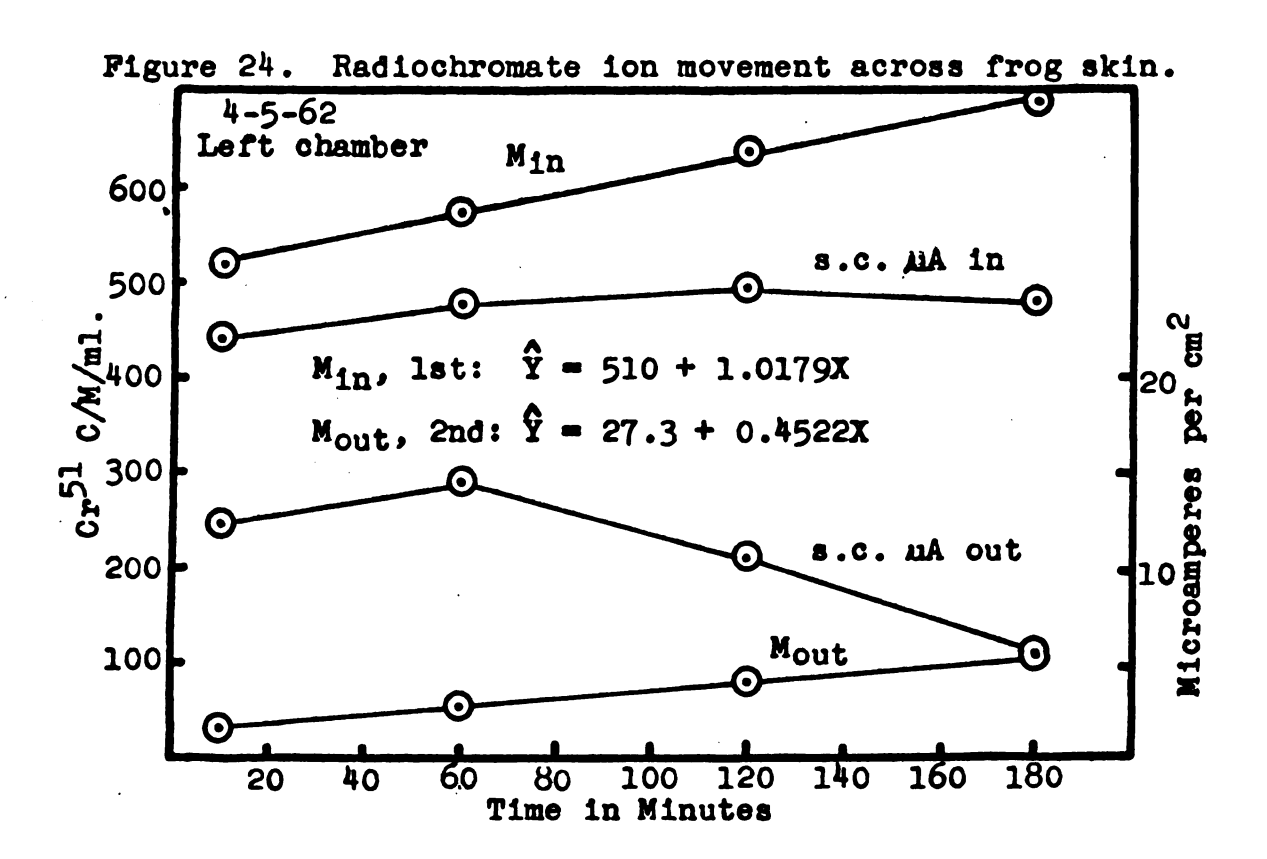
The activity remaining in the frog skin, as well as that activity removed by rinsing the skin in 50 ml. of Ringer's solution, is listed in table 6. In this same table, uptake ratios of radiochromate in skin have been estimated using a wet frog skin weight of 171 mg.

The per cent of radiochromate ion crossing frog skin, as calculated from the corrected regression equations, is









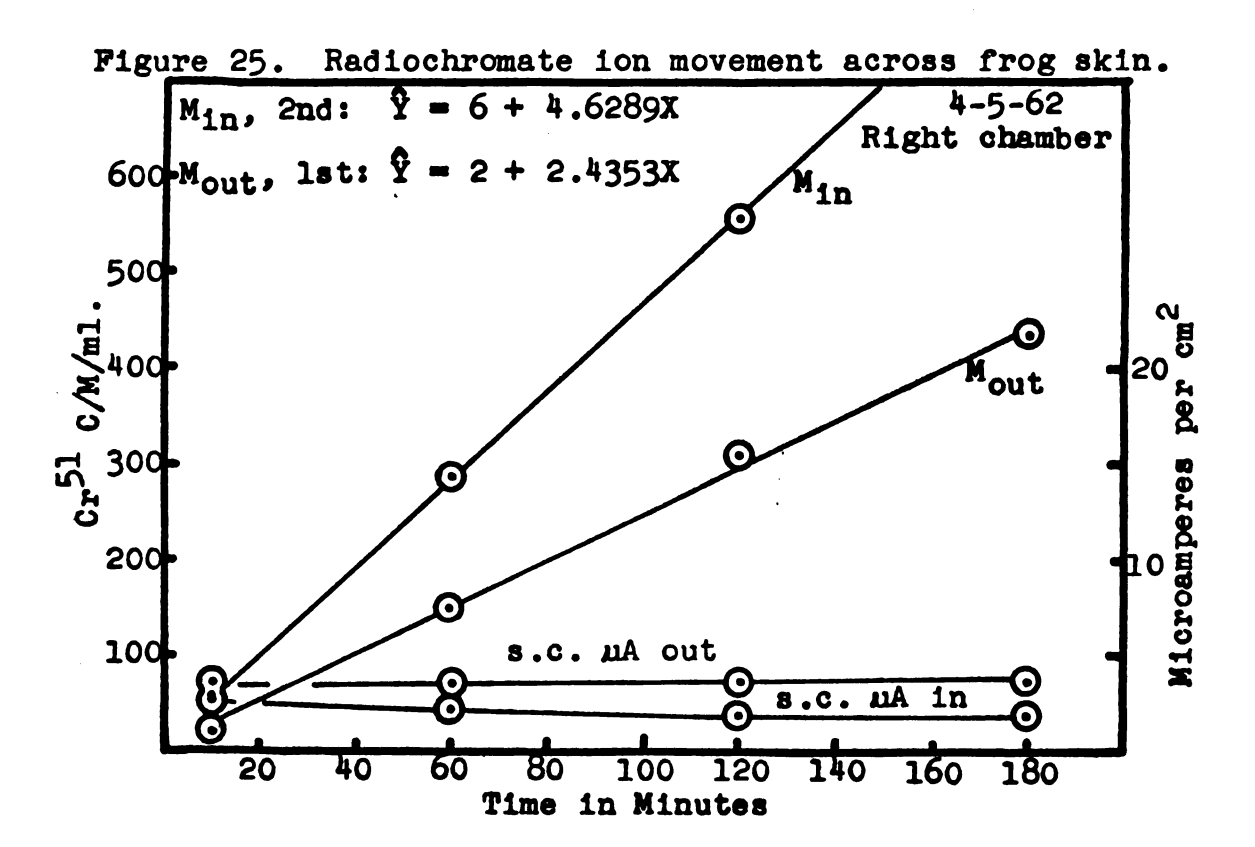


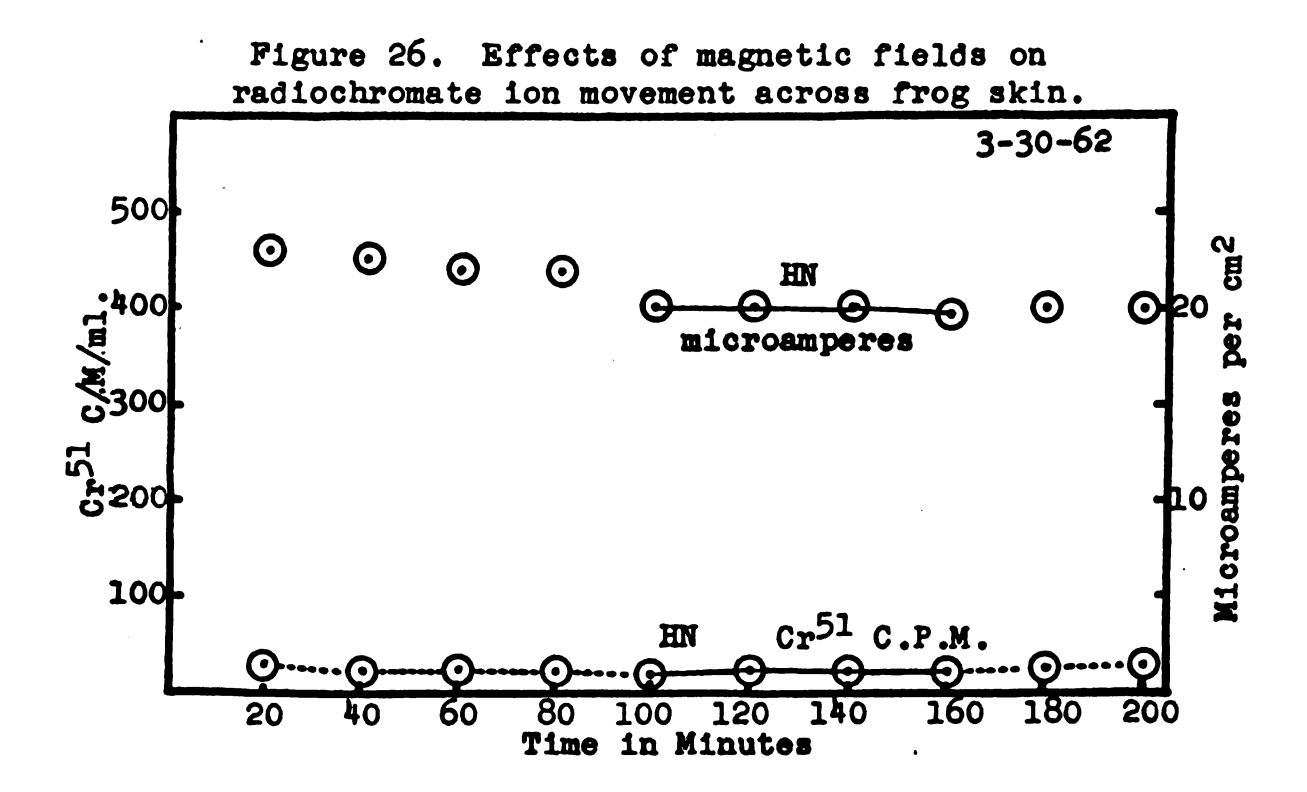
Table 5. Calculated line equations and flux ratios for radiochromate ion movement across frog skin.

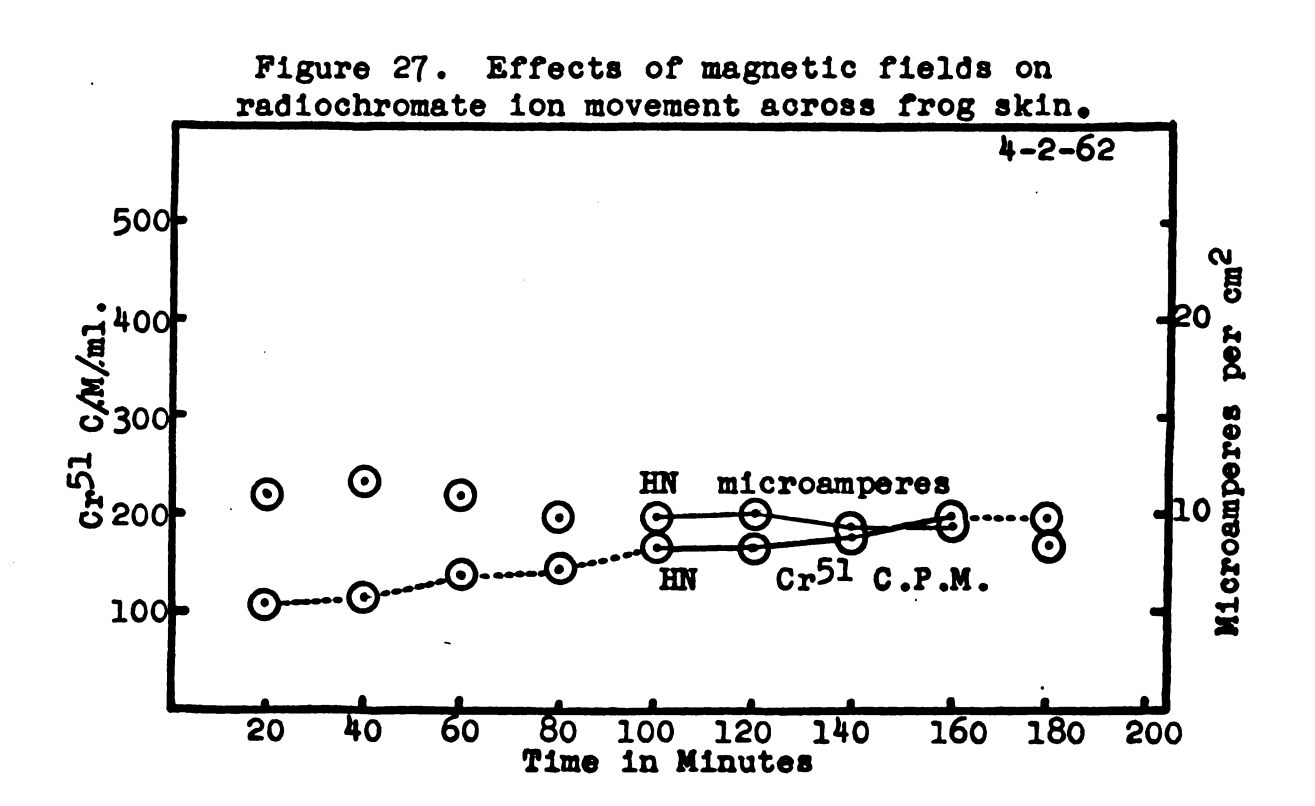
Fig-	Regression Equations $\hat{Y} = a + bX$						M _{in} /M _{out}	
ure	Chamber		in b		ut b	in mV	Meas.	Calc.
20	Left	51.3	0.78	*85.1	0.34	18	2.3	2.0
21	Right	*n:	il	31.0	0.09	20	-	2.2
22	Left	*510	1.02	27.3	0.45	24	2.25	2.6
23	Right	6	4 ,63	*2	2.44	2.0	1.9	1.1

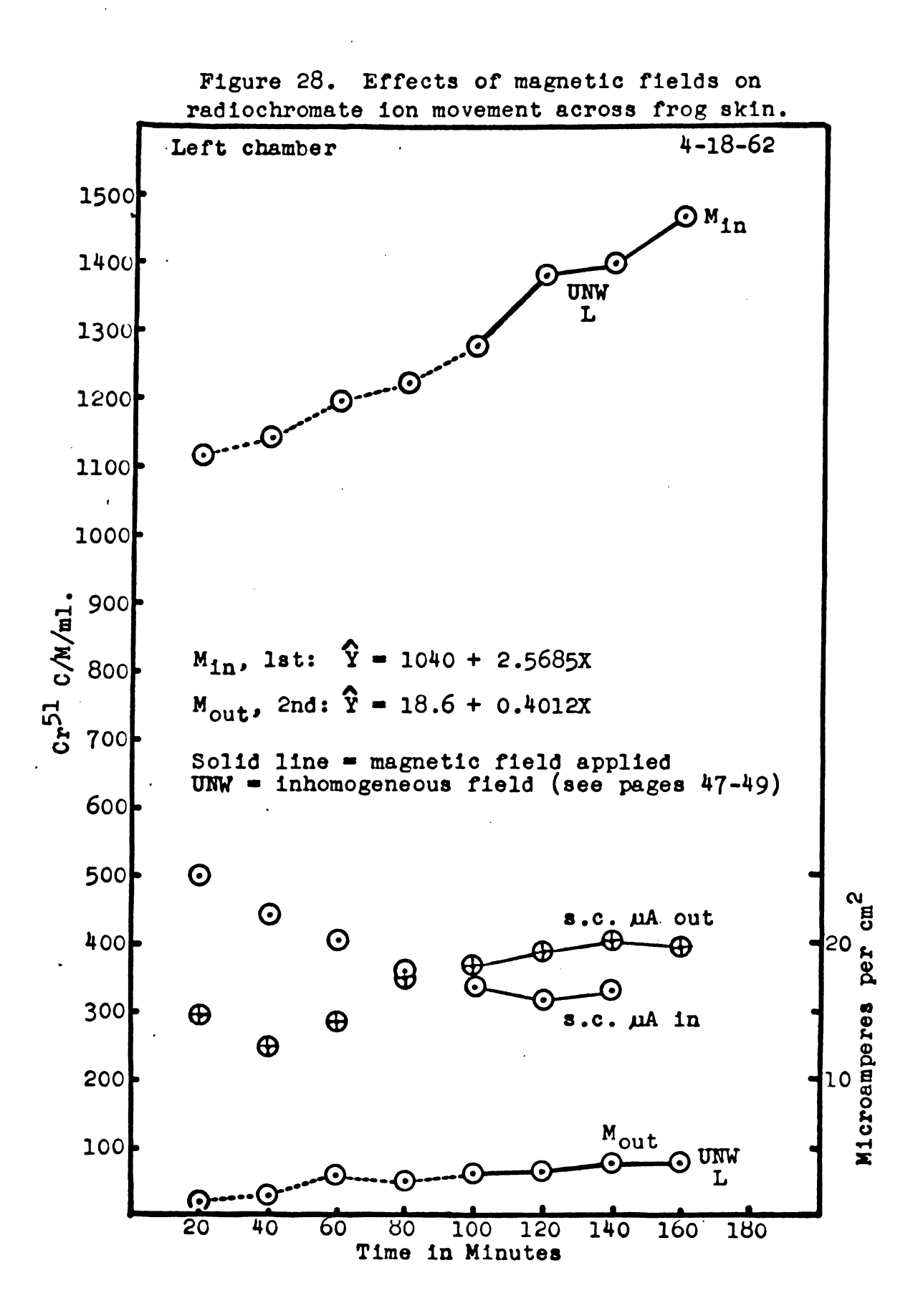
^{*}Radiochromate added to this chamber first.

Table 6. Activity remaining in the frog skins after rinsing in 50 ml. of Ringer's solution.

Fig- ure	Skin, Total C/Min.	50 ml. Ringer's Rinse, Total C/Min.	X Counts of Bathing Solution	C/g. Skin	Skin C/g. Water C/ml.
20	53,333	1,450	54,725	311,889	5.7
21	54,468	2,026	49,032	318,526	6.5
22	82,581	42,900	50,645	482,930	9.5
23	17,124	3,525	45,441	100,140	2.2







2,

2. 2

2

(a) (b) (c)

Table 7. Per cent of activity crossing frog skin in 1, 2 and 3 hours, based on corrected activities.

Figure	Average C/Min/ml.	Calculated Activities C/Min/ml.		C	Skin		M _{in} /M _{out} Ratio Based on C/Min/ml.			
	Opposite Side					2 hr.	3 hr.		2 hr.	3 hr.
20, M _{in}	60,599	98	145	192	0.16	0.24	0.32	C.92	1.15	1.32
20, M _{out}	48,851	106	126	146	0.22	0.26	0.30			
21, M _{in}	nil	nil			nil			-	-	-
21, M _{out}	47,115	36	42	47	0.08	0.09	0.10			
22, M _{in}	49,231	571	632	694	1.16	1 28	1.41	10.6	7.80	6.43
22, M _{out}	52,058	54	81	108	0.10	0.16	021			
23, M _{in}	43,583	284	562	839	0.65	1.29	1.93	1.92	1.91	1.90
23, M _{out}	47,299	148	295	441	0.31	0.62	0.93			

Table 8. Calculated regression equations and flux ratios for radiochromate ion movement across frog skin in the presence of a magnetic field.

		Regr		Equati + bX	ons		Avg.	1	
Figure		rmal tion b	Magn Por a	net tion b		tire ine b	P.D. in mV	Min/Meas.	
24, M _{in}						0.015	30.6		3 • 37
25, M _{out}	95	0.555	114.5	0.395	101	0.471	18.6		2.09
26, M _{in}	1087	1.840	998	2.915	1040	2.568	12.4	6.40	1.64
26, M _{out}	9.5	0.595	32	0.295	18.6	0.401	28.6	6.40	3.11

Table 9. Summary of ion exchange studies of ${\rm Cr}^{51}$ after it had passed through frog skin,

Portion Counted	C/Min/m	1.
Forcion Counted	Side to which Cr ⁵¹ 04 [*] added	Opposite Side
Initial activity	50,196	84
After anion exchange	436	8
After anion and cation exchange	137	3
First wash of anion resin	770	7.5
Second wash of anion resin	70	1.5
First wash of cation resin	17	nil
Second wash of cation resin	1.5	nil
Second wash of cation resin	1.5	nil

tabulated in table 7. Ratios of influx/efflux of radiochromate ion at various times are also included.

The results of radiochromate ion movement across frog skin in the presence of a magnetic field are given in figures 26, 27 and 28 and table 8.

The potential differences observed during the influx period were less than those observed for the efflux portion of figure 28, explaining the difference in calculated values of $M_{\rm in}/M_{\rm out}$.

Ion exchange studies, summarized in table 9, showed that most of the ${\rm Cr}^{51}$ that had crossed the frog skin was of an anionic nature. Consequently, it was assumed that it was still in the chromate ion form.

The Movement of Radiochromate Ion across Fish Skin

The P.D. existing across the skin of a live rainbow trout in a non-anesthetized condition was measured by inserting one Ringer-agar electrode under the abdominal skin midway between the pelvic and pectoral girdles and placing the other Ringer-agar electrode in contact with the water of the tube in which the fish was confined. Under these conditions, a potential of approximately 1 mV was detected that rose to a peak of approximately 1.5 mV during normal opercular movements. The short-circuit current necessary to reduce this voltage to zero varied from 1 to 1.5 microamperes.

A significantly measurable P.D. did not exist across

isolated fish skin. The results of radiochromate ion movement through isolated fish skin are given in figures 29 through 32 with all experimental data tabulated in Appendix F. The calculated regression equations, along with the measured flux ratios, are shown in table 10.

The uptake of radiochromate ion by isolated fish skin is summarized in table 11. An average fish skin weight of 87.93 mg. based on 28 samples was used in calculating the counts per minute per gram of fish skin. The ratio of $\rm Cr^{51}$ counts per gram of fish skin to $\rm Cr^{51}$ counts per ml. of the Ringer's bathing solution equaled 11.37 in all 4 of the fish skins studied.



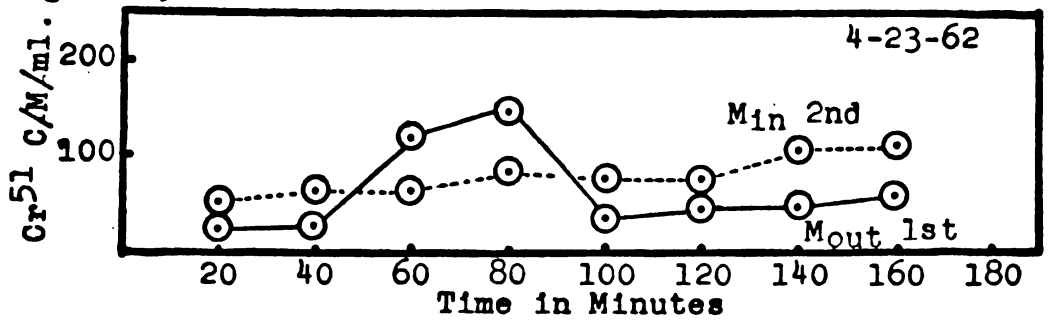


Figure 30. Radiochromate ion movement across fish skin.

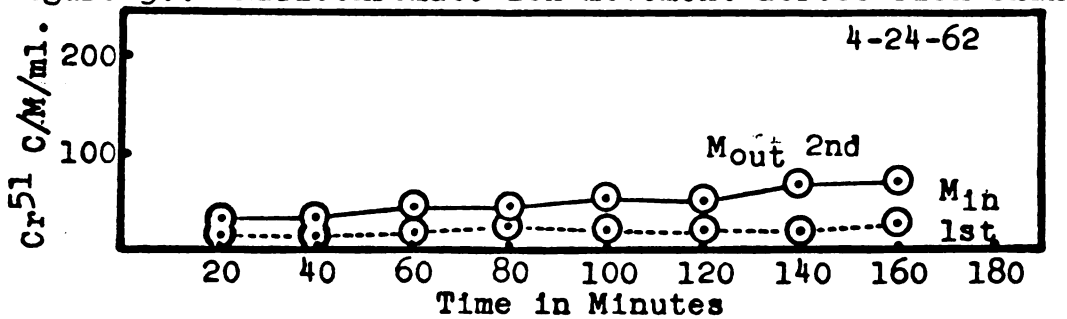
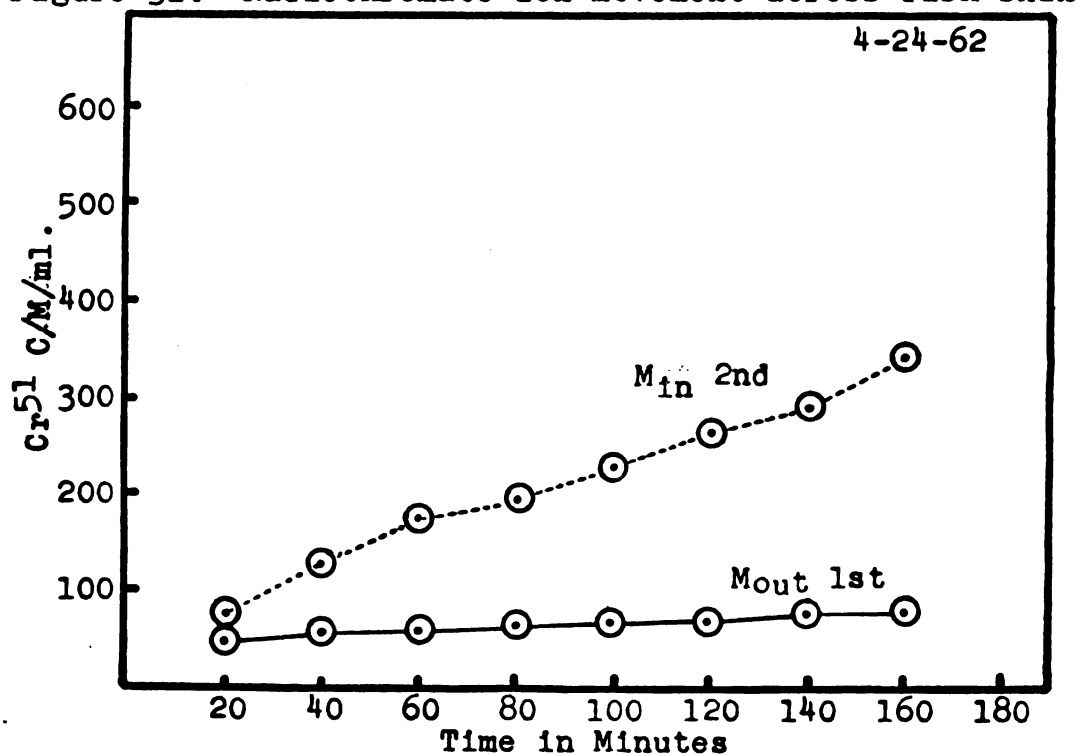


Figure 31. Radiochromate ion movement across fish skin.



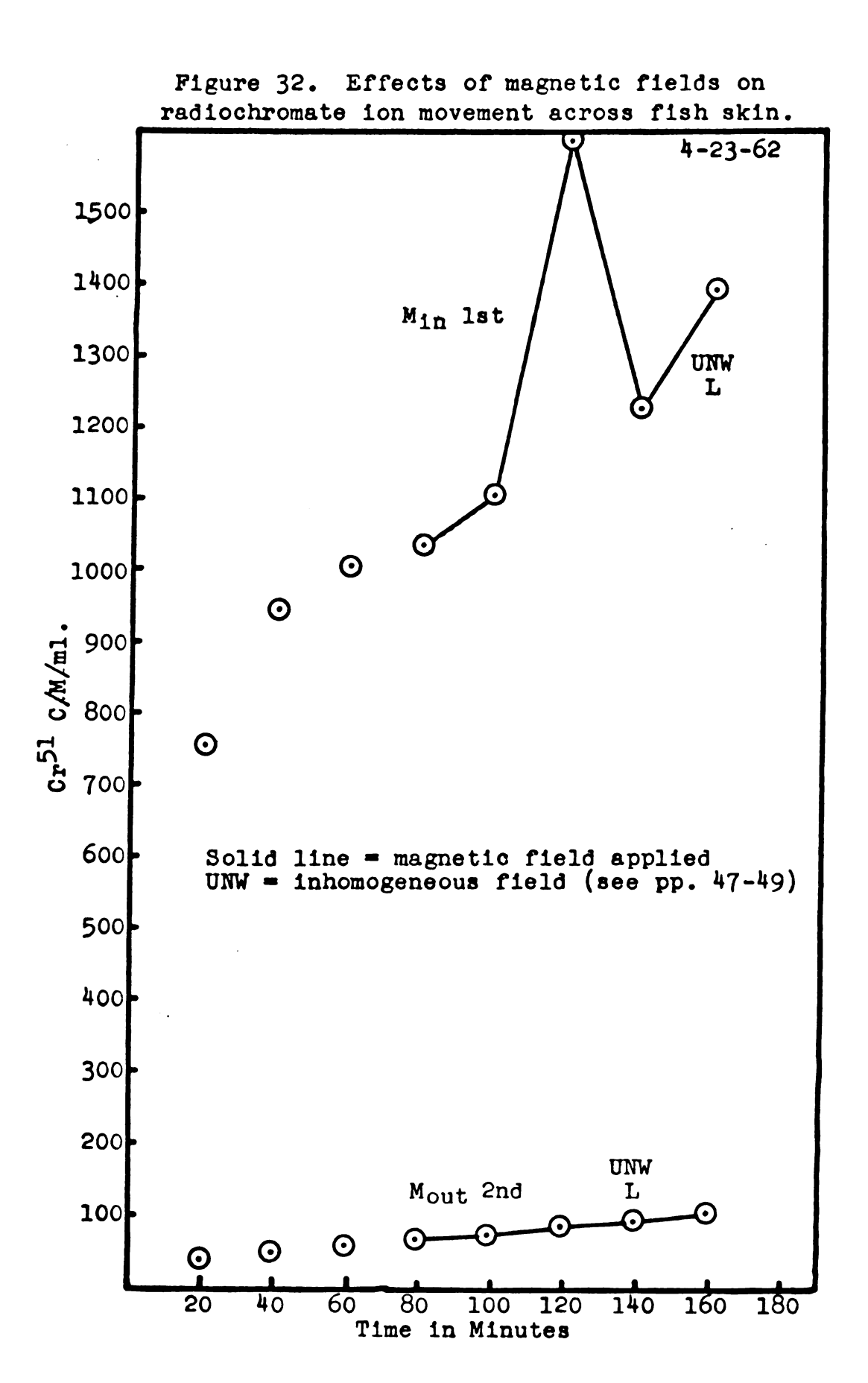


Table 10. Summary of pertinent data regarding radiochromate ion movement across fish skin.

Fig.	Chamber	Regression	M _{in} /M _{out}	
		M _{in}	Mout	<u> </u>
27	Right	$\hat{Y} = 46.8 + 0.35X$	$*\hat{Y} = 32.7 + 2.91X$	0.12
			$*\hat{Y} = 16.5 + 0.30X^{\#}$	1.16
28	Left	$\hat{Y} = 20 + 0.25X$	*Ŷ = 8.3 + 0.06X	4.17
29	Right	*Ŷ = 45 ± 0.17X	$\hat{\mathbf{Y}} = 54 \pm 1.61\mathbf{X}$	0.11
30	Left	$*\hat{Y} = 738 + 3.95X$	$\hat{\mathbf{Y}} = 30 + 0.40\mathbf{X}$	9.90

^{*}Radiochromate added to this side first.

Table 11. Uptake of radiochromate ions by isolated fish skin.

Fig- ure	Skin, Total C/Min.	50 ml. Ringer's Rinse, Total C/Min.	X Counts of Bathing Solution	C/g. Skin	Skin C/g. Water C/ml.
27	49,967	6,300	30,060	568,259	11.37
28	51,200	5,141	28,192	582,281	11.37
29	19,845	6,925	29,885	225,691	11.37
30	41,290	7,625	31,710	469,578	11.37

 $^{\#}_{\text{Observations}}$ for 60 and 80 minutes excluded.

DISCUSSION

Effects of Magnetic Fields on Sodium Ion Transport across Normal Frog Skin

In order to state that a particular experimental technique produced an effect, the results should be reproducible within statistical bounds. Neither homogeneous nor inhomogeneous magnetic fields, in the range of 3500 gauss, produced repeatable effects on the normal short-circuit current of frog skin. As long as the short-circuit chamber was not jarred or bumped, short exposures to magnetic fields, changes in the types of magnetic fields, or continuous exposures to these fields over a period of 10 to 16 hours did not result in effects that were discernible under the conditions of this experiment. Homogeneous magnetic fields up to 10,000 gauss, applied for 15 seconds, produced no effect on short-circuit current. In this latter study, however, inhomogeneous fields were not used, nor was such a field applied over a prolonged period of time.

Although the data of figure C-l are included, there is good evidence to indicate that the changes that occurred upon magnet insertion or removal were artifacts caused by jarring the chamber. Subsequent studies revealed that a mechanical tap on a short-circuit chamber either in or out of a magnetic field would produce a significant drop in frog skin potential, as well as in short-circuit current. The only possible effect

that a magnetic field may have produced was a greater degree of variation of the short-circuit curve, generally occurring between 100 and 200 minutes after the experiment was begun. This phenomenon was observed in less than half of the experimental runs. In view of the fact that an effect should be reproducible and that this variability is obviously not significantly different from the control value at a reasonable confidence level, it was not considered further.

Effects of Magnetic Fields on Sodium Ion Transport across Frog Skin Stimulated with Neurohypophyseal Extract or Epinephrine

The resulting effects of these hormones, when no magnetic field was present, compared favorably with data presented by Ussing and Zerahn (1951), although they utilized separate control studies rather than the pre-administration current values as a control. Calculations based on their data demonstrated that neurohypophyseal hormone stimulation produced an increase in short-circuit current of approximately 75 per cent, while the average increase in this experiment was about 100 per cent. In the case of epinephrine stimulation, they obtained about a 50 per cent increase in short-circuit current, while this experiment produced an average increase of approximately 45 per cent.

A magnetic field applied, following either neurohypophyseal extract or epinephrine administration, produced no significant effect. The application of a magnetic field prior to epinephrine administration likewise produced no effect.

Although the effects of neurohypophyseal extract administration were longer acting when the magnetic field was applied prior to the administration of this hormone, the normal control curve did not diminish as rapidly as did the other curves. Data from a single paired frog skin are shown in figure 14 and it is probable that this figure depicts a normal response for active frog skin.

Increased Potential Following Short-Circuiting of Frog Skin

An increase in potential, following short-circuiting of frog skin, was observed regularly throughout the entire study. Numerous observations, in addition to those listed in the Results section, showed that a magnetic field did not significantly alter this increase.

Evidence has already been presented to indicate the presence of a Na⁺ ion pool in the stratum germinativum cells (Koefoed-Johnsen and Ussing, 1958; Hoshiko and Ussing, 1960; Hoshiko, 1960; Gatzy and Clarkson, 1962). Ussing's active transport model envisions Na⁺ ions as diffusing into the stratum germinativum cells from the outward facing membrane and being transported across the inward facing side of the cell by an active process. The increased after-potential could be explained in a similar manner. Such a model would envision Cl⁻ ions as diffusing through both the outer and

inner membranes of the stratum germinativum cells. If this were so, then a Cl ion pool would also exist in the stratum germinativum. Under non-short-circuit conditions, an excess of Cl ions would exist in these cells due to the active removal of Na tions. The P.D. measured across the skin would reflect this ionic imbalance. Under short-circuit conditions. Cl ions are deposited on the outside Ag-AgCl electrode (outside with respect to the skin). Although the ionic balances on both sides of the frog skin are equal, the site of removal of Cl ions is far removed from the interior of the stratum germinativum cells, the site where the excess occurs. Although these excess Cl ions would diffuse toward the outside of the stratum germinativum cells, there is no large force acting upon them in either direction and they would tend to accumulate inside the cells. When short-circuiting is stopped, the excess Cl ions in the stratum germinativum cells are responsible for the increased after-potential. Within limits, the longer the duration of short-circuiting, the greater would be the amount of Cl ion accumulation.

The downward slopes immediately following the voltage peak attained after short-circuiting ceased, when plotted on semi-logarithmic paper, varied directly in magnitude with the duration of short-circuit current.

Radiochromate Ion Movement across Frog Skin

With a single exception, the linear regression line

resulting from a plot of Cr⁵¹ activity versus time did not extend through zero. These data infer the presence of a 2-component system: a fast component already completed before the first 10 minute sample was obtained, and a slower component extending over the entire three hour period. Figure 25, the one exception to these observations, represents a frog skin in which very low Na⁺ ion transport was taking place, the maximum short-circuit current being 3.5 µA per cm². Another graph of a skin that was accidentally damaged by adding a solution of low pH was similar to this one in appearance. It is probable that figure 25 represents a skin that is not metabolically active, and that slopes of a two-step nature would characterize the response of healthy skins.

In a 2-component system using radiochromate, it would be inadvisable to calculate flux on the basis of the fraction of activity present in a one ml. aliquot appearing on the other side in one hour, as Ussing (1949b) did in the case of iodide ion. Flux ratios based on the slopes of the second slow component are presented in table 5 and they compare closely with calculated values based on the P.D. existing across the skin. Variations that occurred could be due to the non-uniformity of the P.D. throughout the experiment and an average of P.D. measurements will not necessarily be indicative of the true mean P.D. Measured and calculated flux ratios do not agree well in figure 25 which does not possess

a 2-component system. Ussing's method of calculating flux ratios (1949b) assumes a uniform movement of ions across the skin. This method was employed and values, using activity ratios at 1, 2, and 3 hours are shown in table 8.

All Min/Mout flux ratios are expressed in table 12 for comparison. Figures 22, 24, and 28 represent 2-component systems, while figure 25 represents a 1-component system.

In all cases, flux ratios based on the slope of the second component agree more closely with calculated values than do those where the per cent of activity that had crossed the membrane at a given time was used.

Table 12. Flux ratios determined using different criteria

Figure	Flux Ratios Calculated	Flux Ratios Based on: 2nd Component Activities at			
	from Formula	Slopes		2 hr	
22	2.0	2.5	0.9	1.2	1.3
24	2.6	2.3	10.6	7.8	6.4
25	1.1	1.9	1.9	1.9	1.9
28	6.4	2.6	27.8	20.1	16.5

The first rapid increment could be due to clogging of skin membrane pores by radiochromate ions. If this phenomenon occurred, one would expect an increase in the P.D. across the skin if Cl ions diffuse through the same pores. Although potentials did vary in the experiments, none were observed that would be considered abnormally large. There

was no consistent pattern observed in the direction of potential change. All observed changes appeared to be of a random nature within the realm of expected observations. If permanent binding took place, the initial rapid component should not appear when the radiochromate was added to the opposite chamber in the second half of the experiment. only applicable data (figures 22, 24, and 28) do show that the initial rapid component was greater in the first half of the experiment. The half-hour washing in 5 changes of Ringer's solution could have removed some loosely bound radiochromate, accounting for the smaller rapid increase observed in the second half of the experiments. If the diminution of the first rapid component was due to radiochromate ion binding by the skin, the second slower phase must represent a component in which binding is not involved, since flux is apparently a linear function and follows the electrochemical diffusion laws. The P.D. across the skin is not greatly changed, inferring that the route taken by Cl ion across the skin is little affected. Data obtained suggest the possibility of two routes being available for movement of chromate across frog skin. The first route is not available to the Cl ion movement and, while allowing rapid chromate ion movement, is readily occluded by binding. The second route is little affected by chromate ion binding. Another possibility is that radiochromate ions bind rapidly up to a point where the charge on the site is neutralized by the negatively charged ions, without fully occluding the passageway. This would allow radiochromate ions to pass through the site at a reduced rate.

Magnetic fields did not exert any great modification of radiochromate fluxes. However an analysis of slope data indicates some possible effects. In figure 28, magnet insertion increased the slope from a pre-insertion level of 1.840 to 2.915 in influx studies (Min) and decreased the slope from a pre-insertion level of 0.595 to 0.295 in efflux (Mout) studies. Such an effect could be explained by applying the Lorentz equation as the magnetic field was unchanged. Efflux was also decreased (figure 27) with the slope dropping from a pre-insertion level of 0.555 to 0.395 when a homogeneous field, HN, was applied. No examination of slope data was attempted for figure 26 since no appreciable amount of radiochromate ion passed through the skin.

Radiochromate Ion Movement across Fish Skin

In contrast to frog skin, fish skin did not actively transport ions. This is so, both in living fish and isolated fish skin in the short-circuit chamber. The maximum short-circuit current of 1.5µA measured across the abdominal skin of a living rainbow trout could represent a reflection of a higher P.D. existing in some other areas of the body. Although not reported in this work, the P.D. between the left

first afferent artery of the same fish and tap water was measured. It varied from 3.5 to 4.0 mV. Although P.D. measurements vary over different regions of a fish, they are less than those observed in living frogs anesthetized with urethane. In the latter, potentials of 15 mV were measured across abdominal skin with short-circuit current amounting to 150 µA.

Anatomical considerations of the two species tend to support these findings. Although frog skin contains mucus secreting cells, the skin is generally not slimy. Frog skin is loosely attached to the underlying musculature and possesses lymph sacs occupying the space between the skin and musculature. Certain areas of the corium appear to be well vascularized. Trout skin, on the other hand, does possess a protective mucous layer as well as small cycloid scales and is firmly affixed to the underlying musculature.

The data indicate a 2-component system operates in radiochromate ion movement across fish skin. All 8 of the linear regression equations intercepted the Y axis at a point greater than zero. If only a single component system were involved the intercepts would be expected to cross the Y axis near zero and be equally divided above and below it. The initial rapid component was already completed before the first sample aliquot was taken at 20 minutes. The graphs are similar in a general way to those obtained in the frog

skin experiments thus the same interpretation can be made. The initial surge of radiochromate ion across fish skin is due, possibly to its passage through areas where it is bound, thus either completely occluding the area, with other uncharged passage sites being unaffected, or reducing the size of the pore to a point where the charge was neutralized, but still leaving a smaller opening at which binding did not take place. Measured flux ratios of $M_{\rm in}/M_{\rm out}$ were based on slope calculations. Since no P.D. existed, calculated ratios of $M_{\rm in}/M_{\rm out}$ would all equal one. An examination of the four flux ratios, 1.2*, 4.1, 0.1, and 9.9, although indicating the possibility of a net inward flux, does not justify such a conclusion, due to the value less than one. A more detailed study would be necessary before any conclusion other than $M_{\rm in}/M_{\rm out}=1$ could be drawn.

Again, as with frog skin, fish skin took up radiochromate ions from the Ringer bath. All four ratios of skin counts per gram divided by counts per ml. of Ringer's solution equaled 11.37. It is not known whether fish skin takes up radiochromate ion at a highly constant level or whether these similarities represent pure chance. Previously unpublished data concerning radiochromate uptake by rainbow trout, over a 7 day period, indicated that very little radiochromate is bound by the skin. Only three out of fifteen observations showed an accumulation greater than that of the

^{*}Observations for 60 and 80 minutes not included.

aquaria water in which the fish were maintained. These ratios of skin counts per gram divided by water counts per ml. equaled 2.5, 2.2, and 1.2. The ratios of the remaining twelve observations were less than 0.5. This current study showed that rainbow trout skin is capable of binding radio-chromate with ratios (tissue/medium) of about 10. If radiochromate had passed through the skin of living fish in large quantities, then uptake ratios of near 10 should be obtained. As the majority of the ratios was less than 1, radiochromate ion must pass through the skin of a living fish slowly. The movement of radiochromate ion across fish skin detected in this experiment does not necessarily indicate true conditions as they exist in a living fish. The skin was difficult to remove and in the process, mucus and/or scales may have been disturbed.

The data of figure 32 was considered as too variable to examine the slopes for possible effects of an applied magnetic field. This experiment was conducted in a manner similar to the frog skin studies, hence one would expect inward movement to be enhanced somewhat, while outward movement should be diminished as predicted by the Lorentz equation.

SUMMARY AND CONCLUSIONS

- 1. Magnetic fields in the range of 3500 gauss were found to exert no repeatable effects on sodium ion transport across isolated frog skin.
- 2. The total electrical output of 16 frog skins averaged 233 \pm 97 microampere hours or 0.84 \pm 0.35 coulombs, which corresponds to 0.20 \pm 0.08 milligrams of sodium transported.
- 3. Neurohypophyseal hormone stimulation produced an approximate 100 per cent increase in short-circuit current of frog skin. Magnetic fields exerted no influence on this increase.
- 4. Epinephrine stimulation produced an increase of approximately 45 per cent in short-circuit current of frog skin. Magnetic fields exerted no influence on this increase.
- 5. An increased potential difference occurring subsequent to cessation of short-circuiting of frog skin was observed and investigated. It was proposed that this increased electrical potential resulted from Cl⁻ ion accumulation in the stratum germinativum cells when the skin was short-circuited. This increased potential was unaffected by magnetic fields.
- 6. Radiochromate ions crossed frog skin in a two-step process; a rapid initial step completed before the first 10 minute aliquot was taken and a slow second step that remained linear over a three-hour observation period. Radiochromate

flux ratios of M_{in}/M_{out}, determined by using the slopes of the linear regression lines of the second slow components, compared favorably with calculated values. It was thus assumed that the second component represented radiochromate ion movement caused by the electrochemical potential gradient existing across the frog skin. Arguments were presented to support the concept that the first rapid component is quenched due to radiochromate ion binding in or on membrane pores, thereby either diminishing the pore size or occluding it altogether.

- 7. Possible effects of a magnetic field on radiochromate ion movement across frog skin were observed. Such effects could be explained by application of the Lorentz equation.
- 8. Potential differences measured across the skin of living rainbow trout were small and, depending on the site of measurement, varied from 1 to 4 millivolts. A potential difference of 15 millivolts, that short-circuited at 150 microamperes, was measured across the skin of a living frog.
- 9. The possibility of a two-component system of radio-chromate ion movement across fish skin was observed. Since the potential difference across isolated fish skin was zero, all calculated flux ratios of $M_{\rm in}/M_{\rm out}$ should equal one. Although variable, flux ratios based on the ${\rm Cr}^{51}$ activity that crossed the skin ranged both above and below one.

10. Isolated fish skin took up radiochromate ion in amounts ten times greater than that present in the Ringer's bathing solutions. Because skin taken from fish living in water containing radiochromate ion showed little activity, it was concluded that radiochromate ion probably does not cross the skin of living rainbow trout to any great extent.

LITERATURE CITED

- Ackerman, E. 1962. Biophysical Science. Prentice-Hall, Englewood Cliffs. p. 525.
- Amberson, W. R. 1936. On the mechanism of the production of electromotive forces in living tissues. Cold Spring Harbor Symp. Quant. Biol. 4:53-62.
- Andersen, B., and H. H. Ussing. 1957. Solvent drag on non-electrolytes during osmotic flow through isolated toad skin and its response to antidiuretic hormone.

 Acta Physiol. Scand. 39:228-239.
- Barnothy, J. M. 1959. Influence of magnetic fields upon the development of tumors in mice. Proc. 1st Nat'1. Biophy. Conf. Yale Univ. Press, New Haven. p. 735.
- Barnothy, J. M. 1960. Biologic effects of magnetic fields. Vol. 3, pp. 61-64. Medical Physics. O. Glasser, ed. Year Book Publishers, Chicago.
- Barnothy, J. M., M. F. Barnothy, and I. Boszormenyi-Nagy. 1956. Influence of a magnetic field upon the leucocytes of the mouse. Nature. 177:577-578.
- Barnothy, M. F. 1959. Influence of magnetic fields upon the leucocytes of the mouse. Proc. 1st Nat'l. Biophy. Conf. Yale Univ. Press, New Haven. p. 734.
- Barnothy, M. F., and J. M. Barnothy. 1958. Biological effect of a magnetic field and the radiation syndrome. Nature. 181:1785-1786.
- Brachet, J. 1961. The living cell. Sci. Amer. 205:50-61.
- Brown, A. C. 1962. <u>In vivo</u> frog skin short-circuit current and open circuit voltage. Fed. Proc. 21:144.
- Brown, F. A., Jr. 1959. The rhythmic nature of animals and plants. Amer. Sci. 47:147-168.
- Brown, F. A., Jr., M. F. Bennett, and W. J. Brett. 1959. Effects of imposed magnetic fields in modifying snail orientation. Biol. Bull. 117:406.
- Brown, F. A., Jr., M. F. Bennett, and H. M. Webb. 1961.

 A magnetic compass response of an organism. Biol.

 Bull. 119:65-74.

- Brown, F. A., Jr., W. J. Brett, M. F. Bennett, and F. H. Barnwell. 1960. Magnetic response of an organism and its solar relationships. Biol. Bull. 118:367-381.
- Brown, F. A., Jr., W. J. Brett, and H. M. Webb. 1959. Fluctuations in the orientation of the mud snail, Ilyanassa obseleta, in constant conditions. Biol. Bull. 117:406-407.
- Brown, F. A., Jr., H. M. Webb, M. F. Bennett, and F. H. Barnwell. 1959. A diurnal rhythm in response of the snail <u>Hyanassa</u> to imposed magnetic fields. Biol. Bull. 117:405-406.
- Brown, F. A., Jr., H. M. Webb, and W. J. Brett. 1960.
 Magnetic response of an organism and its lunar
 relationships. Biol. Bull. 118:383-392.
- Canessa-Fischer, M., C. M. Edelmann, Jr., and R. P. Davis. 1962. The coupling of ion transport and energy metabolism in the toad bladder. Fed. Proc. 21:148.
- Capraro, V., and G. Bernini, 1952. Mechanism of action of extracts of the posthypophysis on water transport through the skin of the frog (Rana esculenta). Nature. 169:454.
- Clarkson, T. W. 1962. Interdependence between the flows of water and electrolytes across the isolated rat ileum. Fed. Proc. 21:144.
- Cole, K. S. 1949. Dynamic electrical characteristics of the squid axon membrane. Arch. Sci. Physiol. (Par.) 3:253-258.
- Curran, P. F., and J. R. Gill, Jr. 1962. The effect of calcium on sodium transport by frog skin. J. Gen. Physiol. 45:643-649.
- Curran, P. F., F. C. Herrera, and W. J. Flanigan. 1962. Sites of calcium and antidiuretic hormone action on sodium transport by frog skin. Fed. Proc. 21:145.
- Davson, H. 1959. A textbook of general physiology. Little, Brown and Co., Boston. 846 p.
- Eiselein, J. E., H. M. Boutell, and M. W. Biggs. 1961. Biological effects of magnetic fields - negative results. Aerospace Med. 32:383-386.

- Engback, L., and T. Hoshiko. 1957. Electrical potential gradients through frog skin. Acta Physiol. Scand. 39:348-355.
- Francis, W. L. 1933. Output of electrical energy by frog skin. Nature. 131:805.
- Frazier, H. S. 1962. The electrical potential profile of the isolated toad bladder. J. Gen. Physiol. 45:515-528.
- Gatzy, J., and T. W. Clarkson. 1962. Relative ionic permeabilities of the mucosal and serosal surfaces of isolated toad bladder. Fed. Proc. 21:149.
- Heinmets, F., and A. Herschman. 1961. Considerations on the effects produced by superimposed electric and magnetic fields in biological systems and electrolytes. Phys. Med. Biol. 5:271-288.
- Hevesy, G., E. Hofer, and A. Krogh. 1935. The permeability of the skin of frogs to water as determined by D₂O and H₂O. Skand. Arch. Physiol. 72:199.
- Hodgkin, A. L., A. F. Huxley, and B. Katz. 1952. Measurement of current-voltage relations in the membrane of the giant axon of Loligo. J. Physiol. 116:424-428.
- Hodgkin, A. L., and R. D. Keynes. 1955. The potassium permeability of a giant nerve fiber. J. Physiol. 128:61-88.
- Hokin, L. E., and M. R. Hokin. 1960. Phosphatidic acid as a carrier for Na⁺ ions. Fed. Proc. 19:130.
- Holter, H. 1961. How things get into cells. Sci. Amer. 205:167-180.
- Hoshiko, T. 1960. Frog skin epithelial cell membrane resistance. Fed. Proc. 19:127.
- Hoshiko, T. 1961. Effect of sodium replacement by guanidine and hydrazine on frog skin current. Fed. Proc. 20:142.
- Hoshiko, T., and L. Engbaek. 1956. Microelectrode study of the frog skin potential. 20th Int. Physiol. Cong., Brussels. p. 443.
- Hoshiko, T., and J. P. Seldin. 1962. Ionic requirements for secretion by frog skin glands. Fed. Proc. 21:151.

- Hoshiko, T., and H. H. Ussing. 1960. The kinetics of Na²⁴ flux across amphibian skin and bladder. Acta Physiol. Scand. 49:74-81.
- Huber, G. S., and R. A. Phillips. 1962. Effect of <u>Cholera</u> <u>vibrio</u> products on active transport. Fed. Proc. 21:144.
- Huf, E. 1935. Versuche über den zusammenhang zwischen stoffwechsel, potentialbildung und funktion der froschhaut. Pflugers Arch. ges. Physiol. 235:655-673.
- Huf, E. G. 1937. Die reproduzierbarkeit des reidschen versuchs. Pflugers Arch. ges. Physiol. 238:97-102.
- Huf, E. G., and N. S. Doss. 1959. Effect of temperature on electrolyte metabolism of isolated frog skin. J. Gen. Physiol. 42:525-531.
- Huf, E. G., N. S. Doss, and J. P. Wills. 1957. Effects of metabolic inhibitors and drugs on ion transport and oxygen consumption in isolated frog skin. J. Gen. Physiol. 41:397-417.
- Huf, E. G., L. L. Eubank, A. D. Campbell, and B. B. Taylor. 1962. Effects of redox systems on active ion transport in frog skin. Fed. Proc. 21:145.
- Karger, W. 1962. Oscillatorische phänomene des elektrischen potentials an der isolierten froschhaut nach temperaturwechsel. Pflugers Arch. ges. Physiol. 274:331-339.
- Karger, W., und D. Krause. 1962. Der einfluss von temperaturstörungen auf potential und kurzschlussstrom der isolierten froschhaut bei verwendung impenetrabler anionen. Pflügers Arch. ges. Physiol. 274:340-344.
- Katz, J. 1960. The biology of heavy water. Sci. Amer. 203:106-116.
- Katzin, L. J. 1940. The use of radioactive tracers in the determination of irreciprocal permeability of biological membranes. Biol. Bull. 79:342.
- Kirschner, L. B. 1953. Effect of cholinesterase inhibitors and atropine on active sodium transport in frog skin. Nature. 172:348.
- Kitching, J. A., and J. E. Podfield. 1960. Permeability of ciliates to heavy water. J. Exp. Biol. 37:73-82.

- Knoll, J. 1959. Accumulation and elimination of hexavalent chromium in rainbow trout. Master's Thesis. Mich. State Univ., East Lansing.
- Knoll, J., and P. O. Fromm. 1960. Accumulation and elimination of hexavalent chromium in rainbow trout. Physiol. Zool. 33:1-8.
- Koblick, D. 1958. The characterization and localization of frog skin cholinesterase. J. Gen. Physiol. 41:1129-1134.
- Koefoed-Johnsen, V., H. Levi, and H. H. Ussing. 1952. The mode of passage of chloride ions through the isolated frog skin. Acta Physiol. Scand. 25:150-163.
- Koefoed-Johnsen, V., H. H. Ussing, and K. Zerahn. 1952. The origin of the short-circuit current in the adrenaline stimulated frog skin. Acta Physiol. Scand. 27:38-48.
- Koefoed-Johnsen, V., and H. H. Ussing. 1953. The contributions of diffusion and flow to the passage of D₂O through living membranes. Effect of neurohypophyseal hormone on isolated anuran skin. Acta Physiol. Scand. 28:60-76.
- Koefoed-Johnsen, V., and H. H. Ussing. 1956. Nature of the frog skin potential. 20th Int. Physiol. Cong., Brussels. p. 511.
- Koefoed-Johnsen, V., and H. H. Ussing. 1958. The nature of the frog skin potential. Acta Physiol. Scand. 42:298-308.
- Krogh, A. 1937. Osmotic regulation in the frog (\underline{R} . esculenta) by active absorption of chloride ions. Skand. Arch. Physiol. 76:60-74.
- Krogh, A. 1938. The active absorption of ions in some freshwater animals. Z. vergl. Physiol. 25:335-350.
- Leaf, A. 1960. Some actions of neurohypophyseal hormones on a living membrane. J. Gen. Physiol. 43(5):175-189(Part 2).
- Leaf, A., J. Anderson, and L. B. Page. 1957. Active sodium transport by the isolated toad bladder. J. Gen. Physiol. 41:657-668.

- Leaf, A., and A. Renshaw. 1957. The anerobic active ion transport by isolated frog skin. Bio. J. 65:90-93.
- Linderholm, H. 1954. On the behavior of the "sodium pump" in frog skin at various concentrations of sodium ions in the solution on the epithelial side. Acta Physiol. Scand. 31:36-61.
- Lindley, B. D., and T. Hoshiko. 1962. Osmotic and solvent drag effects of D_2O on isolated frog skin. Fed. Proc. 21:151.
- Lund, E. J., and P. Stapp. 1947 Use of the iodine coulometer in the measurement of bioelectrical energy and the efficiency of the bioelectrical process. p.235-254. In E. J. Lund and P. Stapp, Bioelectric fields and growth, Univ. Texas Press, Austin.
- Maffly, R. H. and I. S. Edelman. 1961. Relationship of carbohydrate metabolism to sodium transport. Fed. Proc. 20:137.
- Marmont, G. 1949. Studies on the axon membrane. J. Cell. Comp. Physiol. 34:351-382.
- Meyer, K. H., and P. Bernfeld. 1946. The potentiometric analysis of membrane structure and its application to living animal membranes. J. Gen. Physiol. 29:353-378.
- Montgomery, D. J., and A. E. Smith. 1959. Do magnetic fields affect living processes? Unpublished.
- Ottoson, D., F. Sjostrand, S. Stenstrom, and G. Svaetichin.
 Microelectrode studies on the E.M.F. of the frog skin
 related to electron microscopy of the dermo-epidermal
 junction. Acta Physiol. Scand. 29(Suppl. 106):611-624.
- Pauling, L. C. 1960. The nature of the chemical bond. 3rd ed. Cornell Univ. Press, Ithaca. p. 611-617.
- Peterson, M. J., and I. S. Edelman. 1962. Reversibility of calcium inhibition of vasopressin action on the toad bladder. Fed. Proc. 21:146.
- Prescott, D. M., and E. Zeuthen. 1953. Comparison of water diffusion and water filtration across cell surfaces. Acta Physiol. Scand. 28:77-94.

- Robertson, D. J. 1962. The membrane of the living cell. Sci. Amer. 206:64-72.
- Scheer, B. T. 1962. Electrochemical diffusion. Science. 135:313-314.
- Sidel, V. W., and J. F. Hoffman. 1961. Water transport across membrane analogues. Fed. Proc. 20:137.
- Skjelkvale, L., V. K. Nieder, and E. G. Huff. 1960. Metabolic studies on frog skin epithelium. J. Cell. Comp. Physiol. 56:43-54.
- Stapp, P. 1941. Efficiency of electrical energy production by surviving frog skin, measured by iodine coulometer. Proc. Soc. Exp. Biol. 46:383-384.
- Ussing, H. H. 1949a. The active transport through the isolated frog skin in the light of tracer studies. Acta Physiol. Scand. 17:1-37.
- Ussing, H. H. 1949b. The distinction by means of tracers between active transport and diffusion. Acta Physiol. Scand. 19:43-56.
- Ussing, H. H. 1952. Some aspects of the application of tracers in permeability studies. Advanc. Enzymol. 13:21.
- Ussing, H. H. 1960a. The alkali metal ions in isolated systems and tissues. Handbuch Exp. Pharmakol. 13:1-195.
- Ussing, H. H. 1960b. The frog skin potential. J. Gen. Physiol. 43(5):135-147.
- Ussing, H. H., and K. Zerahn. 1951. Active transport of sodium as the source of electric current in the short-circuited isolated frog skin. Acta Physiol. Scand. 23:110-127.
- Zerahn, K. 1956. Oxygen consumption and active sodium transport in the isolated and short-circuited frog skin. Acta Physiol. Scand. 36:300-318.

APPENDIX A

SUBSTANCES AFFECTING SODIUM TRANSPORT ACROSS FROG SKIN

Table A-1. Agents stimulating active sodium transport in amphibian skin (Ussing, 1960)

Group	Substance	Dose	Applied on
Neurohypo- physeal	vasopressin	0.1-4.0 I.U./25 ml.	inside
hormones	oxytocin	0.1-2.0 I.U./25 ml.	inside
Oxidants	permanganate	$3 \cdot 10^{-4} \text{ M/1.}$	inside
	bromine	$1 \cdot 10^{-3} \text{ M/1}.$	inside
	periodate	5 · 10 M/1.	inside
Reductants	BAL	$3 \cdot 10^{-4} \text{ M/1}.$	inside
Heavy metals	Ag ⁺	$1 \cdot 10^{-4} \text{ M/1.}$	inside
Alkaloids	atropine	$0.3-9 \cdot 10^{-4} \text{ M/1.}$	outside
	curare	$0.1-1.3 \cdot 10^{-4} \text{ M/1}.$	outside
Diuretics	mersalyl	10-4	inside
	aminophylline	2 • 10-3	inside

Table A-2. Agents inhibiting sodium transport in amphibian skin (Ussing, 1960)

Group	Substance	Dose giving at least 50% inhibition M/1.	Applied on
Metabolic inhibitors	cyanide	3 · 10 ⁻⁵	inside
IMITOTOOLS	fluoroacetate	1 · 10 ⁻³	inside
	azide	1 • 10-3	inside
	diethylmalonate	i · 10 ⁻³	inside
	iodoacetate	1 • 10-3	inside
	2,4 dinitrophenol	5 · 10 ⁻⁵	inside outside both sides
	arsenite	1 · 10 ⁻⁴	inside
	fluorije	1 · 10-2	inside
Cholines-	(TEP) tetraethyl- pyrophosphate eserin	6 · 10 ⁻³	inside
terase inhibitors		1 • 10-2	outside
Sulfonamides	p-toluenesulfonamide	1.8 • 10-3	inside
	sulfanilamide	2 · 10 ⁻³	inside
Narcotics	co ₂	5%	both sides
Cardiac glucosides	g-strophanthin	1 · 10-6	inside

Table A-3. Effect of various metabolites on $\rm O_2$ -consumption of epithelial homogenate (Skjelkvale et al., 1960)

12 umoles of each substrate	0 ₂ consumption		
in 3 ml.	Total	Net	
	µ1/hr/200	mg wet tissue	
a. No substrate	4 C	-	
b. Pyruvate	48	8	
Fumarate	161	121	
Fumarate + pyruvate	223	183	
c. Succinate	162	122	
Succinate + pyruvate	227	187	
d. Citrate	173	133	
Citrate + pyruvate	171	131	
Citrate + pyruvate + fumarate	199	159	
e. ∝-Ketoglutarate	203	163	
1-Glutamate	221	181	
∠-Ketoglutarate + 1-glutamate	233	193	

APPENDIX B

PHYSICAL PROPERTIES OF MAGNETISM

PHYSICAL PROPERTIES OF MAGNETISM

The Development of a Magnetic Field

Electric currents (charges in motion) and magnetism are intimately related phenomena. Oersted first demonstrated that a compass needle was deflected when placed near a wire carrying current. Ampère demonstrated that two parallel wires carrying current in the same direction attract each other. Such electromagnetic effects involve three-dimensional relationships which are considered in Ampère's Field Law:

$$dH = id\overline{1} \frac{\overline{r}}{r^3}$$

where:

dH = differential magnetic field intensity

i = current

 $d\overline{l}$ = differential length of current

 \overline{r} = radius vector

r = distance from a point charge

The magnitude of a magnetic field at a point r is directly proportional to the current element $id\overline{l}$. The direction of the field is indicated by the right hand rule, i.e., if the thumb of the right hand points in the direction of current flow, the curled fingers will indicate the direction of the magnetic field around such current flow.

Electrostatics (electric charges at rest) and magnetism

are also intimately related. Where charged bodies at rest are small compared with the distance from their centers, the electrical displacement exerted by them can be expressed by Coulomb's Law:

$$dD = dq \frac{\overline{r}}{r^3}$$

where:

D = electrical displacement

q = charge

Although charged particles are responsible for establishing magnetic fields, such fields can also influence charged particles. The total force experienced by a charged object moving in an electric and magnetic field is given by the Lorentz Equation:

$$dF = dq \ (\overline{E} + \frac{v}{c} \times \overline{\beta})$$

where:

F = force experienced by a charged object
moving in a magnetic field

q = charge on the object

v = velocity of the object

c = velocity of light

 $\overline{\mathbf{E}}$ = electric field strength

 $\bar{\beta}$ = magnetic field strength

Such a force is the sum of electric field strengths and magnetic field strengths. Heinmets and Herschman (1961) consider the process as one in which the first term, dq $\overline{\mathbf{E}}$, causes a velocity of charged particles, while the second term, dq $\frac{\mathbf{v}}{\mathbf{c}} \times \overline{\mathbf{\beta}}$, is capable of changing the direction in which the particles move. They reported that bacteria in a modified microelectrophoresis chamber moved in a straight line when under the influence of only an electric field but changed the direction of movement 20° when a magnetic field was applied, although still proceeding in a straight line.

Special simple assemblages of charges, possibly in motion, include monopoles and dipoles.

Monopoles

A group of localized charges when observed from a distance can be considered as comprising one point.

The force exerted vectorally from such a point can be described by the integral form of Coulomb's Law:

$$\overline{D} = \int dq \frac{\overline{r}}{r^3} = \frac{\overline{r}}{r^3} q$$

Dipoles

Dipoles can also develop from such groups of localized charges where both positive and negative components are present.

Although monopoles can be present in electrostatic

charges, they are unknown in magnetic fields. The simplest element to consider from the standpoint of magnetic fields is the current loop. Mathematical treatment shows that at large distances from a closed loop, the magnetic field has the form shown in figure B-1. At a distance r, such a field has a radial component and a tangential component:

$$H_{\text{radial}} = -\frac{2M}{r^3} \cos \theta$$

$$H_{tangential} = \frac{M}{r3} \sin \theta$$

where:

M = iA

i = current flowing in the loop

A = area of the loop

Diamagnetism (Pauling, 1960)

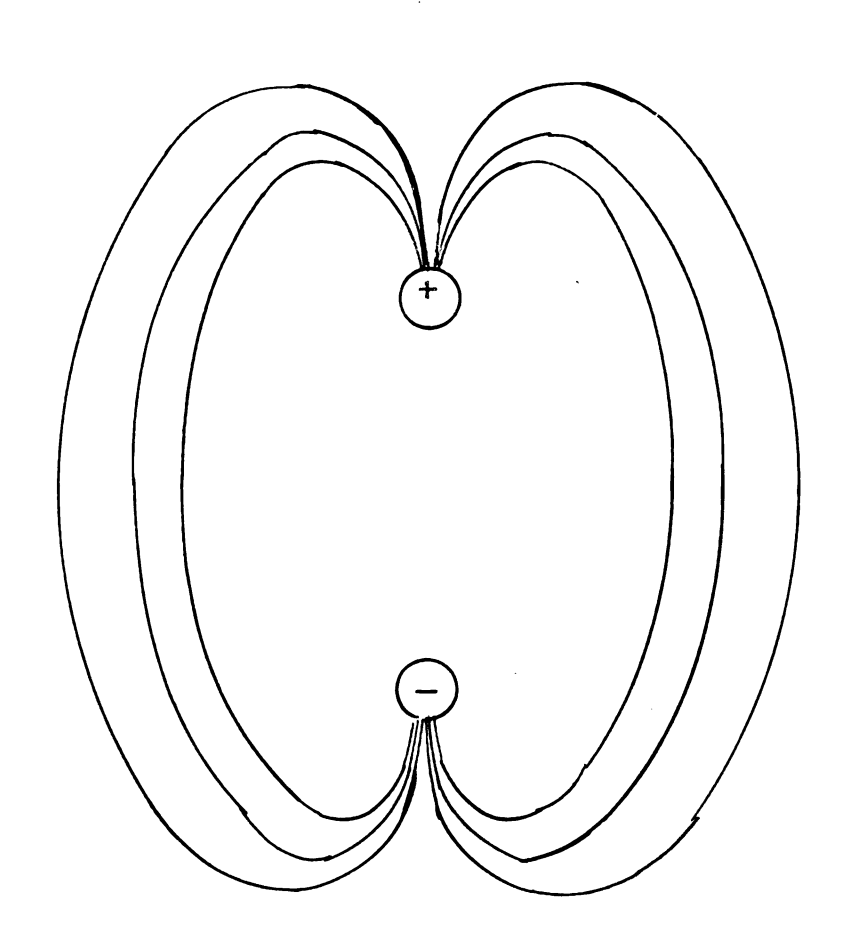
A sample of a diamagnetic substance placed in an inhomogeneous magnetic field is acted upon by a force tending to push it away from the strong field region. This force is proportional to the diamagnetic susceptibility of the substance, which is defined as the ratio of the induced moment, μ , to the field strength, H:

$$\mu = \chi H$$

where:

 χ = magnetic susceptibility

Figure B-1. The magnetic field surrounding a closed loop as viewed from a great distance.



The effect of the application of a magnetic field to an atom or monatomic ion is to cause the electrons to assume an added rotation about an axis parallel to the field direction and passing through the nucleus. This rotation is called the Larmor precession. For spherically symmetrical atoms, the molar diamagmetic susceptibility is:

$$\chi_{\text{molar}} = -\frac{\text{Ne}^2}{6\text{mc}^2} \sum_{i} \overline{r}_{i}^2$$

where:

 χ_{molar} = molar diamagnetic susceptibility

N = Avogadro's number

e = charge of electron

m = mass of electron

c = velocity of light

r2= average distance squared of the electron from the nucleus

Diamagnetic susceptibility is in general independent of the temperature. Diamagnetic substances of biological interest include hydrogen, carbon, nitrogen, phosphorus, sulphur, chlorine, copper, zinc and water.

Paramagnetism (Pauling, 1960)

Paramagnetic substances, when in a magnetic field of ordinary strength, develop a magnetic moment in the field direction that is proportional to the strength of the field.

Most paramagnetic substances have susceptibilities a hundred or a thousand times as great as the customary diamagnetic susceptibilities, and with opposite sign (mass susceptibility (per g) + 10^{-4} or 10^{-3} , as compared with about -1 x 10^{-6} for diamagnetic substances). The molar paramagnetic susceptibility is given by Curie's Law:

$$\chi_{\text{molar}} = \frac{c_{\text{molar}}}{T} + D$$

where:

 χ_{molar} = molar paramagnetic susceptibility

 $C_{molar} = molar Curie constant$

T = absolute temperature

D = the diamagnetic contribution
 (negative value)

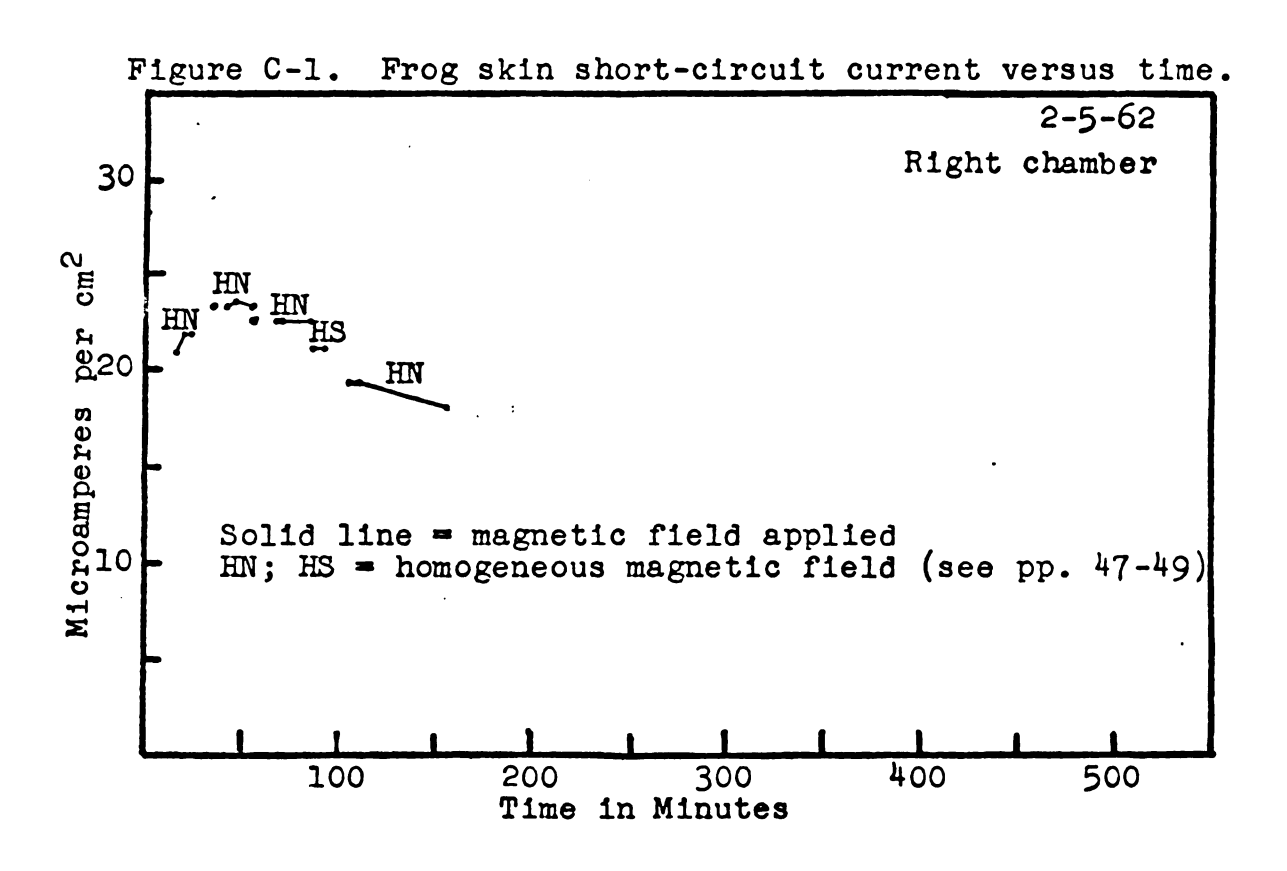
Paramagnetic susceptibility is strongly dependent on temperature as is apparent in Curie's equation. This equation applies to gases, solutions, and some crystals. Paramagnetic substances of biological interest include oxygen, sodium, potassium, and calcium.

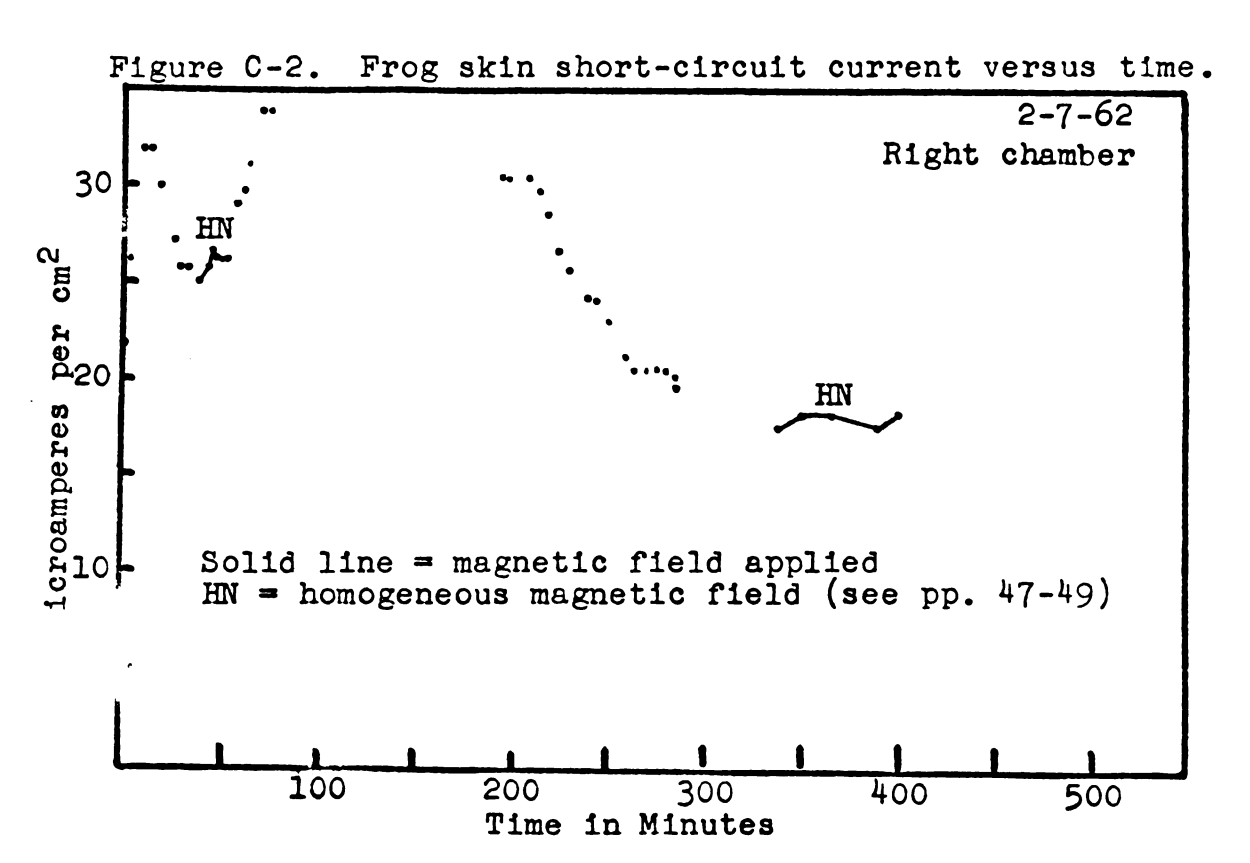
Other Types of Magnetism

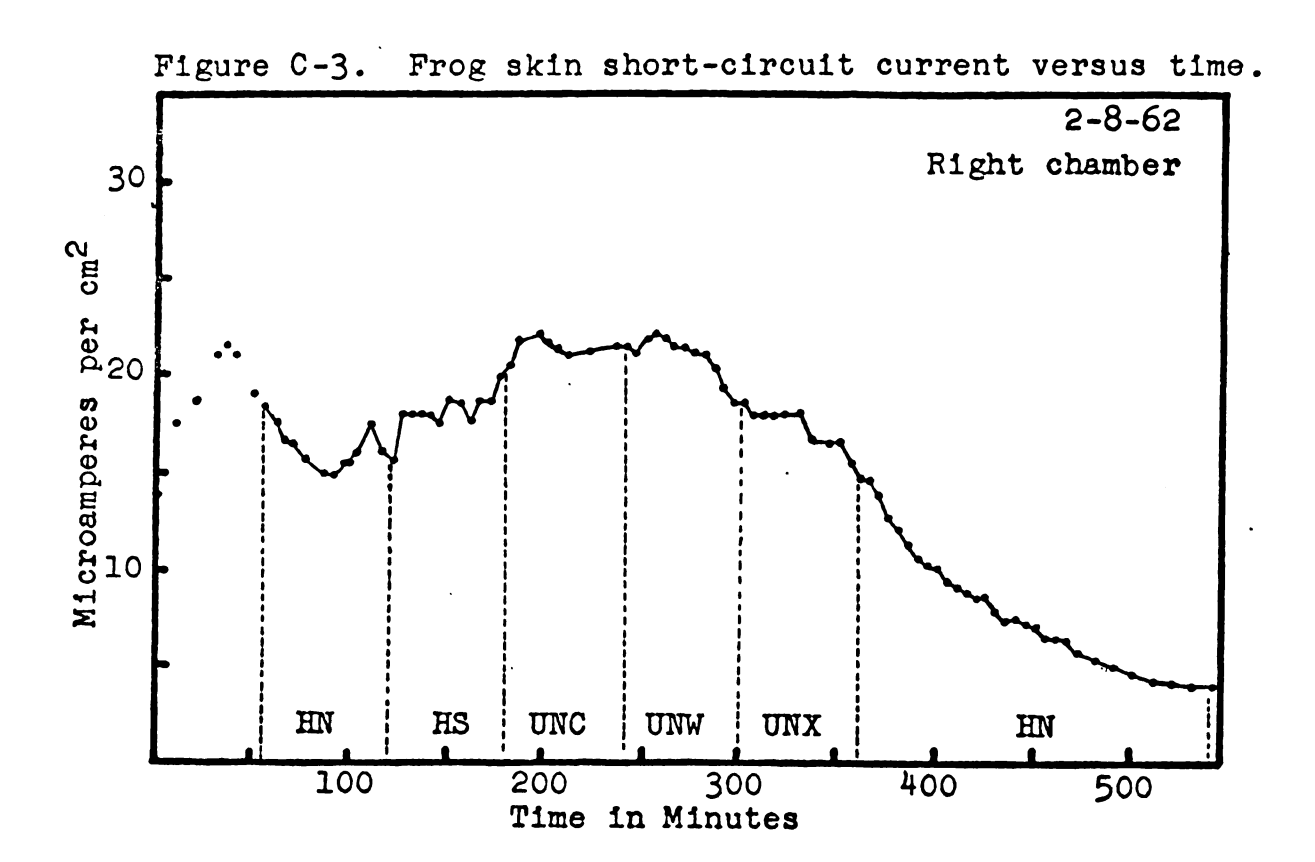
Ferromagnetism, antiferromagnetism, and ferrimagnetism occur when there are strong cooperative interactions of electron spins at the atomic level. As a result, they are important only in condensed and concentrated substances at low temperatures. Only rarely will such cooperative phenomena be of interest from a biological standpoint.

APPENDIX C

SHORT-TERM BIOMAGNETIC STUDIES

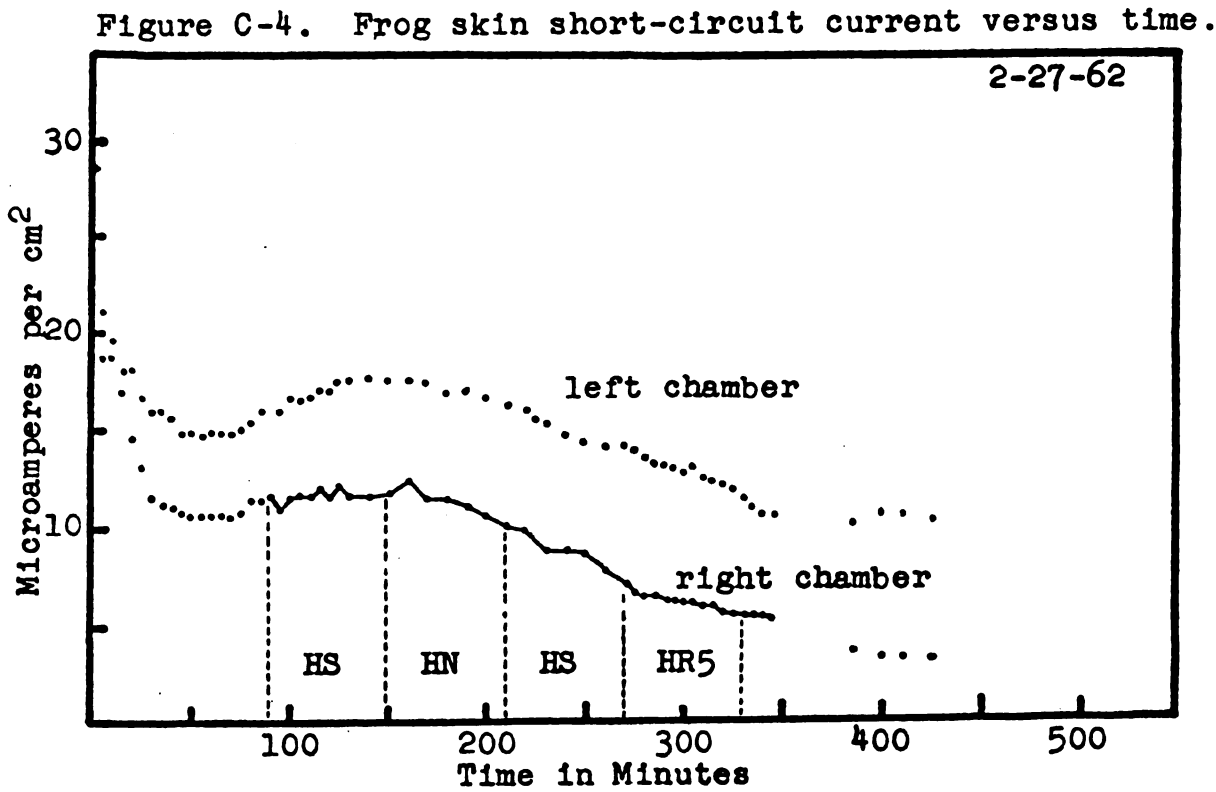


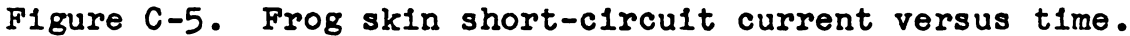


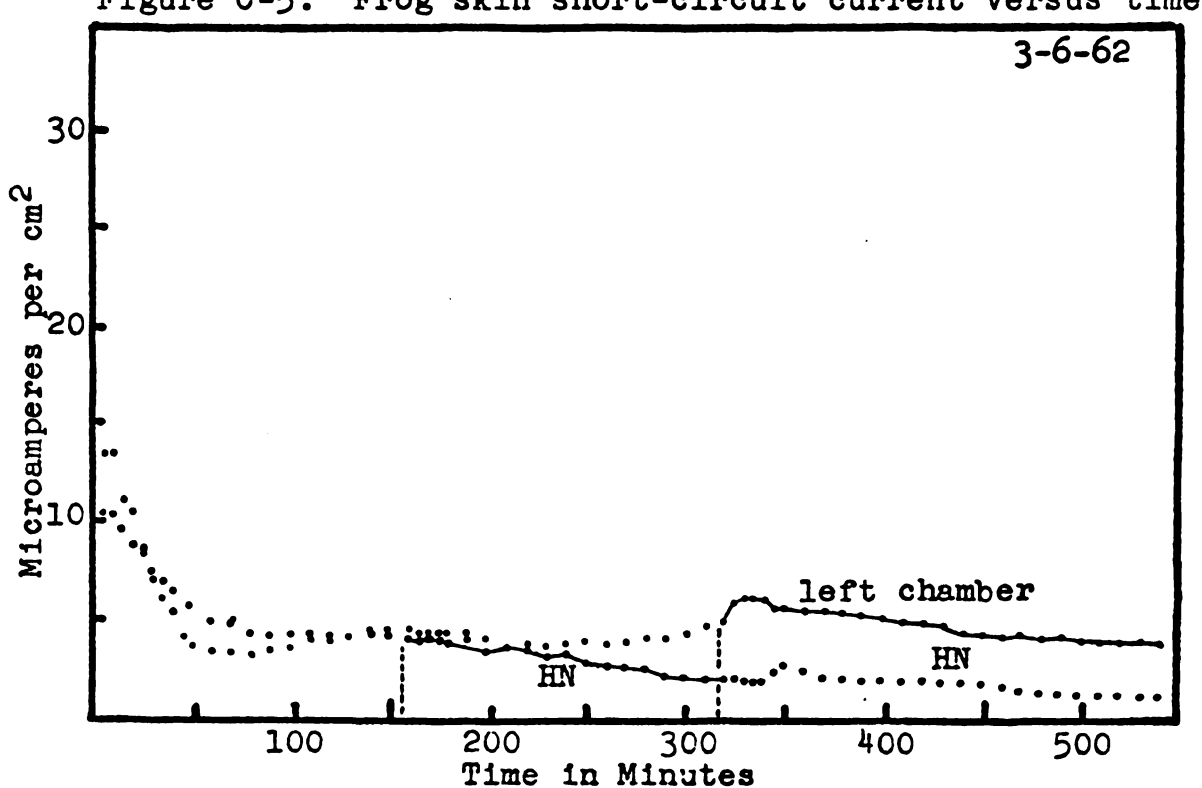


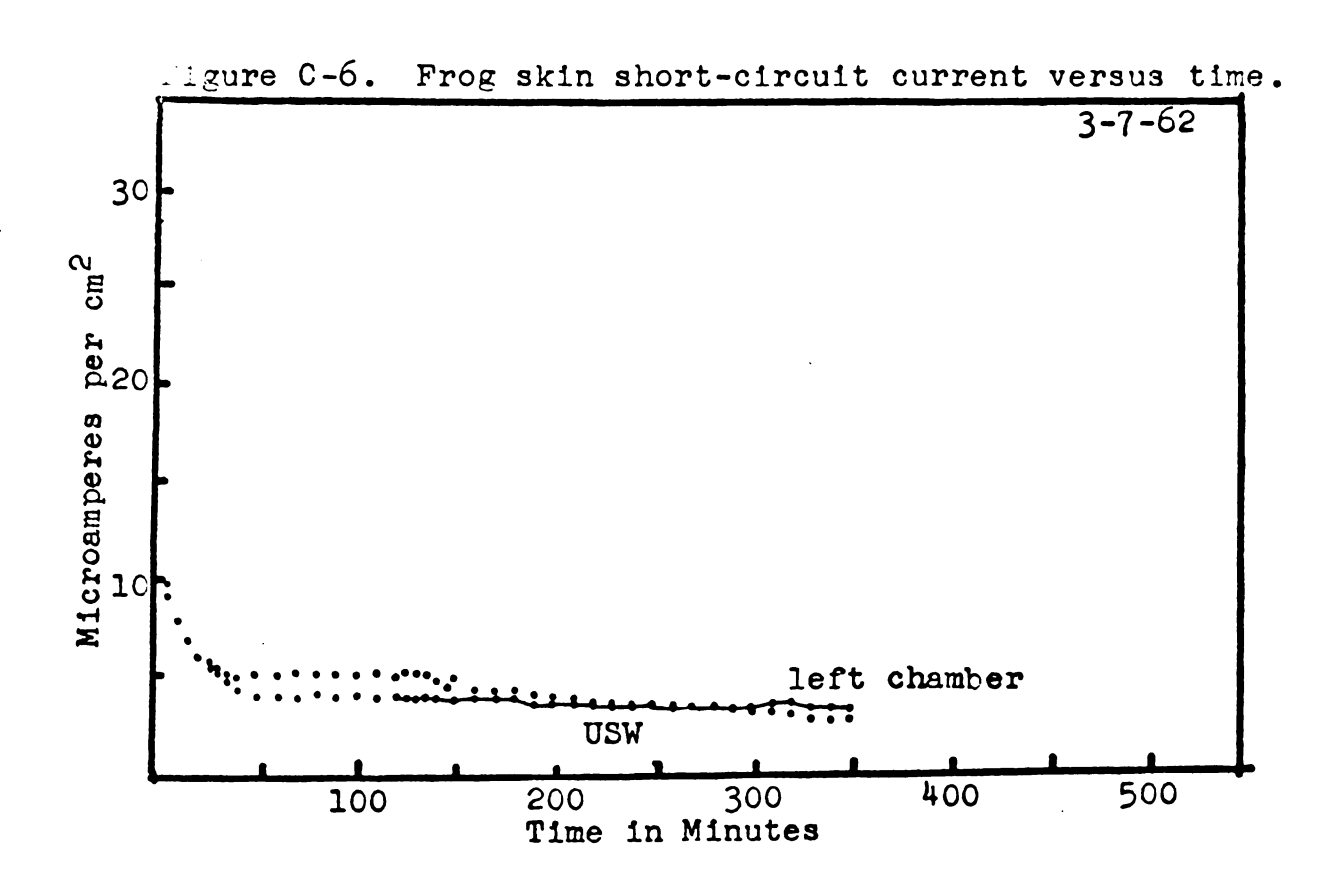
HN; HS = homogeneous field (see pages 47-49)

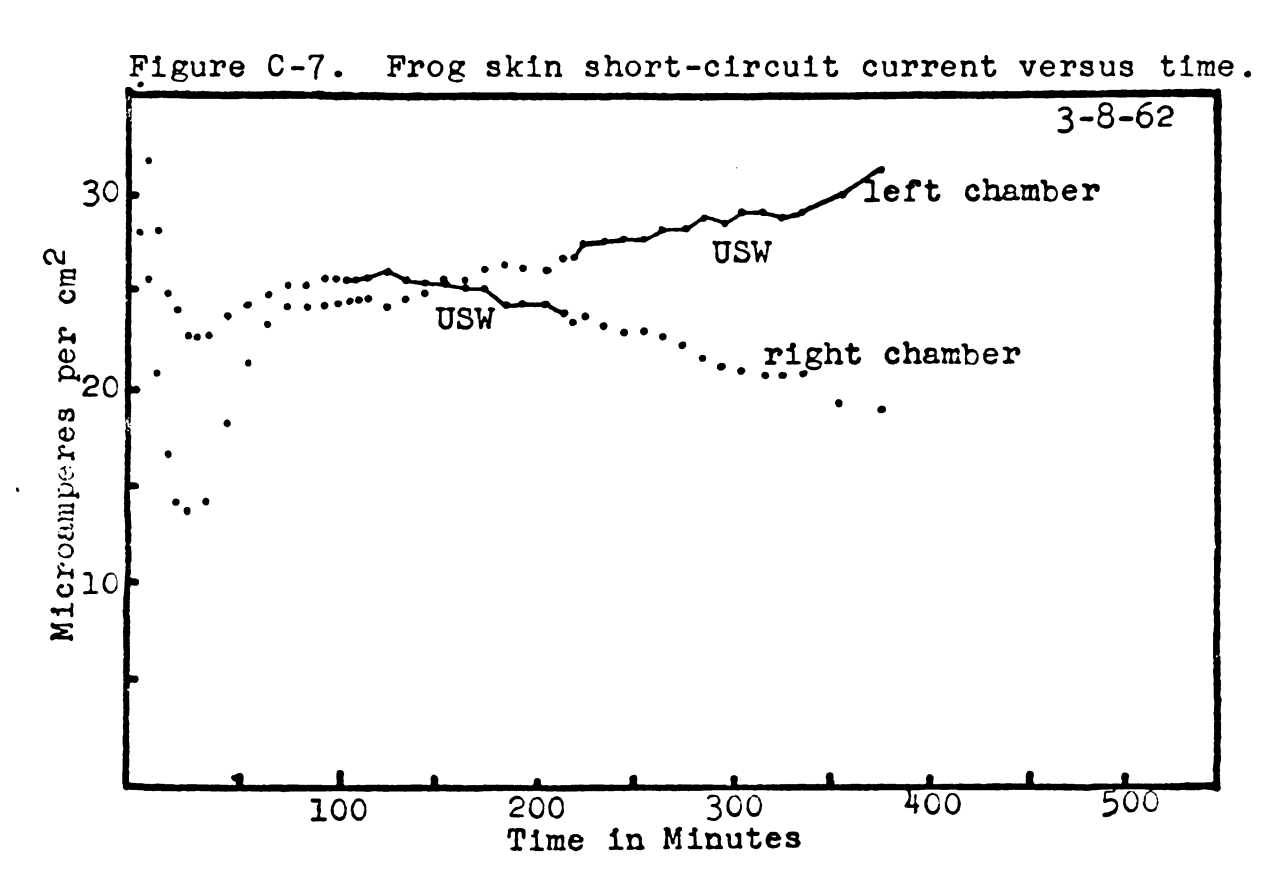
UNC; UNW; UNX = inhomogeneous field (see pages 47-49)











APPENDIX D

TEN-HOUR BIOMAGNETIC STUDIES

Table D-1. The total short-circuit current (microampere hours) produced by frog skins.

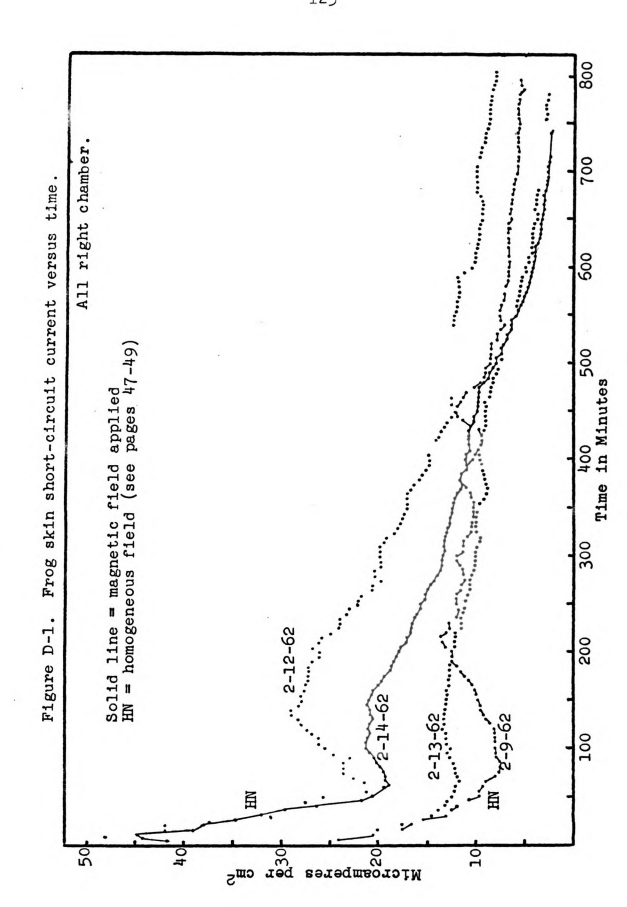
Figure	Total Microampere Hours	Total Coulombs
D-1	147	53
D-1	322	116
D-1	130	47
D-1	169	61
D-2, left	353	127
D-2, right	258	93
D-3, left	359	129
D-3, right	333	120
D-4, left	240	86
D-4, right	117	42
D-5, left	244	88
D-5, right	182	66
D-6, left	115	41
D-6, right	82	30
D-7, left	133	48
D-7, right	91	33

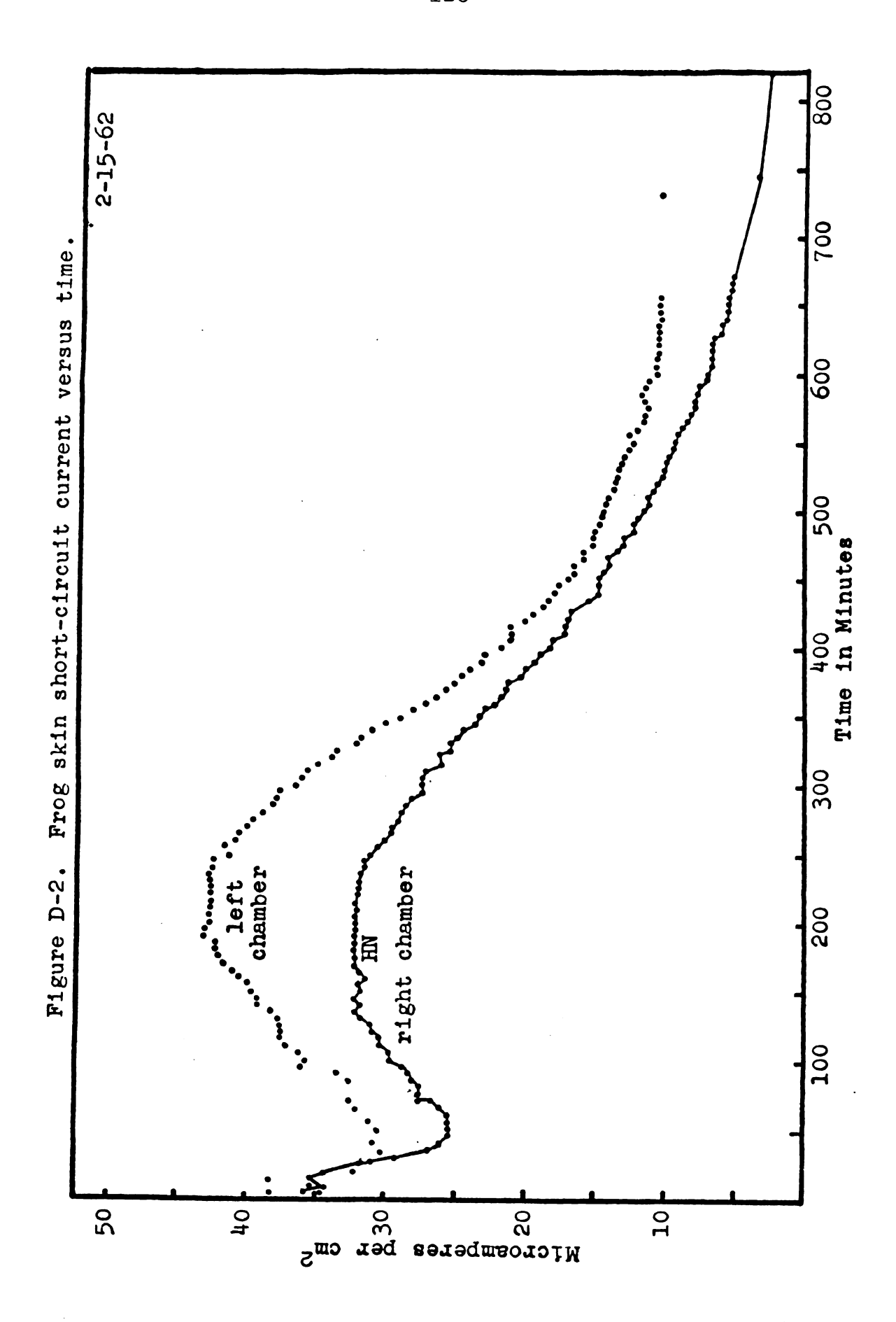
The area under the curve remaining after the termination of the experiment was estimated by extrapolation.

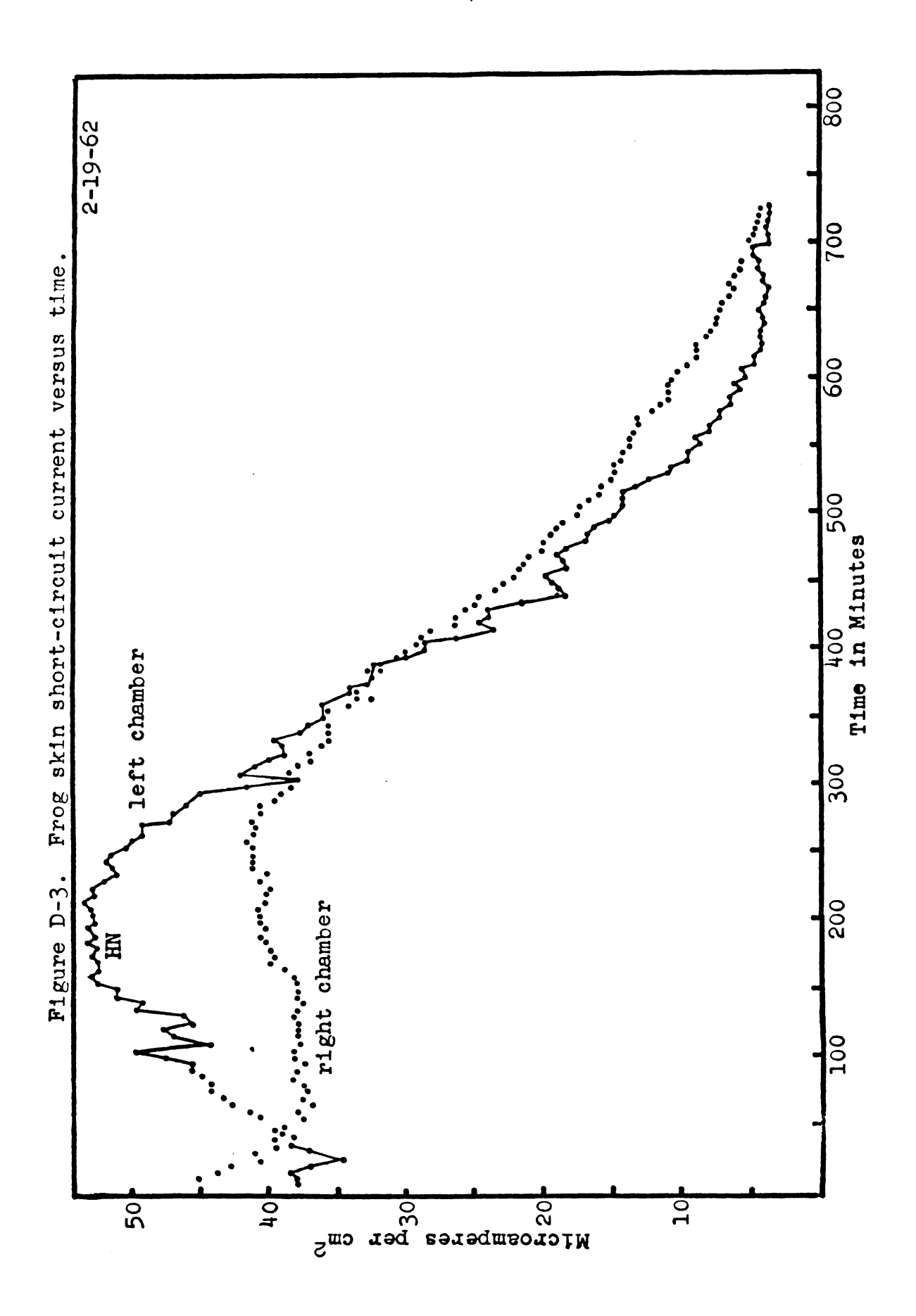
 $\overline{X} = 233 \pm 97$ microampere hours.

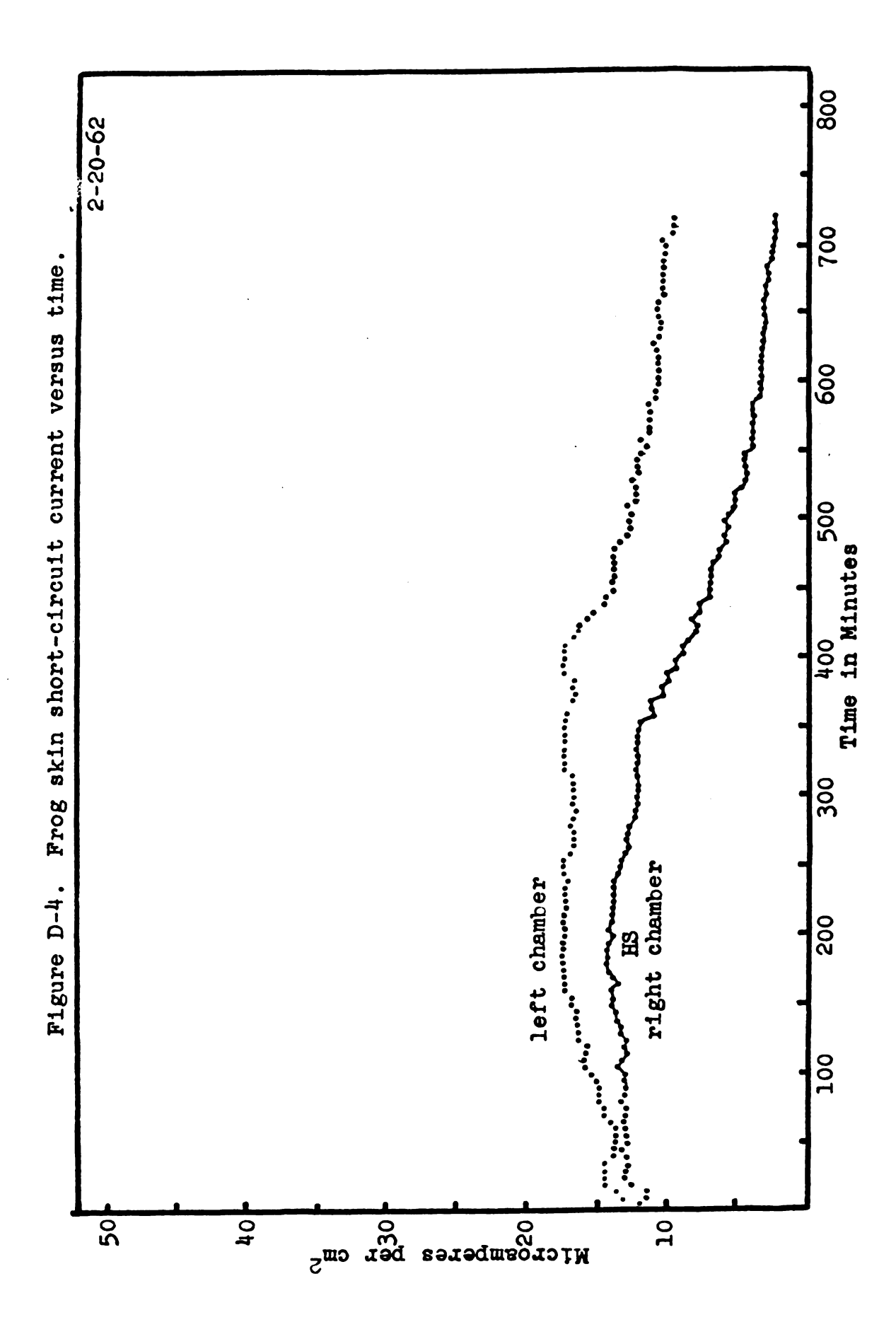
 $\overline{X} = 84 + 35$ coulombs.

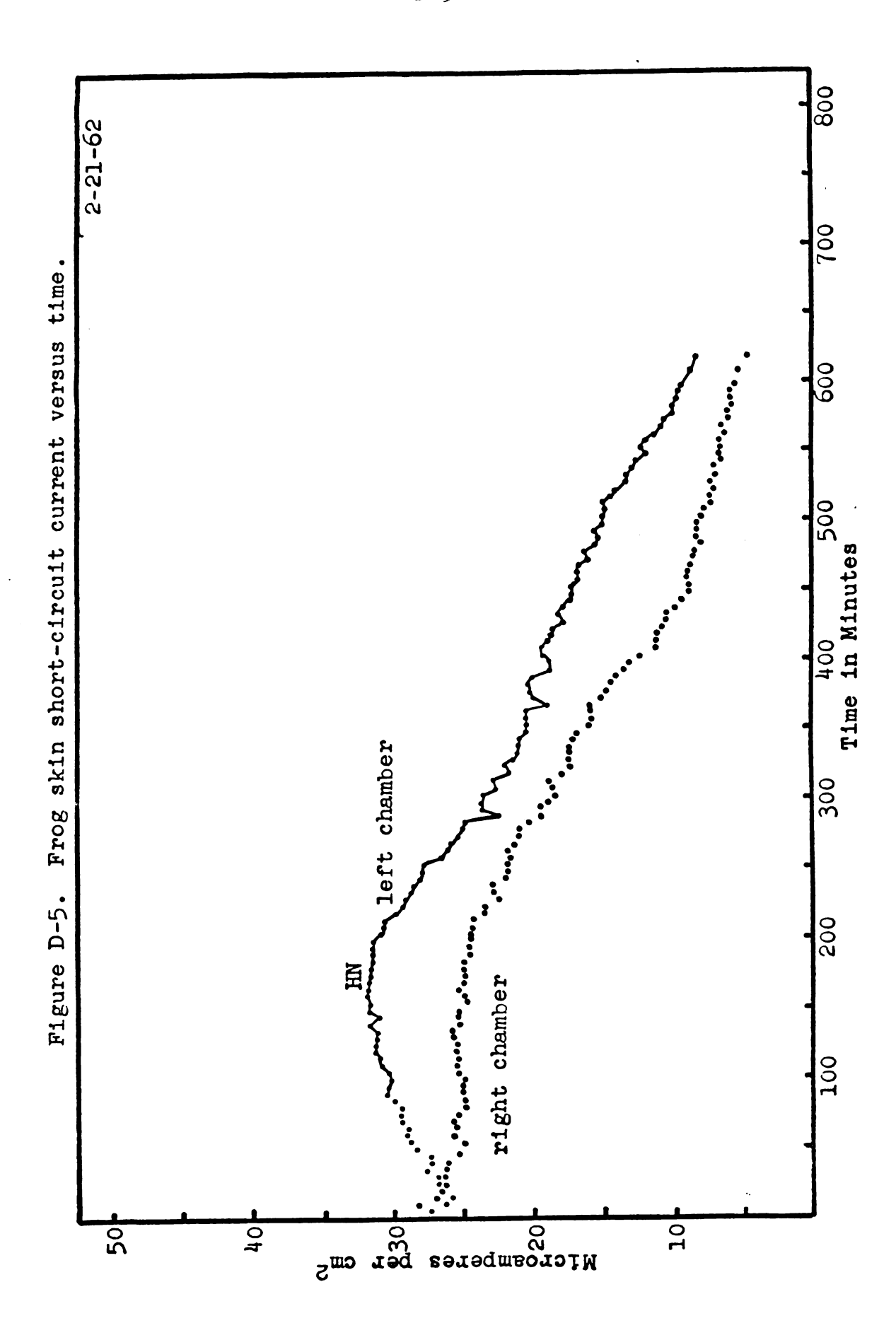
 \overline{X} = 20 $\frac{+}{-}$ 8 milligrams sodium transported.

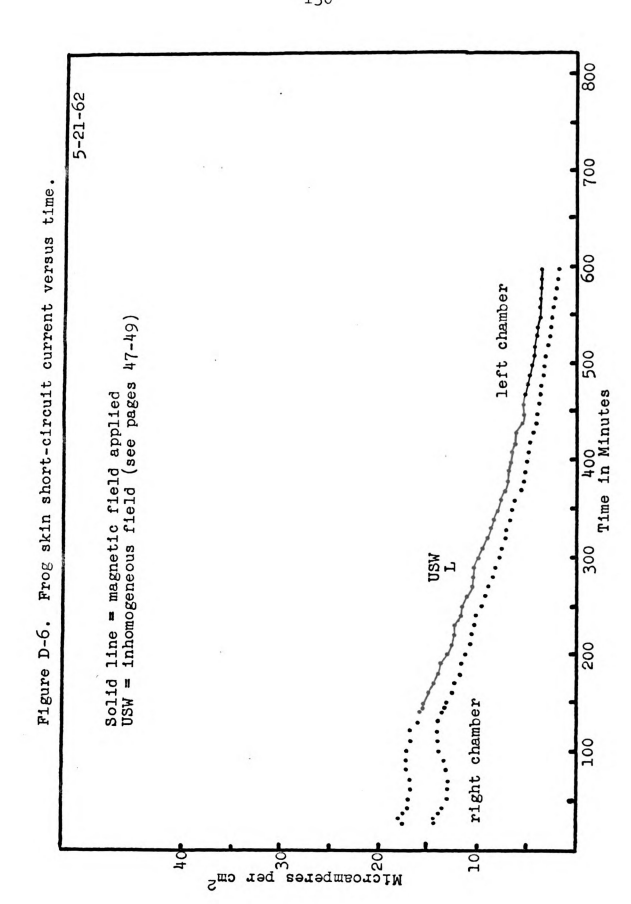


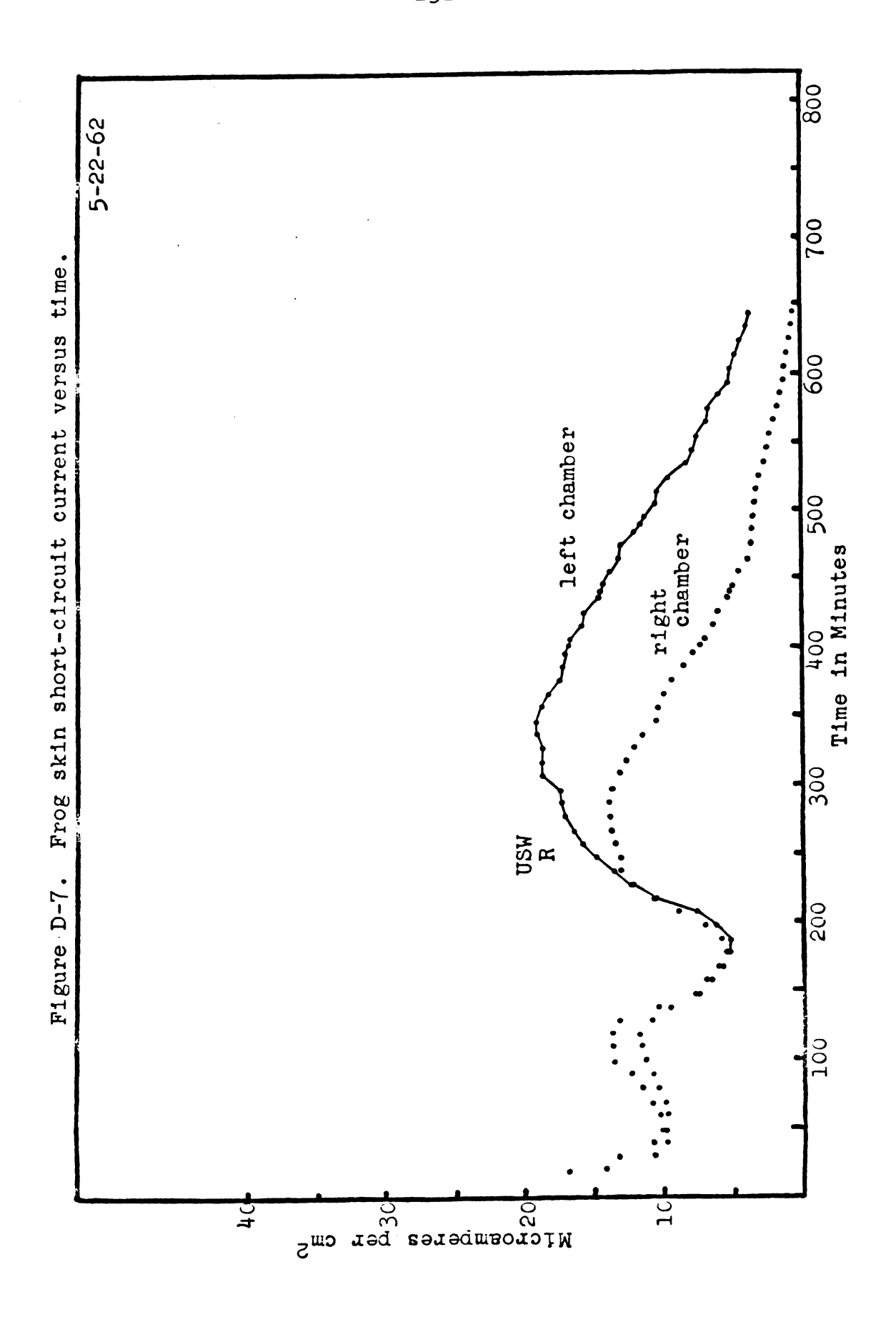












APPENDIX E

MOVEMENT OF RADIOCHROMATE ION ACROSS FROG SKIN

Table E-1. Movement of radiochromate ion across frog skin (figure 20, left chamber)

Total	Exp.	P.D.	s.c. µA	C/Min	/ml.		ected n/ml.
Min.	Min.	mV	per cm2	inside	outside	inside	outside
Mout:							
130	0	Approx.	l µc	Cr^{51} added	to insi	de chamb	er.
140	10	17	16.8	51,200	87		87
190	60	18	20.0	50,195	110		108
250	120	20	16.5	48,300	130		125
310	180	22	15.8	45,710	157		146

M _{in} :							
380	0	Approx.	1 µc	Cr ⁵¹ a	.dded	to outside	chamber.
390	10	21	10.9		66	60,953	66
440	60	18	8.1		89	59,535	87
500	120	16.5	6.1	1	61	60,953	147
560	180	14.5	5.3	2	22	60,953	193

^{53,333} C/Min in skin after rinsing in 50 ml. Ringer's.
1,450 C/Min in the 50 ml. Ringer's rinse.

Table E-2. Movement of radiochromate ion across frog skin (figure 21, right chamber)

Total	Exp.	P.D.	s.c. µA	C/Mir	n/ml.		ected n/ml.
Min.	Min.	mV	per cm2	inside	outside	inside	outside
M _{in} :							
110	0	Approx.	1 µc	Cr ⁵¹ added	l to outs	ide cham	ber.
120	10	18	17.5	l	51,200	-	
170	60	20	14.7	0	51,200	-	
230	120	22	13.0	3	51,200	-	
290	180	23.5	10.5	0	50,195	-	

M _{out} : 360	O	Approx.	1 µc	Cr^{51} added	to inside	chamber.
370	10	26	6.3	51,200	36	36
420	60	23	4.9	47,408	29	30
480	120	16	3.5	45,715	45	43
540	180	11	2.5	44,138	53	49

54,468 C/Min in skin after rinsing in 50 ml. Ringer's. 2,026 C/Min in the 50 ml. Ringer's rinse.

Table E-3. Movement of radiochromate ion across frog skin (figure 22, left chamber)

Total	Exp.	P.D.	s.c. µA	C/M	C/Min/ml.		Corrected C/Min/ml.	
Min.	Min.	mV	per cm2	inside	outside	inside	outside	
M _{in} :								
100	0	Approx.	l µc	Cr ⁵¹ add	ed to outs	side cham	ber.	
110	10	22	22.0	518	49,231	518		
160	60	26	23.8	577	49,231	572		
220	120	30	24.6	654	49,231	637		
280	180	29	23.8	724	49,231	690		

M _{out} :						
355	0	Approx.	1 µc	Cr^{51} added	to inside	chamber.
365	10	20	12.3	53,334	31	31
415	60	29	14.4	54,468	58	56
475	120	22	10.5	51,200	86	80
535	180	14	5.6	49,231	124	109

82,581 C/Min in skin after rinsing in 50 ml. Ringer's. 42,900 C/Min in the 50 ml. Ringer's rinse.

Table E-4. Movement of radiochromate ion across frog skin (figure 23, right chamber)

Total	Exp.	P.D.	s.c. µA	C/Min	/ml.		ected n/ml.
Min.	Min.	mV	per cm2	inside	outside	inside	outside
M _{out} :							
170	0	Approx.	1 µc	Cr^{51} added	to insi	de chamb	er.
180	10	1.85	3.5	47,408	21		21
230	60	1.8	3.5	47,408	161		150
290	120	1.8	3.5	46,973	347		307
350	180	1.75	3.5	47,408	511		432

M _{in} :						
400	0	Approx.	l µc	${\tt Cr}^{51}$ added	to outside	chamber.
410	10	0.6	2.5	54	44,138	54
460	60	0.5	2.1	305	44,138	285
520	120	0.4	1.8	628	43,390	556
580	180	0.4	1.8	1,006	42,667	843

^{17,124} C/Min in skin after rinsing in 50 ml. Ringer's.
3,525 C/Min in the 50 ml. Ringer's rinse.

Table E-5. Movement of radiochromate ion across frog skin in the presence of a magnetic field (figure 24, left chamber)

Total	Exp.	P.D.	s.c. µA	C/Min/ml.
Min.	Min.	in mV	per cm2	inside outside
M _{in} :				
100	0	Approx. 1 µc	c Cr ⁵¹ added	to outside chamber
120	20	31	22.8	27.2
140	40	30	22.4	20.3
160	60	30	21.8	21.1
180	80	30	21.8	21.8
187		Magnet posit	cioned: HN	
200	100	29	20.2	17.5
220	120	30	20.0	20.1
240	140	31	20.0	21.6
260	160	31	19.7	22.3
263		Magnet remov	red.	
280	180	32	20.0	24.9 60,952
300	200	32	20.0	28.0

Table E-6. Movement of radiochromate ion across frog skin in the presence of a magnetic field (figure 25, left chamber)

Total			s.c. μΛ	C/Min	ı/ml.	Corrected C/Min/ml.	
Min.	Min.	mV	per cm ²	inside	outside	inside	outside
M _{out} :							
215	0	Approx.	2 µc	Cr ⁵¹ added	to insid	de chamb	er.
235	20	19	10.9	91,429	108		108
255	40	22	11.6	91,429	112		112
275	60	20	10.9	89,825	135		133
295	80	18	9.8	86,780	141		138
298		Magnet	positi	ioned: HN			
315	100	19	9.8	85,333	164		157
335	120	19	10.0	82,581	166		159
355	140	18	9.3	82,581	175		166
375	160	18	9.5	81,270	196		181
376		Magnet :	remove	ed.			
395	180	16.5	8.4	80,000	197		182
415	200	16.5	<u>-</u>	-	209	****	190

Table E-7. Movement of radiochromate ion across frog skin in the presence of a magnetic field (figure 26, left chamber)

Total	Exp.	P.D.	s.c. µA	C/Mir	1/ml.		rected n/ml.
Min.	-	mV	per cm2	inside	outside	inside	outside
M _{in} :							
65	0	Approx.	2 µc	${\tt Cr}^{51}$ added	l to outs	ide cham	ber.
85	20	18	24.9	1,115		1,115	
105	1 4 O	15	22.1	1,139		1,138	
125	60	13	20.2	1,200		1,194	
145	80	12	17.9	1,228		1,219	
148		Magnet	positi	oned: UNT	1		
165	100	10	16.7			1,274	
185	120	10	15.8	1,423		1,377	
205	140	9	16.5	1,444		1,393	
225	160	-	_	1,541		1,463	
Both	chambe	rs rinse	d five	times wit	h Ringer	's solut	ion.
Mout:							
290	0	Approx.	2 µc	${\tt Cr}^{51}$ added	to insi	de chamb	er.
310	20	23	14.7		19		19
330	40	22	12.3		30		30
350	60	26	14.2		61		59
370	80	30	17.5		50		49
374		Magnet	positi	oned: UNI	1		
390	100	32	18.3	2	66		62
410	120	32	19.3		70		65
430	140	32	20.0		85		76
	- 6 -				0.0		-0

19.7

APPENDIX F

MOVEMENT OF RADIOCHROMATE ION ACROSS FISH SKIN

Table F-1. Movement of radiochromate ion across fish skin (figure 27, right chamber)

Total	Exp.		in/ml.			ected n/ml.
Min.	Min.	inside	outside	- -	inside	outside
Mout:						
25	0	Approx. 3	µc Cr ⁵¹	added	to inside	chamber.
45	20		23			23
65	40		28			28
85	60	29,425	119			112
105	80		148			138
125	100		37			45
145	120	29,091	49			55
165	140		52			57
185 Both M _{in} :	160 chambers r	insed five ti	63 Emes with	n Ringe	er's solut	65
210	0	Approx. 3)	ic Cr ⁵¹ e	ıdded .	to outside	chamber.
230	20	51			51	
250	40	65			64	
270	60	66	30,118		65	
290	80	86			83	
310	100	79			77	
330	120	89			85	
350	140	109	31,605		100	
370	160	112			102	

^{41,967} C/Min in skin after rinsing in 50 ml. Ringer's.

^{6,300} C/Min in the 50 ml. Ringer's rinse.

Table F-2. Movement of radiochromate ion across fish skin (figure 28, right chamber)

Total	Exp.	C/Min/ml. inside outside				Corrected C/Min/ml.		
Min.	Min.				inside outside			
M _{in} :								
25	0	Approx. 2	uc Cr ⁵¹	added	to	outside	chamber.	
45	20	8				8		
65	4 O	9				9		
85	60	12	29,425			12		
105	80	20				19		
125	100	15				15		
145	120	15				15		
165	140	12	29,425			13		
185	160	21				19		
	chambers r	insed five ti	lmes with	h Ring	er's	s soluti	ion.	
Mout:								
240	0	Approx. 2	µc Cr51	added	to	inside	chamber.	
260	20		27				27	
280	40		29				29	
300	60	27,527	37				36	
320	80		39				38	
340	100		48				46	
360	120		45				44	
380	140	26,392	63				58	
400	160		68				62	

^{51,200} C/Min in skin after rinsing in 50 ml. Ringer's.

^{5,141} C/Min in the 50 ml. Ringer's rinse.

Table F-3. Movement of radiochromate ion across fish skin (figure 29, left chamber)

Total	Exp.	C/Min/ml.				Corrected C/Min/ml.		
Min.	Min.	inside outside				nside	outside	
M _{out} :								
25	0	Approx. 2	µc Cr ⁵¹ a	dded	to :	inside	chamber.	
45	20		47				47	
65	40		53				53	
85	60	30,843	55				55	
105	80		59				59	
125	100		63				62	
145	120		65				64	
165	140	30,843	71				69	
185	160		75				72	
	chambers rin	nsed five ti	mes with 1	Ringe	r's	soluti	lon.	
M _{in} :								
240	0	Approx. 2 µ	c Cr ⁵¹ add	ded t	ο οι	ıtside	chamber.	
260	20	7 7				77		
280	40	125				123		
300	60	171	29,091			165		
320	80	191				183		
340	100	224				211		
360	120	260				240		
380	140	287	28,764			279		
400	160	338				316		

^{19,845} C/Min in skin after rinsing in 50 ml. Ringer's. 6,925 C/Min in the 50 ml. Ringer's rinse.

Table F-4. Movement of radiochromate ion across fish skin in the presence of a magnetic field (figure 30, left chamber)

	Total Min.		C/Min/ml.			Corrected C/Min/ml.		
			inside	outside		inside	outside	
M _{in} :	20	0	Approx. 2	μc Cr ⁵¹	added	outside	chamber.	
	40	20	755			755		
	60	4 O	944			936		
	80	60	1,005	31 , 605		992		
	100	80	1,032			1,016		
	106		Magnet pos	sitioned:	UNT L			
	120	100	1,105			1,077		
	140	120	1,602	31,220		1,475		
	160	140	1,226			1,189		
	180 cham 210	160 bers rin: O	1,390 sed five to Approx. 2					
M _{out} :	230	20	Approx. 2	36	added	1115100	36	
	250	40		47			47	
	270	60	32,305	56			. 55	
	290	80		66			64	
	295		Magnet pos	itioned:	UNT L			
	310	100		72			69	
	330	120		83			78	
	350	140		93			85	
	370	160		105			94	

^{41,290} C/Min in skin after rinsing in 50 ml. Ringer's.

^{7,625} C/Min in the 50 ml. Ringer's rinse.

.

